



# Probabilistic Analysis of Flexible Riser Responses in Storms

By

Curtis John Armstrong  
BE (Ocean Engineering) (Hons)  
National Centre for Maritime Engineering and Hydrodynamics  
Australian Maritime College

Submitted in fulfilment of the requirements for the degree of Doctor of Philosophy

University of Tasmania

March, 2019

# Declarations

## **Statement of Originality**

This thesis contains no material which has been accepted for a degree or diploma by the University or any other institution, except by way of background information and duly acknowledged in the thesis, and to the best of my knowledge and belief no material previously published or written by another person except where due acknowledgement is made in the text of the thesis, nor does the thesis contain any material that infringes copyright.

## **Authority of Access**

This thesis is not to be made available for loan or copying for two years following the date this statement was signed. Following that time the thesis may be made available for loan and limited copying and communication in accordance with the Copyright Act 1968.

## **Published Work Contained in Thesis**

The publishers of the papers comprising Chapters 2 to 6 hold the copyright for that content, and access to the material should be sought from the respective publisher. The remaining non-published content of the thesis may be made available for loan and limited copying and communication in accordance with the Copyright Act 1968.

Curtis John Armstrong

# Statements of Co-Authorship

The following people and institutions contributed to the publication of work undertaken as part of this thesis:

Candidate:	Curtis Armstrong,	University of Tasmania
Author 1:	Dr. Yuriy Drobyshevski,	INTECSEA Pty. Ltd.
Author 2:	Dr. Christopher Chin,	University of Tasmania
Author 3:	A. Prof. Irene Penesis,	University of Tasmania
Author 4:	Mr. Alexander Waterhouse,	University of Tasmania
Author 5:	Mr. Christopher Dunn,	University of Tasmania

## Author details and their roles:

---

### Paper 1, Investigation into Application of Environmental Contours for Analysis of Floating Systems:

Located in chapter 2, Authors 1, 2, and 4 were contributors to this paper.

Candidate contributed approximately 75% to the planning, execution and preparation of the work for the paper. Authors 1 and 4 contributed to the conception and design of the project and the analysis and interpretation of the research data. Author 2 contributed to the interpretation of the work by critically revising the paper.

Candidate (75%)	Author 1 (15%)	Author 2 (5%)	Author 4 (5%)
-----------------	----------------	---------------	---------------

---

### Paper 2, Comparative Study on Probability Distributions of Riser Responses

Located in chapter 3, Authors 1, 2, and 5 were contributors to this paper.

Candidate contributed approximately 75% to the planning, execution and preparation of the work for the paper. Authors 1 and 5 contributed to the conception and design of the project and the analysis and interpretation of the research data. Author 2 contributed to the interpretation of the work by critically revising the paper.

Candidate (75%)	Author 1 (15%)	Author 2 (5%)	Author 5 (5%)
-----------------	----------------	---------------	---------------

---

### **Paper 3, Probabilistic Analysis of Extreme Riser Responses for a Weather-vaning FPSO in Tropical Cyclones**

Located in chapter 4, Authors 1, 2, and 3 were contributors to this paper.

Candidate contributed approximately 75% to the planning, execution and preparation of the work for the paper. Author 1 contributed to the conception and design of the project and the analysis and interpretation of the research data. Authors 2 and 3 contributed to the interpretation of the work by critically revising the paper.

Candidate (75%)	Author 1 (15%)	Author 2 (5%)	Author 3 (5%)
-----------------	----------------	---------------	---------------

---

### **Paper 4, Application of Frequency Domain Methods for Response Based Analysis of Flexible Risers**

Located in chapter 5, Authors 1 and 2 were contributors to this paper.

Candidate contributed approximately 80% to the planning, execution and preparation of the work for the paper. Author 1 contributed to the conception and design of the project and the analysis and interpretation of the research data. Author 2 contributed to the interpretation of the work by critically revising the paper.

Candidate (80%)	Author 1 (15%)	Author 2 (5%)
-----------------	----------------	---------------

---

### **Paper 5, Variability of Extreme Riser Responses Due to Wave Frequency Motions of a Weather-vaning FPSO**

Located in chapter 10, Authors 1, 2, and 3 were contributors to this paper.

Candidate contributed approximately 75% to the planning, execution and preparation of the work for the paper. Author 1 contributed to the conception and design of the project and the analysis and interpretation of the research data. Authors 2 and 3 contributed to the interpretation of the work by critically revising the paper.

Candidate (75%)	Author 1 (15%)	Author 2 (5%)	Author 3 (5%)
-----------------	----------------	---------------	---------------

---

## Signatures

We the undersigned agree with the stated “proportion of work undertaken” for each of the published (or submitted) peer-reviewed manuscripts contributing to this thesis:

Signed:

\_\_\_\_\_  
Dr. Christopher Chin  
Supervisor  
The Australian Maritime College  
University of Tasmania

\_\_\_\_\_  
Prof. Shuhong Chai  
Head of School  
The Australian Maritime College  
University of Tasmania

Date:

\_\_\_\_\_  
28 MARCH 2019

\_\_\_\_\_  
28 March 2019

# Acknowledgements

Firstly, I would like to thank The Australian Maritime College (The University of Tasmania) and INTECSEA for providing joint funding to this project, as well as for the supportive communities that each is comprised of.

Endless thanks are owed for the quality of supervision provided by Yuriy Drobyshevski, Christopher Chin, and Irene Penesis; Yuriy, for his wealth of technical knowledge and distinctive ability to educate and inspire thought; Chris, for his guidance, encouragement, understanding, and sense of humour that has made all students at AMC feel welcome since their first days on campus; and Irene, for the steadfast support and the clarity she provides in any situation.

I would also like to say thank you for the help provided by Marius Martens and Dan Brooker during my tenures at the INTECSEA office in Perth, WA. Their insights and assistance with riser analysis was invaluable to the progression of this research. Furthermore, I would like to acknowledge the assistance provided to me by Alexander Waterhouse and Christopher Dunn during their undergraduate studies at AMC, their work provided vital results and assistive tools throughout various stages of the research.

And finally, to my parents, Robert and Suzanne Armstrong, for their unwavering support and love throughout all my endeavours, and for being the greatest teachers in my life. Thank you both.

# Table of Contents

Chapter 1 THESIS INTRODUCTION .....	1-1
1.1 INTRODUCTION.....	1-2
1.2 BACKGROUND/LITERATURE REVIEW.....	1-2
1.2.1 Conventional Design Approach for Riser Systems.....	1-2
1.2.2 Global Analysis .....	1-3
1.2.3 Riser Properties and Analysis .....	1-4
1.2.4 Response Based Analysis .....	1-4
1.2.5 Integrated System Design (Mooring, Riser and Floating Systems Integration).....	1-7
1.2.6 Environmental Contour Line (Surface) Methods (Traditional) .....	1-8
1.3 OBJECTIVES .....	1-11
1.4 METHODOLOGY .....	1-11
1.5 NOVEL ASPECTS .....	1-12
1.6 THESIS STRUCTURE .....	1-12
1.6.1 Chapter 1.....	1-12
1.6.2 Chapter 2.....	1-12
1.6.3 Chapter 3.....	1-13
1.6.4 Chapter 4.....	1-13
1.6.5 Chapter 5.....	1-13
1.6.6 Chapter 6.....	1-13
1.6.7 Chapter 7.....	1-14
1.6.8 Chapter 8.....	1-14
1.6.9 Chapter 9 – APPENDIX A .....	1-14
1.6.10 Chapter 10 – APPENDIX B .....	1-14
1.6.11 Chapter 11 – APPENDIX C .....	1-14
Chapter 2 INVESTIGATION INTO APPLICATION OF ENVIRONMENTAL CONTOURS FOR ANALYSIS OF FLOATING SYSTEMS .....	2-1
2.1 ABSTRACT.....	2-2
2.2 KEYWORDS .....	2-2
2.3 NOMENCLATURE.....	2-2
2.4 INTRODUCTION.....	2-2
2.5 THE ENVIRONMENTAL CONTOUR METHODS .....	2-3
2.5.1 Joint Probability Model .....	2-3
2.5.2 Constant Probability Density Contour .....	2-4
2.5.3 IFORM Contour.....	2-4
2.5.4 Exceedance Contour .....	2-5
2.6 ANALYSIS METHODS .....	2-6
2.6.1 Contour Sensitivity Analysis .....	2-6
2.6.2 Offshore System Response Studies .....	2-7
2.7 RESULTS AND DISCUSSION.....	2-8
2.7.1 Comparison of the Contours .....	2-8

2.7.2	Sensitivity of Responses .....	2-10
2.8	CONCLUSIONS .....	2-13
2.9	ACKNOWLEDGEMENTS .....	2-14
2.10	APPENDIX – Tabulated Environmental Contour Line Response Results .....	2-15
Chapter 3 COMPARATIVE STUDY ON PROBABILITY DISTRIBUTIONS OF RISER RESPONSES .....		3-1
3.1	ABSTRACT .....	3-2
3.2	KEYWORDS .....	3-2
3.3	INTRODUCTION.....	3-2
3.4	PROBABILITY DISTRIBUTIONS OF RISER RESPONSES .....	3-3
3.4.1	Normal Distribution .....	3-3
3.4.2	Beta Distribution.....	3-3
3.4.3	Birnbaum-Saunders Distribution .....	3-4
3.4.4	Burr Distribution.....	3-4
3.4.5	Gamma Distribution .....	3-5
3.4.6	Generalised Extreme Value (GEV) Distribution .....	3-5
3.4.7	Lognormal Distribution .....	3-5
3.4.8	Weibull Distribution .....	3-6
3.4.9	Rayleigh Distribution.....	3-6
3.4.10	Hermite Moments Model.....	3-6
3.5	GOODNESS OF FIT (GOF) METHOD .....	3-8
3.5.1	Goodness of Fit Tests for Normality .....	3-8
3.5.2	Goodness of Fit Tests for Specific Distributions .....	3-8
3.5.3	Application of Goodness of Fit Tests .....	3-10
3.6	CASE STUDY DATA .....	3-11
3.6.1	Vessel and Riser System Model .....	3-11
3.6.2	Metoccean Data .....	3-12
3.6.3	Software and Model Setup.....	3-13
3.7	RESULTS AND DISCUSSION.....	3-13
3.7.1	Storm 1 .....	3-13
3.7.2	Storm 2 .....	3-17
3.8	SUMMARY AND CONCLUSIONS.....	3-22
3.8.1	Summary of Goodness of Fit Tests.....	3-22
3.8.2	Distribution Moments and Classification .....	3-22
3.8.3	General Conclusions and Future Work.....	3-23
3.9	ACKNOWLEDGEMENTS .....	3-24
Chapter 4 PROBABILISTIC ANALYSIS OF EXTREME RISER RESPONSES FOR A WEATHER-VANING FPSO IN TROPICAL CYCLONES .....		4-1
4.1	ABSTRACT .....	4-2
4.2	NOMENCLATURE.....	4-2
4.3	INTRODUCTION.....	4-2
4.4	METHOD FOR PROBABILISTIC ANALYSIS.....	4-4
4.4.1	Global Performance and Riser Response Analysis .....	4-4



4.4.2	Short Term (Interval) Response Distribution.....	4-5
4.4.3	Medium Term (Storm) Response Distribution .....	4-7
4.4.4	Conditional Storm Response Distribution in Asymptotic Form .....	4-7
4.4.5	Equivalent Interval and Duration.....	4-9
4.4.6	3-Hour Design Event .....	4-11
4.5	CASE STUDY .....	4-11
4.5.1	FPSO Vessel, Mooring System and Riser Details .....	4-11
4.5.2	Metoccean Data .....	4-12
4.5.3	Modeling Approach and Software .....	4-13
4.6	RESULTS AND DISCUSSION.....	4-14
4.6.1	Short Term (Interval) Distributions .....	4-14
4.6.2	Medium Term (Storm) Distributions .....	4-16
4.6.3	Equivalent Intervals and their Durations .....	4-20
4.6.4	Comparison of Maximum Storm and 3-Hour Design Responses .....	4-22
4.6.5	Comparison of MPM Responses during Storm .....	4-26
4.6.6	Conditional Storm Distributions .....	4-29
4.7	CONCLUSIONS .....	4-31
4.8	ACKNOWLEDGMENT .....	4-32
Chapter 5 APPLICATION OF FREQUENCY DOMAIN METHODS FOR RESPONSE BASED ANALYSIS OF FLEXIBLE RISERS .....		5-1
5.1	ABSTRACT .....	5-2
5.2	NOMENCLATURE .....	5-2
5.3	INTRODUCTION.....	5-3
5.4	DESIGN DATA .....	5-3
5.4.1	FPSO Vessel Details .....	5-3
5.4.2	Riser System .....	5-3
5.4.3	Metoccean Data .....	5-4
5.5	METHODOLOGY .....	5-5
5.5.1	General.....	5-5
5.5.2	Vessel Heading and Offset .....	5-5
5.5.3	Post Processing .....	5-6
5.5.4	Sea Elevation Results.....	5-9
5.5.5	Curvature Components .....	5-11
5.6	RESULTS AND DISCUSSION.....	5-11
5.6.1	“Linear” Response Power Spectral Densities .....	5-11
5.6.2	Curvature Component Power Spectral Densities (Mid Water Arch and Sag Bend) .....	5-11
5.6.3	Curvature Component at Hang-off Power Spectral Densities .....	5-12
5.6.4	Response Amplitude Operators .....	5-13
5.6.5	Storm Response Most Probable Maximums .....	5-14
5.6.6	Applicability of Frequency Domain Analysis for Extreme Riser Responses .....	5-16
5.7	CONCLUSIONS .....	5-17
5.8	ACKNOWLEDGEMENTS .....	5-18

Chapter 6 METHODS FOR ANALYSIS OPTIMIZATION .....	6-1
6.1 Introduction .....	6-2
6.2 General Formulation for Interval Response Distribution .....	6-3
6.3 Reduction of the number of time domain realizations.....	6-3
6.4 Hybrid LF + WF Method .....	6-4
6.5 Frequency Domain Method.....	6-7
6.5.1 Distribution of the Dynamic Response Component.....	6-7
6.5.2 Static Response Component .....	6-9
6.5.3 Turret Excursion Envelopes.....	6-10
6.5.4 Definition of Waypoints .....	6-13
6.5.5 Waypoint Heading Definition.....	6-15
6.6 Case Studies .....	6-16
6.6.1 FPSO Vessel/Riser System (OrcaFlex)/Mooring System (ARIANE) Details .....	6-16
6.6.2 Metocean Data .....	6-16
6.7 Results and Discussion.....	6-17
6.7.1 Time Domain LF Responses.....	6-17
6.7.2 Hybrid LF+WF Method.....	6-19
6.7.3 Polar Coordinate and Waypoint Heading Findings .....	6-23
6.7.4 Use of Response Isolines .....	6-27
6.8 Summary and Conclusions .....	6-32
Chapter 7 SUMMARY, CONCLUSIONS AND FUTURE WORK .....	7-1
7.1 Summary and Conclusions .....	7-2
7.2 Limitations and Considerations of Numerical Analyses for RBA of Flexible Risers .....	7-5
7.3 Future Work .....	7-7
Chapter 8 REFERENCES.....	8-1
Chapter 9 APPENDICES .....	9-1
9.1 Storm #1 (Benign) and Storm #2 (Severe) Metocean Parameters .....	9-1
9.2 Hermite Extreme Value Distribution.....	9-3
9.3 Polar Coordinate Equations of an Ellipse.....	9-3
9.4 Equations for Vessel Headings.....	9-5
Chapter 10 VARIABILITY OF EXTREME RISER RESPONSES DUE TO WAVE FREQUENCY MOTIONS OF A WEATHER-VANING FPSO .....	10-1
10.1 ABSTRACT .....	10-2
10.2 NOMENCLATURE .....	10-2
10.3 INTRODUCTION.....	10-2
10.4 DESIGN DATA .....	10-3
10.4.1 FPSO Vessel Details .....	10-3
10.4.2 Riser System .....	10-3
10.4.3 Metocean Data .....	10-4
10.5 METHODOLOGY .....	10-4
10.5.1 Vessel Heading and Offset .....	10-4
10.5.2 Interval Response Distributions.....	10-5

10.5.3	Storm Distributions.....	10-6
10.5.4	3-Hour Design Maximum.....	10-6
10.5.5	Equivalent Interval and Design Storm Durations .....	10-6
10.5.6	Storm Distribution in Asymptotic Form .....	10-7
10.6	RESULTS AND DISCUSSION.....	10-7
10.6.1	Gumbel Fitting.....	10-7
10.6.2	Storm Distributions.....	10-9
10.6.3	Equivalent Interval Duration (EID) .....	10-11
10.6.4	3-Hour Design MPMs.....	10-12
10.6.5	Storm MPM Comparisons .....	10-12
10.6.6	Storm Distributions in Asymptotic Form.....	10-12
10.7	CONCLUSIONS .....	10-14
10.8	ACKNOWLEDGEMENTS.....	10-14
10.9	ANNEX A: Storm MPM Comparisons .....	10-15
10.10	ANNEX B: Equivalent Interval Duration.....	10-17
10.11	ANNEX C: Asymptotic Form of Storm Distribution .....	10-17
10.12	ANNEX D: Metocean Data .....	10-19
Chapter 11 SENSITIVITY OF VESSEL RESPONSES TO ENVIRONMENTAL CONTOURS OF EXTREME SEA STATES.....		11-1

# List of Figures

Figure 1-1 – “Figure 1: $H_s - T_p$ contours and TLP/Spar iso-response lines” [16]	1-9
Figure 1-2 – FORM Linearization of Failure Boundary in U-Space [28]	1-10
Figure 2-1: Exceedance Contour Definition	2-5
Figure 2-2: Riser Lazy Wave Configuration	2-8
Figure 2-3: World Wide Trade contour lines with return periods of 1, 10, 100, 1000 and 10000 years	2-9
Figure 2-4: $T_p$ difference between contour lines against $H_s$ for World Wide Trade	2-9
Figure 2-5: Contour plots with response iso-lines for semi-submersible heave response in the North Atlantic	2-10
Figure 2-6: Contour plots with response iso-lines for ship shaped FSO wave induced bending moment response in the West Shetlands Location	2-11
Figure 2-7: CPD 100, 1,000 and 10,000-year Contours with Hang off Tension Riser Response for West Shetlands Location	2-12
Figure 2-8: IFORM 100, 1,000 and 10,000-year Contours with Hang off Curvature Riser Response for World Wide Trade Location	2-13
Figure 2-9: Exceedance 100, 1,000 and 10,000-year Contours with Hang off Curvature Riser Response for West Shetlands Location	2-13
Figure 3-1: OrcaFlex model setup. Circles represent response location	3-12
Figure 3-2: Peak metocean parameters and headings for Storm 1	3-13
Figure 3-3: Peak metocean parameters and headings for Storm 2	3-13
Figure 3-4: Hang off tension (Storm 1) with fitted Normal distribution	3-14
Figure 3-5: Hang off curvature (Storm 1) with fitted Burr PDF	3-15
Figure 3-6: Sag bend curvature (Storm 1) with fitted Hermite PDF	3-15
Figure 3-7: Declination angle (Storm 1) with fitted Weibull PDF	3-16
Figure 3-8: Declination angle (Storm 1) with fitted Hermite PDF	3-17
Figure 3-9: Hang-off tension (Storm 2) with fitted Normal distribution	3-19
Figure 3-10: Normal dist. QQ plot fitted to hang-off tension (Storm 2)	3-19
Figure 3-11: Hang off tension (Storm 2) with fitted Hermite PDF	3-19
Figure 3-12: Hang off curvature (Storm 2) with fitted Hermite PDF	3-20
Figure 3-13: MWA Curvature (Storm 2) with fitted GEV PDF	3-21
Figure 3-14: Sag bend curvature (Storm 2) with fitted Hermite PDF	3-21
Figure 4-1: OrcaFlex riser model (red circles indicate locations of responses)	4-12
Figure 4-2: Metocean heading angle	4-13
Figure 4-3: Turret movement tracks from Ariane time histories	4-14
Figure 4-4: Sample Gumbel distribution fit CDF/empirical CDF	4-15
Figure 4-5: CDF of tension response	4-16
Figure 4-6: Truncated CDFs of tension response	4-16
Figure 4-7: LF+WF storm 1 sag bend curvature interval CDFs and storm CDF	4-17
Figure 4-8: LF+WF storm 1 turret heave interval CDFs and storm CDF	4-18
Figure 4-9: LF+WF storm 2 hang-off curvature interval CDFs and storm CDF	4-18

Figure 4-10: LF+WF storm 2 MWA curvature interval CDFs and storm CDF .....	4-19
Figure 4-11: LF+WF storm 2 sag bend curvature interval CDFs and storm CDF.....	4-19
Figure 4-12: WF-only storm 2 effective hang-off tension interval CDFs and storm CDF .....	4-20
Figure 4-13: LF+WF storm 2 effective hang-off tension interval CDFs and storm CDF.....	4-20
Figure 4-14: Equivalent Metocean Parameters for Hang-off Tension, MWA Curvature and Turret Heave: Storm 1 (Interval 29) .....	4-22
Figure 4-15: Metocean Parameters of "Benign" Storm 1 Interval 30. Equivalent Metocean Parameters for Hang-off Curvature, Sag-bend Curvature and Hang-off Declination Angle .....	4-24
Figure 4-16: Equivalent Metocean Parameters for Turret Heave: Storm 2 (Interval 73) .....	4-24
Figure 4-17: Metocean Parameters of "Severe" Storm 2 Interval 74. Equivalent Metocean Parameters for Hang-off Tension.....	4-24
Figure 4-18: Equivalent Metocean Parameters for Hang-off Curvature and Hang-off Declination Angle: Storm 2 (Interval 75) .....	4-25
Figure 4-19: Equivalent Metocean Parameters for Sag Bend Curvature: Storm 2 (Interval 83) .....	4-25
Figure 4-20: Equivalent Metocean Parameters for MWA Curvature: Storm 2 (Interval 92) .....	4-25
Figure 4-21: Storm 2 effective hang-off tension MPMs.....	4-26
Figure 4-22: Storm 2 sag bend curvature MPMs.....	4-27
Figure 4-23: Storm 2 MWA curvature MPMs.....	4-27
Figure 4-24: Storm 2 hang-off curvature MPMs .....	4-28
Figure 4-25: Storm 2 turret heave MPMs .....	4-28
Figure 4-26: Storm 2 declination angle MPMs.....	4-29
Figure 4-27: Asymptotic and exact CDFs of effective hang-off tension: Storm 2 .....	4-30
Figure 4-28: Asymptotic and exact CDFs of Hang-off curvature: Storm 2 .....	4-30
Figure 5-1: OrcaFlex Riser Model (Red circles indicate locations of monitored responses) .....	5-4
Figure 5-2: Model Coordinate System.....	5-5
Figure 5-3: Sea Elevation Time History with Sample Windowing (Storm 2 Case 74) .....	5-7
Figure 5-4: Windowed Sea Elevation PSD's (Storm 2 Case 74).....	5-7
Figure 5-5: Averaged Windowed Sea Elevation PSD for Seed 1 (Storm 2 Case 74).....	5-7
Figure 5-6: All Seeds Sea Elevation PSD's (Storm 2 Case 74).....	5-8
Figure 5-7: Windowing Size Effect on Sea Elevation PSD's (Storm 2 Case 74) .....	5-8
Figure 5-8: Number of FFT Windows vs. Significant Wave Heights (From 0 <sup>th</sup> Spectral Moment) (Storm 2 Case 74).....	5-9
Figure 5-9: Storm 1 Case 30 Sea Elevation PSDs .....	5-9
Figure 5-10: Storm 2 Case 74 Sea Elevation PSDs .....	5-9
Figure 5-11: Storm 2 Case 74 Hang-off Tension PSDs.....	5-11
Figure 5-12: Storm 2 Case 74 MWA X-Curvature PSD showing excellent agreement between time and frequency domain results.....	5-12
Figure 5-13: Storm 2 Case 74 MWA Y-Curvature PSD with reduced agreement between time and frequency domain results due to response magnitude .....	5-12
Figure 5-14: Storm 2 Case 74 Hang-off X-Curvature PSD .....	5-13

Figure 5-15: Effective Tension RAOs .....	5-13
Figure 5-16: Y-Curvature at the Hang-off RAOs .....	5-14
Figure 5-17: Hang-off tension Storm 2 most-probable maximums .....	5-14
Figure 5-18: Turret heave Storm 2 most-probable maximums .....	5-15
Figure 5-19: Hang-off curvature Storm 2 most-probable maximums.....	5-15
Figure 5-20: Sag-bend curvature Storm 2 most-probable maximums .....	5-16
Figure 5-21: MWA curvature Storm 2 most-probable maximums .....	5-16
Figure 6-1: Storm 2, Interval 76, Seed 1 Turret Track with WF FD Waypoints Distributed at 36s Intervals .....	6-5
Figure 6-2: Turret Excursion Envelope Examples With $S_{0,0}$ and Waypoints, $K_{x,x}$ for Two Intervals.....	6-9
Figure 6-3: Static Response Shift of Cumulative Probability Function for Waypoint, $K$ .....	6-10
Figure 6-4: Turret Excursion Maximums for Storm 2 .....	6-11
Figure 6-5: Turret Time History Tracks, Envelope and FD Solver Waypoints .....	6-11
Figure 6-6: Constant Probability Density Contours.....	6-12
Figure 6-7: Bivariate Normal Distribution of Turret Offset Tracks .....	6-13
Figure 6-8: Ellipsoidal Contours Generated by Bivariate Normal Distribution with Waypoints and Headings.....	6-13
Figure 6-9: Delaunay Triangles (LEFT) and Corresponding Waypoints Overlaid on Turret Tracks (RIGHT) .....	6-14
Figure 6-10: Polar Coordinate Generated Waypoints (White Marker) with Associated Radii and Angles.....	6-15
Figure 6-11: OrcaFlex Riser Model (Red circles indicate locations of responses) .....	6-16
Figure 6-12: Storm 2 LF Tension Response MPMs .....	6-17
Figure 6-13: Storm 2 LF Hang-off Curvature Response MPMs .....	6-18
Figure 6-14: Storm 2 LF Sag Bend Curvature Response MPMs.....	6-18
Figure 6-15: Storm 2 LF Wave Curvature Response MPMs .....	6-19
Figure 6-16: Storm 2, Interval 76, Seed 1 LF and WF Components of Turret Heave Response .....	6-20
Figure 6-17: Storm 2, Interval 76, Seed 1 LF and WF Components of Hang-off Tension Response .....	6-21
Figure 6-18: Storm 2, Interval 76, Seed 1 LF and WF Components of Hang-off Curvature Response .....	6-21
Figure 6-19: Storm 2, Interval 76, Seed 1 LF and WF Components of Sag Bend Curvature Response.....	6-22
Figure 6-20: Storm 2, Interval 76, Seed 1 LF and WF Components of Wave Curvature Response.....	6-22
Figure 6-21: Storm 2 Heave MPMs.....	6-23
Figure 6-22: Heading Sample Size Dependency for Storm 2 Turret Heave MPMs .....	6-24
Figure 6-23: 20K Point $\pm$ 2 Std. Dev. Heading for Storm 2 Turret Heave MPMs .....	6-24
Figure 6-24: Storm 2 Hang-off Tension MPMs .....	6-25
Figure 6-25: Storm 2 Hang-off Curvature MPMs .....	6-26
Figure 6-26: Storm 2 Sag Bend Curvature MPMs.....	6-26
Figure 6-27: Storm 2 Wave Curvature MPMs.....	6-27
Figure 6-28: Effective Hang Off Tension FD Simulation MPMs Scatter.....	6-28
Figure 6-29: Effective Hang Off Tension Maximum Response Interval (76) Response Isolines .....	6-28
Figure 6-30: Hang Off Curvature FD Simulation MPMs Scatter .....	6-29
Figure 6-31: Hang Off Curvature Maximum Response Interval (76) Response Isolines .....	6-29
Figure 6-32: Sag Bend Curvature FD Simulation MPMs Scatter .....	6-30
Figure 6-33: Sag Bend Curvature Maximum Response Interval (106) Response Isolines .....	6-30

Figure 6-34: Wave Curvature FD Simulation MPMs Scatter .....	6-31
Figure 6-35: Wave Curvature Maximum Response Interval (75) Response Isolines .....	6-31
Figure 6-36: Turret Heave FD Simulation MPMs Scatter .....	6-32
Figure 9-1: Storm 1 Metocean Parameters .....	9-1
Figure 9-2: Storm 2 Metocean Parameters .....	9-2
Figure 9-3: Base Ellipse Diagram.....	9-3
Figure 10-1: OrcaFlex Riser Model (Red circles indicate locations of responses).....	10-4
Figure 10-2: Model Coordinate System.....	10-5
Figure 10-3: Turret Heave Squared Response MLE Fit CDF (Storm 1 Interval 30) .....	10-7
Figure 10-4: Turret Heave Squared Response MLE Fit Quantile-quantile Plot (Storm 1 Interval 30) .....	10-8
Figure 10-5: Turret Heave Squared Response MLE Fit PDF (Storm 1 Interval 30) .....	10-8
Figure 10-6: Turret Heave Response Method of Moments Fit PDF (Storm 1 Interval 30) .....	10-8
Figure 10-7: Storm 1 Effective Hang-off Tension CDFs and Storm MPM.....	10-9
Figure 10-8: Storm 2 Effective Hang-off Tension CDFs and Storm MPM.....	10-10
Figure 10-9: Storm 2 Curvature: Sag Bend CDFs and Storm MPM .....	10-10
Figure 10-10: Storm 2 Curvature: Hang-off CDFs and Storm MPM .....	10-11
Figure 10-11: Asymptotic and Product of Interval CDFs of Storm 2's Hang-off Tension Storm Distribution...10-13	
Figure 10-12: Asymptotic and Product of Interval CDFs of Storm 1's Hang off Curvature Storm Distribution 10-13	
Figure 10-13: Storm 1 Responses.....	10-15
Figure 10-14: Storm 1 Curvature Responses .....	10-15
Figure 10-15: Storm 2 Responses.....	10-16
Figure 10-16: Storm 2 Curvature Responses .....	10-16
Figure 10-17: Metocean Heading Angle .....	10-19

# List of Tables

Table 2-1: FPSO General Particulars.....	2-7
Table 2-2: Riser Properties .....	2-7
Table 2-3: Responses and their Locations .....	2-8
Table 2-4: Vessel Sensitivity: Semi-Submersible Heave .....	2-15
Table 2-5: Vessel Sensitivity: Ship Shaped FSO Wave Induced Bending Moment.....	2-15
Table 2-6: Vessel Sensitivity: Riser Hang-off Tension .....	2-16
Table 2-7: Vessel Sensitivity: Riser Hang-off Curvature .....	2-16
Table 3-1: Vessel general particulars.....	3-11
Table 3-2: Mooring line properties.....	3-11
Table 3-3: Riser properties .....	3-11
Table 3-4: Response locations and corresponding static responses .....	3-12
Table 3-5: Storm metocean data magnitudes and directions .....	3-12
Table 3-6: GOF tests for turret heave and hang off tension (Storm 1). .....	3-14
Table 3-7: Curvature responses goodness of fit results for Storm 1 .....	3-15
Table 3-8: Declination angle response GOF results for Storm 1 .....	3-16
Table 3-9: GOF tests for turret heave and hang off tension (Storm 2). .....	3-17
Table 3-10: Hang off tension responses GOF results for Storm 2 .....	3-18
Table 3-11: Curvature responses GOF results for Storm 2.....	3-20
Table 3-12: Declination angle response GOF results for Storm 2 .....	3-21
Table 3-13: Best fit parent distributions .....	3-22
Table 3-14: Moments and Classification Storm 1 .....	3-22
Table 3-15: Moments and Classification Storm 2 .....	3-22
Table 4-1: FPSO general particulars.....	4-11
Table 4-2: Mooring line properties.....	4-11
Table 4-3: Riser properties .....	4-12
Table 4-4: Responses and their locations.....	4-12
Table 4-5: Peak values of metocean parameters and their associated headings .....	4-13
Table 4-6: Current Profile.....	4-13
Table 4-7: Storm response MPMs .....	4-16
Table 4-8: Equivalent Intervals for Response MPM: Storm 1 .....	4-21
Table 4-9: Equivalent Intervals for Response MPM: Storm 2.....	4-21
Table 4-10: Metocean parameters of Equivalent Intervals and % of Peak Metocean parameters (Table 4-5) ..	4-21
Table 4-11: 3-Hour design MPMs for Max Hs intervals (30 and 74) in Storm 1 and 2 with % differences from storm MPMs .....	4-23
Table 4-12: Parameters of Conditional Distributions: Storm 1 .....	4-29
Table 4-13: Parameters of Conditional Distributions: Storm 2 .....	4-29
Table 5-1: FPSO General Particulars.....	5-3
Table 5-2: Riser Properties .....	5-4



Table 5-3: Responses and their Locations .....	5-4
Table 5-4: Metocean parameters of selected intervals with Maximum Hs .....	5-5
Table 5-5: Processing Time Comparison.....	5-17
Table 6-1: Responses and their Locations .....	6-16
Table 6-2: Riser RBA Method Processing Times and File Requirements.....	6-32
Table 10-1: FPSO General Particulars.....	10-3
Table 10-2: Riser Properties .....	10-4
Table 10-3: Responses and their Locations .....	10-4
Table 10-4: Storm Response MPMs.....	10-10
Table 10-5: Equivalent Interval Durations .....	10-11
Table 10-6: Equivalent Interval Duration MPMs .....	10-12
Table 10-7: 3-Hour Design MPMs with % Differences from Storm MPMs .....	10-12
Table 10-8: 3-Hour Design Storm Equivalent Interval Durations .....	10-12
Table 10-9: Parameters of Asymptotic Distribution: Storm 1 .....	10-13
Table 10-10: Parameters of Asymptotic Distribution: Storm 2 .....	10-13

# Abstract

Dynamic flexible risers are an essential component which governs design of a floating production system, especially for offshore fields with harsh environment. Current design practices for flexible risers do not always capture the probabilistic nature of the offshore environment and its effects on the risers in a consistent manner. Unlike hulls and mooring systems of floating vessels, the probabilistic design methods for riser systems are somewhat lagging due to their complex structure, nonlinear mechanical properties and responses. As probabilistic response based design methods are increasingly in use for fixed and floating structures, inclusion of the riser systems into the framework of these methods is a logical extension. In this work, probabilistic prediction of extreme riser responses is investigated for a short and medium-term exposure periods, the latter being associated with a storm event. Investigation of several critical responses at several locations along a flexible riser supported by a weathervaning turret-moored vessel was conducted.

Probability distributions of the response processes, of the extreme responses in stationary intervals and in a complete storm, their sensitivities and variability were investigated comprehensively. The contributing metocean effects were examined where possible, and the wave frequency (WF) and low frequency (LF) (slow drift) components of the riser responses were studied in isolation and then combined. This approach allowed for a breakdown of the effects on each critical response, with the overall objective of developing a comprehensive storm-based response based design process, which would be applicable to all riser responses.

Initial steps included gauging the applicability of various typical distribution models to describe stochastic response processes as well as the extreme value distributions of isolated WF and coupled LF+WF responses. This was followed by the development of the maximum response distribution in a storm and its asymptotic formulation in a conditional format, with results indicating accurate representation of the numerical probability functions. Variability of flexible riser responses in two storms was investigated, including differences between the responses, effects of various metocean parameters and representation of the maximum riser response in a storm by the most contributing interval (sea state).

Another focus of the work was assessment of the practicality of the application of the probabilistic design methods to industry projects. Initial efforts to generate the riser response data sufficient to predict long term responses at long return periods by time domain analysis revealed major ‘big data’ restrictions, most significantly the computational efficiency of time domain methods and contemporary hardware. This prompted the focus to be extended to both the time and frequency domain analyses, respective solver strengths and limitations. Observing these limitations, optimization of the riser response analysis was studied using various methods including frequency domain and hybrid time - frequency domain approaches. Further work is recommended to develop these conceptual processes, however initial efforts provided promising insights and results towards the development of response based design methods for flexible risers.

Chapter 1

THESIS INTRODUCTION

## 1.1 INTRODUCTION

Response Based Analysis (RBA) is a probabilistic approach for the analysis of offshore systems, which is closely related to the structural reliability methods. RBA predicts N-year return period responses (loads) and associated metocean conditions by analyzing statistics of the floating system responses at the site. RBA is a promising alternative to the conventional design approach; the latter being based on the analysis of the system in extreme N-year return period metocean conditions often resulting in over-conservative predictions. Current practices are less computationally demanding and so require less turnaround time. However, Winterstein [1] highlights a similar progression in statistical analysis whilst writing about response surface models, saying "...early probability work adopted these models [e.g. normal and lognormal] as much for the sake of computational convenience as for accuracy." Therefore, with the continuous advancement of modern computing, advancement of the processes used should also be developed for improved accuracy.

To date, published research within the RBA field is limited to fixed and floating offshore structures, whereas the probabilistic analysis of dynamic risers received minimal attention. This is largely due to difficulties associated with the non-linearity of the riser responses and their strong dependency on the global behaviour of the floater, which make the probabilistic description of the complete system rather complex.

Dynamic risers are an essential component which governs the design of the floating production system, especially for offshore fields with harsh environment. Current design practices do not always provide for an adequate level of integration between the floating structure, mooring system and the risers. This results in different approaches used for the analysis of risers and the floating structure, as well as vague assumptions regarding design metocean conditions and, ultimately, an inefficient design or possible damage or failure of the risers. Therefore, development of consistent probabilistic methods for the analysis of the floating structure, moorings and the risers will contribute to improved safety and efficiency of floating production systems.

## 1.2 BACKGROUND/LITERATURE REVIEW

### 1.2.1 Conventional Design Approach for Riser Systems

Various codes, standards, and recommended practices exist for the design, installation and operation of offshore systems and form the foundation of many studies within these fields. They are comprehensive and continually updated alongside the industries progress as well as current research influences. Det Norske Veritas (DNV) and the American Petroleum Institute (API) codes are the two most commonly used in the offshore oil and gas industry and so a brief overview of the codes relevant to this research project is provided below:

The standard, DNV-OS-F201: Dynamic Risers [2], focuses on establishing safe practices in regards to steel risers for drilling, production/injection processes, completion/workover, and the transportation of hydrocarbons. In addition to new built risers, the standard is applicable for the modification, operation and upgrading of existing risers. The document is inclusive of design, materials, fabrication, testing, operation, and maintenance and assessment of risers.

DNV-RP-F204: Riser Fatigue [3] is an additional steel riser fatigue recommended practice which is intended to accompany the DNV-OS-F201 standard. The document complies with the standards outlined in DNV-OS-F201. This document is comprehensive in its recommended practices for riser fatigue analysis when the riser is subjected to fluctuating, repeating loads. Vortex Induced Vibration (VIV) loads are also outlined in the recommended practices.

In addition to the two primary riser design documents listed, DNV-OSS-302: Offshore Service Specification [4] provides an overview of other DNV documents and their uses. In terms of hierarchical listing of DNV documents the OSS type is governing, followed by standards and then recommended practices. DNV-OSS-302 indexes the standards and recommended practices and provides brief explanations of when they are intended to be applied in the design process of offshore riser systems. The OSS further lists standards and recommended practices provided by similar organizations to DNV and API.

Two API documents are similar in content to DNV's riser standards and practices and include API RP-17B: Recommended Practice for Flexible Pipe [5] and API 17J: Specification for Unbonded Flexible Pipe [6]. DNV-OSS-302 recommends that mixing of the DNV and API standards and recommended practices is to be avoided due to differences in safety factors and some practices. However, it is noted if they are to be mixed that the accompanying reports be clearly noted.

### 1.2.2 Global Analysis

Global analysis of an offshore installation is inclusive of all systems, primarily the floater, mooring and riser systems. A global analysis of all these systems links all their parameters to form broad responses for the system as a whole. Garret [7] discusses the processes of a global analysis and the methods used to couple each of the systems present in a case study involving a semisubmersible platform, 16 mooring lines and 20 risers. Modelling of the rigid bodies, elastic rods and connecting links are detailed to make the coupling of systems possible. The task is inclusive of concept selection to final design, installation and operation which the author describes as a daunting task involving close to 1000 load cases for completion of the global analysis. The novelty of the research conducted was performing fully coupled analyses in the frequency domain with the intent of reducing computational demand. Garret concludes that sufficient accuracy and efficiency are gained when analyses are performed in the frequency domain. Efficiencies are stated to be in the order of two to three times in magnitude in favour of frequency domain simulations with no loss of accuracy.

Extending Garret's work, Low [8] presented a hybrid global coupled analysis which uses both time and frequency domains for low frequency (LF) and high frequency (HF) responses respectively. The hybrid method is stated to be nearly as accurate as a fully coupled time domain analysis but with the enormous benefit of requiring less than a tenth of the computational effort. The analysis was performed with in-house software, however the author notes that the method is compatible with other software packages capable of coupled analyses.

Building on the hybrid methodology of frequency domain analyses, Low [9] investigates the effect of water depth, and hence the introduction of further non-linearities to the global system in shallow waters. It is found that the accuracy of the hybrid model severely decreases upon the reduction of water depth. The non-linearities that arise in shallow water affect the restoring forces caused by the mooring lines as well as causing large changes to the configuration of the lines and their dynamic response characteristics (damping). Low [9] presents a solution in the form of transferring wave frequency response statistics from the frequency analysis to time domain analysis in order to compute linearized drag forces.

When considering time and frequency domains as well as coupled and uncoupled responses there are no distinguishable differences in the safety load factors applied by design codes. Because of this, Vasudevan and Westlake [10] propose the use of less conservative safety factors when conducting the more accurate time domain/fully coupled analyses as well as using the more conservative factors when frequency domain/uncoupled analyses are performed. Appropriate safety factors need developing in conjunction with the development of new design methods such as RBA.

### 1.2.3 Riser Properties and Analysis

Understanding the properties of a riser flowline, including materials, structural configuration and failure modes is significant to design process development. Failure modes of risers are predominantly caused by tension and curvature responses as well as clashing of subsea lines arising from interference scenarios. Fatigue must also be considered as risers are subject to various cyclic loading from the wave loads as well as VIV fatigue.

In their study, Witz and Tan [11] identify the dominant mechanism affecting the curvature of risers as the slip mechanism that exists between structural component layers. The authors present mathematical models for the calculation of internal stresses and potential failure modes resulting from curvature limits being exceeded. The governing component layer for resistivity to failure is understandably the armor layer (commonly helical). The curvature response also initiates a twisting response within the riser component layers, highlighting the complexity of failure modes of risers. Due to the complexity of riser behavior, caution must be taken when interpreting standard riser global dynamic analysis software packages (such as Orcaflex) that utilize line element models that are unable to capture these complex behaviors [12].

### 1.2.4 Response Based Analysis

As previously mentioned, current literature regarding RBA has been limited in scope to fixed structures and floating hulls; the literature reviewed is presented below.

In a study conducted by Forristall [13], response functions of a structure were generated using a multivariate regression analysis since the structure would be exposed to wind, wave and current forces separately. When these functions were then applied to an entire database of oceanographic hindcasts the resultant 100 year response was approximately 15% less than the response calculated by the statistical model that assumed all environmental maximums occurred simultaneously. Forristall [13] developed methods of filtering the hindcast datasets to reduce the sample size that would be exposed to the multivariate response functions including various joint statistical distributions, selection criteria filters and binning functions. These functions also provided statistical indicators of their simultaneous occurrence. The study opens the argument that the statistical models used are too conservative:

*“The strongest winds, waves, and currents do not necessarily occur at the same time in a storm, and it is unnecessarily conservative to set design criteria as if they did” – Forristall [13]*

Response based analysis reduces the conservative approaches of statistical metocean analysis methods by finding true responses to actual environmental data. Tromans [14] identifies the highly conservative practice of assuming that 100-year wind, wave, and current conditions occur simultaneously. Instead Tromans proposes a method of obtaining responses from storm events (in place of sea states) and retrieving the associated statistical properties. The term “Response Based” environmental design conditions is offered and is the basis for the Response Based Analysis method.

Incecik [15] first introduces an analysis procedure based upon the structure variable approach which involves the analysis of wind, wave and current loads on offshore platforms and finds that the most severe moorings loads do not necessarily occur while these loads act collinearly nor at the extreme N-year environmental predictions. This immediately highlights the drawback of the conventional reliability methods such as environmental contour lines as these methods assume the extreme sea states are responsible for the extreme responses [16]. The study employs the transformation of the environmental time series into a time series of forces using their response function. Once response functions are established, Incecik outlines the pros and cons of time domain versus frequency domain analysis methods:

- Frequency domain is less computationally demanding, however is unable to deal with non-linearities that time domain can identify
- Non-linearities associated with floating systems include viscous damping and mooring forces

In another study, Ahilan [17] investigates the advantages and disadvantages of Direct Simulation Approach (DSA: an analysis method synonymous with RBA) and the Reliability Analysis Approach (RAA). For the particular case studies provided the RAA provided design responses within 7% of those identified by the full DSA analysis. Given this difference, the author suggests that RAA, being less computationally demanding and requiring less simplification of the physics model, is the preferable approach in these cases. The author continues to say that case-by-case verification is required as the results are site and structure specific.

DSA, although capable of identifying ‘unlikely’ but still pertinent environmental conditions that may result in failure responses, is unable to determine the most likely combination of parameters that would result in a 100 year response. Ahilan suggests the application of response surface models to the DSA to reduce the number of cases whilst maintaining the models statistical properties as well as allowing for a more robust physics model to be used.

The Reliability Analysis Approach relies on the following arguments:

- a) Assume that the physical response of a system near failure can be defined by a function of the basic variables that influence the system
- b) The basic variables themselves can be described individually and/or jointly by probability distributions
- c) The probability of failure can then be computed by transforming any arbitrary distribution of the basic variables close to the point of failure into equivalent normal distributions *exactly*

Standing [18] presents the findings of a Joint Industry Project (BMT and Noble Denton) for the application of Response Based Design for Floating Production Storage Offloading (FPSO) vessels. The findings identified a possible reduction of design excursions and line tension by 20%, setting a precedent for the benefits of RBA. Furthermore, the study identifies other key benefits such as quantifying probabilities of exceeding design loads and excursions, the ability to apply a systematic approach for selection of design metocean conditions and associated directional properties. First order reliability (FORM) and second order reliability (SORM) methods in conjunction with long term simulation/extreme value analysis for comparative purposes formed the basis of the reliability analysis of this study. The RBA analysis was found to be a reliable method when API or Lloyd’s safety factors were used, with the two methods providing factors consistent with DNV. The study acknowledges the computational complexity compared to ‘traditional’ methods but highlights the various advantages including reduced loads on the design. In regards to the comparison of long term simulation and the application of FORM and SORM Probability Density Functions (PDFs), each method provided ‘similar estimates for 100-year responses and their associated metocean conditions’; the author further acknowledges due to this similarity, the less computationally demanding FORM and SORM methods are favourable for this reason. The study also reveals that the extreme responses of the vessel are most commonly caused by the extreme environmental conditions (hurricanes) contained within the recorded environmental data. The author labels these events as primary causation of extreme responses with storm and eddy current events being of secondary influence, however, they are not negligible in the model fitting.

Perdrizet [19] investigates the application of a long term probabilistic failure response of riser systems. The investigation involves the non-linear extreme response of a riser connected to an FPSO subjected to wave induced loads in a stationary sea state. Perdrizet refers to Response Based Design approaches which aim to directly evaluate the most probable failure point and associated failure probabilities. Short term extreme responses in conjunction with long term methods (all sea states method used) are utilized for this investigation. Perdrizet concludes that the introduction of long term variables in the short term problem, although attractive for design, validating the approach was ‘not straightforward’.

Sousa [20] proposes a computationally feasible methodology for calculating long term extreme responses in conjunction with calibrating loading conditions based on the long term responses identified. Sousa lists two possible flaws with the traditional method of long term metocean analysis; the first being the possibility of low period riser responses being overlooked due to their omission by the traditional statistical analysis, and, the potential for overestimating the riser responses arising due to the consideration of artificial extreme sea states.

Building on previous studies, Drobyshevski [21] investigates the application of Response Based Analysis with focus upon Design Metocean Conditions (DMC), their theoretical background and the numerical method used for the determination of the DMC. A case study of an Floating Storage Offloading (FSO) type turret-moored vessel was performed with the environmental model generated using directional sea spectra from the Synthetic Tropical Cyclone data base and the Random Tropical Cyclone data base. The approach presented provides a consistent method of predicting the DMC’s with N-year responses. The approach involves application of the ‘random event’ method as well as the introduction of two parameters including the N-year return design event and the C-Parameter (contribution parameter). The method proposed allows for several DMC to be determined for a single response. The C-Parameter may be used as a tool for ranking intervals with the N-year return design event. The maximum C-Parameter provides a definition for the interval and metocean condition at which the Most Probable Maximum (MPM) Response on a design return period is most likely to be exceeded. This combination of factors may then be used to define the DMC.

Zhang [22] investigated the statistical properties of riser analysis in irregular and regular sea states with focus placed upon the dynamic and stationery properties of the systems. The effect of the number of wave components implemented for these analysis was studied by performing separate tests consisting of 200 and 3000 components; the difference in the cumulative distributions was minimal leading to the conclusion that a large quantity of wave components is not paramount for the generation of the cumulative distribution in this analysis. A probability distribution study was conducted with the application of five different distribution theories, including:

- Normal Distribution
- Rayleigh Distribution
- Weibull Distribution
- Generalized Pareto Distribution (GPD)
- Gumbel Distribution

The study concluded various advantages and disadvantages of each distribution with respect to their ability to accurately describe irregular waves, top tensions, and top angle, curvature and sag bend responses. Zhang suggests that the normal distribution accurately represented the first two parameters listed, the Weibull or Gumbel distributions appropriate for all



other responses and advising the Rayleigh and GPD distributions were inadequate for all riser distributions. The study also found that all riser responses and irregular waves could be regarded as an ergodic stationery process. From these cumulative investigations, the author proposes the conclusion that riser systems may be regarded as linear systems in contrast to the high non-linearity that is currently implemented in software models.

#### 1.2.5 Integrated System Design (Mooring, Riser and Floating Systems Integration)

Another progressive field of study for improved offshore system design is the integration of the mooring, riser and floating structure systems using coupled analysis. Traditional analysis methods address each system separately and various design codes exist for mooring, risers and floating structures independently. As RBA requires simulation of the system when exposed to hind cast metocean data, a fully coupled analysis of all systems is the ideal method to ensure the responses are predicted as accurately as possible. Integrated analysis methods and various applicable processes have been identified for use in the proposed research.

Firstly, Connaire [23] presents a study of various methods of integrated design of mooring and riser systems for an FPSO installation. Three methods are presented with varying complexity from the least computationally demanding to the most:

1. The first method is the most simplified and involves the summation of drag forces of each system. However it assumes the effects of riser stiffness, added mass and damping contributions are of negligible magnitude.
2. The second approach involves the analysis of riser and mooring system stiffness and attempts to couple their analysis through application of finite element models. This method establishes reaction forces of the systems when exposed to current loading.
3. The final method which is also the most computationally demanding requires the 3D modelling of each system and applies a finite element time domain dynamic riser and mooring system model for this purpose. This method allows for the inclusion of the added mass and damping contributions of the riser and mooring systems.

After comparing the three methods, Connaire [23] recommends that for a detailed analysis and design verification, the approach of intermediate complexity be used where the water depths, current velocities and number of risers are large. In contrast, for shallow water designs and less extreme environment, the mean riser and mooring line current loads appear to be sufficient for design as these loads are not major contributors to vessel response and loading. Stiffness and damping from Steel Catenary Riser's (SCR) are essential to the accuracy of integrated mooring and riser analysis for deep-water applications.

A joint industry project conducted by Goodwin [24] focuses on the reiteration of safety factors through reliability analysis of various offshore vessels and their mooring and riser systems. Through logic guided process loops, the safety factors are optimized so that the difference between the target and predicted probabilities of exceedance states is minimalized; if the difference is too large, re-evaluation of the response surfaces and reliability analysis is performed thus refining the predictive model.

The integration of the riser, mooring and the vessel global performance for the FPSO in harsh environmental conditions was investigated by Martens [25]. The mooring and riser analyses were performed for a common set of design cases by capturing the consistent information on vessel heading and motion behaviour between the two analyses, rather than different sets of design cases and assumptions. The directionality of metocean conditions was also exploited in the time

domain. Compass octants are utilised to discretise the metocean conditions, FPSO headings and turret offsets. Due to the excessive time that the time domain coupled analysis requires, a screening method is proposed by the author and a flow diagram provided for a simplified description.

A methodology from preliminary to advanced integration of mooring and riser design into a design spiral is presented by Giron [26]. A detailed proposition for an integrated design method is provided with accompanying steps and design flow-chart. Giron [26] lists the currently separate design codes for mooring and riser analysis and proposes a method of integrating the codes into the design loop:

- Mooring systems: API RP 2SK, DNV OS E301 and ISO 19901-7
- Rigid Risers: API RP 2RD, DNV OS F201
- Flexible Risers: API Spec 17J, API RP 17B, DNV-OS-F201, DNV-OSS-302, DNV-RP-F204

#### 1.2.6 Environmental Contour Line (Surface) Methods (Traditional)

These methods aim to avoid the long term response prediction (as done in RBA) by replacing it with a short term response analysis for a limited set of metocean conditions. Such conditions are identified on the environmental contour lines corresponding to a given exceedance probability  $q$  or return period  $N$ . There are two common methods for generating the environmental contours: Inverse first order reliability method (IFORM) and constant probability density (CPD).

Winterstein [27] investigates the extrapolation (inflation) of metocean parameters as required in the design of offshore structures/vessels in order to obtain the appropriate safety factors. The paper identifies the uncertainty that a maximum parameter will not always occur during a maximum sea-state and thus introduces an uncertainty factor (omission factor).

Winterstein [27] addresses the fact that specific metocean parameters such as significant wave height,  $H_s$ , and zero-up crossing period,  $T_z$ , may collectively be parameters of concern during the design of an offshore structure as their combined contribution to loading is most significant. This therefore calls for the investigation of methods of combining the probabilities of the two parameters occurring concurrently. The FORM approach “typically seeks the failure probability,  $p_F$ , associated with exceeding a known response capacity,  $y_{cap}$ ” [27], whereas with known data and probabilistic models the response capacity is what is sought rather than known, hence the introduction of the Inverse FORM Method, IFORM. Winterstein identifies the main benefit of the IFORM method as its ability in regards to “decoupling the description of the environment variables  $X$  and  $Y$ ” [27] where  $X$  may be the equivalent of  $H_s$  and  $Y$  of  $T_z$ .

The paper further investigates the assumption that a maximum parametric value is produced by the maximum sea state and thus proposes that the maximum may occur in a sea state other than the maximum. As a result the introduction of an uncertainty factor in order to account for the occurrence of such a phenomenon is investigated. This uncertainty factor allows for inflation (extrapolation) of the contour lines in order to obtain desired return periods. As a result of this investigation the question arises as to the appropriate range for the omission factor; the author suggests a range of “.05 - .25 and most often from .10 to .20” [27] when using the approach outlined in the paper. Winterstein [16] further investigates trends between 100-year contour lines and indicates that an increased decay rate with respect to probability is indicative that the location requires a smaller load factor. Winterstein [16] presents the example of the Gulf of Mexico’s decay rate (lower) versus that of the North Sea (higher) inferring that the more concentrated density of the North Sea points toward a more reliable design case. This trend may prove disruptive to the investigations of variation in contour lines methods when

comparing different locational parameters. A statement regarding IFORM method is also of interest with respect to the function and possible trends of the contour line method: “...the writers believe this 100-year FORM contour provides a useful tool for extreme load estimation, *increasingly accurate as the return period increases*” [16]. Winterstein [16] progresses to investigate the ratios of simulation and contour based vessel responses and compares them for two platform types, Tension Leg Platform (TLP) and a Spar. Winterstein utilizes the isoline response (iso-response) to display this relationship effectively as shown in Figure 1-1.

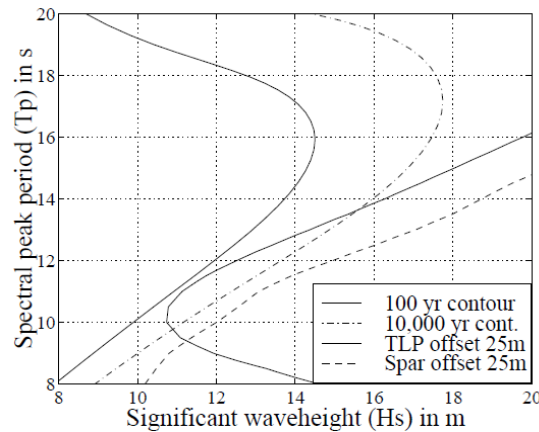


**Figure 1-1 – “Figure 1:  $H_s - T_p$  contours and TLP/Spar iso-response lines” [16]**

Upon his investigation, Winterstein finds that, in the case of the TLP, case-specific multipliers (particularly surge motion) are not preserved adequately if a Gaussian model is applied. This observation may require investigation of the contour line type’s variance between vessel types. The paper also reiterates the primary assumption, previously mentioned in Environmental Contour Lines: A Method for Estimating Long Term Extremes by a Short Term Analysis [28], that the true limit state function is linearized within the U-space.

Haver [29] identifies the primary advantage of the generation of contour lines as being their ability to produce long term extremes from a short term sample. The use of other methods of sample probability for long term extremes requires a large number of categorized short term conditions. As a result the paper labels these systems as ‘inconvenient’ and implies that they are limited by their dependence on time domain analyses and model testing. The paper also queries the issue that contour lines accuracy is dependent on the adequacy of how the sample accounts for short term variability. The other two methods provided for comparison of their ease of use with respect to long term extreme response analysis are the All Sea States approach and the Random Storms approach. The All Sea States approach utilizes step functions to predict long term extremes and analyses ‘all sea states’ thus logging data inclusive of minimums. On the other hand, the Random Storms method assumes equal probability of storms occurring and analyses the maximums that occur within the storm data set. Both of these methods may be convenient for short term analyses, however, for long term specific load cases a large amount of testing and data acquisition is required. The FORM and IFORM Methods are also addressed in regards to their transformations of probability density functions in both the U-space and back to the physical parameter space. The IFORM method is referred, “The main idea of this method is that we know the probability of exceedance and that we aim for the corresponding response level” [29].

Bitner-Gregersen [30] proposes a method of combining the probability functions of environmental parameters inclusive of their directional properties in the hopes of producing a directional probabilistic description of combined seas. Standard probability functions are omnidirectional i.e. they do not take into account the directional components of the parameters.

Quantiles are investigated by Haver and Winterstein [28] as they attempt to identify sources of randomness within the long term methods of sea-state prediction. Haver compares the environmental contour line method with these long term methods and produces quantile ranges between the extreme sea state parameters. Haver also identifies that, “...the only approximation is the FORM Linearization of the failure boundary” [28]. Figure 1-2 illustrates the failure boundaries, the design point (intersection) and the contour associated with the design point (circle). The  $u_2$  variable from the Rosenblatt transformation to the U-space has been omitted from the figure due to its randomness (the  $u_2$  variable is the transformed value of the probability of a peak period occurring with respect to the wave height). This linearization is inferred to be the cause of quantile variation.

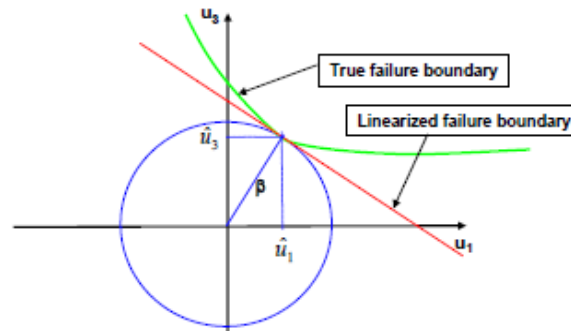


**Figure 1-2 – FORM Linearization of Failure Boundary in U-Space [28]**

Ruichao [31] investigates multiple methods of long-term extreme structure responses including the All Sea States approach, the Peak-over Threshold method and Contour lines (FORM). The author identifies the contour line as the most commonly used method for long term statistical analysis of sea states due to its simple to develop requirement of a short term response analysis. Other methods become convoluted and inefficient for such long term requirements as they require full long term response analyses. Again, short term variability of the response of contour lines is addressed and a percentile of 85 – 95% is recommended for the compensation of its randomness. It is suggested that, for the estimation of extreme response, the focus in terms of model fit should be upon the upper tail of the response distribution.

A comparative study of the two prominent environmental contour line generation methods, IFORM and CPD, is performed by Armstrong [32]. The study includes case studies of three locations (West Shetlands, North Atlantic and World Wide) as well as two vessel types including an FPSO and Semisubmersible platform. The study identifies sensitivities of the contour lines to long period ranges; with the most extreme differences between the responses found to be in the order of 7.0% for 100 year return period response and 9.0% for 10 year return periods. In addition to these differences, uncertainties in the responses would arise when vessel response isolines interacted tangentially to the contour lines. The study highlighted the inconsistencies and uncertainties that affect these surface models and recommended that these significant differences be taken into account during the design process.

An example of an application of surface models is presented by Baarholm [33] whose work involved the application of q-probability contour lines to estimate the responses of a flexible riser in a lazy wave configuration. The system was of non-linear nature and therefore required detailed time domain analysis rather than frequency. Baarholm [33] employs 40 strategically distributed sea-states determined by the contour lines with known q-probabilities. The FEM system is then subjected to these 40 sea-states for a 3-hour time period. From these FEM time domain analyses, Gumbel parameters are drawn to form the distribution that is later used for prediction of the extreme values of the responses.

### 1.3 OBJECTIVES

Current riser analysis methods are secondary to the floating and mooring systems, thus a more robust and global method that may directly associate the riser's extreme responses to metocean datasets is required. In order to develop such methods, the following research questions provided objectives that defined the thesis scope of work:

1. What are the statistical properties of the critical responses that govern the design of a flexible riser system (tension, curvature)? How the non-linearity of the riser system (geometrical, structural, hydrodynamic non-linearity) is reflected in the statistical properties of these critical responses?
  - a. What types of the probability distributions are applicable to modelling stochastic processes of flexible riser responses?
  - b. How to determine the maximum riser response and to estimate its variability in a stationary sea state of a given duration (e.g. from 0.5 to 3.0 hours), based on the time domain or frequency domain simulations?
  - c. How to determine the maximum riser response and to estimate its variability in a storm which consists of several stationary sea states?
2. What is typical correlation between the maximum riser responses and metocean parameters in a storm?
3. How the time domain and frequency domain analysis methods can be used for the probabilistic analysis of riser responses?
  - a. What is the applicability of frequency domain analysis methods for the prediction of extreme responses of flexible risers?
  - b. Are there any alternative (hybrid) analysis methods and what their limitations are, in terms of their accuracy to replicate a complete time-domain simulation?
  - c. How the demands for the computational resources compare between various analysis methods?

### 1.4 METHODOLOGY

The work undertaken in order to address the research questions was scheduled in 5 phases:

Phase 1: A literature review was performed to assess current analysis practices, standards and conceptual approaches to offshore system design with additional focus on the riser system.

Phase 2: An assessment of existing methods for design of floating systems, with emphasis on the methods for prediction of extreme motions and riser responses was performed in order to identify strengths, limitations and sensitivities that can be improved by applying a more advanced response based methods.

Phase 3: Investigation of the statistical properties of the riser responses including distributions of their stochastic processes and distributions of extreme riser responses within the short term (sea state) and medium term (storm) events.

Phase 4: Investigation into the uses and limitations of frequency domain spectral analysis in place of time domain based methods for developing the short term and medium term response distributions.

Phase 5: Investigation of alternative “hybrid” - time and frequency domain approaches, for the prediction of extreme riser responses and their distributions.

## 1.5 NOVEL ASPECTS

This work significantly expands on knowledge of the statistical properties of flexible risers and investigates both established and new conceptual analysis methods. This research contributes towards the development of an efficient methodology for the response based analysis in storms which is an entirely novel approach when applied to flexible riser design.

- A novel ‘exceedance’ environmental contour was compared against established CPD and IFORM methods. Three floating systems as well as a flexible riser system were investigated for the sensitivities of their extreme responses to the contour methods.
- A comprehensive statistical analysis of riser responses was performed with nine conventionally used probability distribution sand a Hermite moment model. The latter was proved an excellent universal model for a range of riser responses.
- Riser responses induced by wave frequency effects were compared between the time and frequency domain analysis methods. Thus, limitations of frequency domain simulations and the effect of linearization were identified for non-linear riser systems.
- Variability of riser responses were investigated for wave frequency (WF) and low frequency (LF) motions and their sensitivities to metocean parameters were identified and the contribution of LF motions to response variability was quantified. The distribution of the response in a storm was developed in the asymptotic form conditional on the storm MPM, which is an extension of the earlier work by Tromans and Vandersohuren [34],
- A novel approach to riser response analysis was conceptualized utilizing the FPSO turret excursion contours with frequency domain simulations performed at a number of waypoints on each contour.

## 1.6 THESIS STRUCTURE

The research is presented in the form of journal and conference papers whose findings contribute towards the development of a methodology for response based design of flexible riser systems. Each paper is presented as a chapter within the thesis as outlined below.

### 1.6.1 Chapter 1

Chapter 1 introduces the thesis subject and develops the research questions and objectives based on the established knowledge within the offshore industry. A glossary of offshore systems and their key design considerations are introduced whose understanding lays the foundation of the research methodology. Identification of the scope, its limitations and considerations are discussed.

### 1.6.2 Chapter 2

This paper focuses on the application of existing method of environmental contours for the prediction of design responses of floating systems and investigates their sensitivities and limitations. Two common types of contours describing the extreme Hs-Tp combinations, constant probability density (CPD) and inverse first order reliability method (IFORM), and a more novel exceedance contour are compared. The case studies included three locations for variation in the sea state

environment and three different offshore systems: a semisubmersible, Floating Storage Offloading (FSO) vessel and an FPSO. The turret moored FPSO with a flexible riser in a lazy-wave configuration was also investigated for the extreme riser tension and curvature at the hang off. The results provide insight into the sensitivity of the riser responses to contour methods. The case studies highlight the uncertainties that are inherent in the current design practices point to opportunities for their improvement.

#### 1.6.3 Chapter 3

Having identified the uncertainties and limitations of current practices, Chapter 3 follows by initializing the development of a more robust design process based on riser responses rather than metocean-centric data. In order to develop a statistically based design method for any system, the statistical properties of the system must first be understood. A comprehensive statistical analysis of riser responses was conducted in order to establish the “parent” distributions of the riser responses that governed the short term and medium extreme response predictions. This study tested suitability of nine standard distribution types as well as of a more novel Hermite moment method for modelling riser responses. Several goodness of fit tests and visual goodness of fit methods were used. The statistical properties of six riser responses were established for two case studies that included storms categorized as ‘benign’ ( $H_s \sim 7.5\text{m}$ ) and ‘severe’ ( $H_s \sim 15\text{m}$ ).

#### 1.6.4 Chapter 4

Chapter 4 expands on the method introduced in Chapter 10 with the inclusion of low frequency motions of the FPSO turret. The method proposed in this paper is the ‘ideal’ method where the probabilistic analysis of the riser responses is entirely time-domain based. The papers method and results provide a baseline to which more efficient processes may be compared. The asymptotic forms of the storm Cumulative Distribution Functions (CDF)s are generated; their parameters are computed and discussed for riser responses in two cyclonic storms, where excitation is caused by both wave and low frequency (slow drift) motions. Within the scope of this work, it was confirmed that the full time domain method was unfeasible to be used for several storms, as the process time for a single 86-hour storm was approximately one week, excluding pre-configuring of simulation files and post processing. A full RBA process will require hundreds to thousands of storms, effectively requiring years to complete the analysis at current computation rates.

#### 1.6.5 Chapter 5

Having identified processing time as a serious limitation to the feasibility of riser response based analysis, this paper sought to provide a comparison of the time and frequency domain methods. Given the non-Gaussian form of critical riser responses found in Chapter 3, use of a frequency domain solver that require linearization of the system mechanical properties presented a challenge to conserve the effects of these non-linearity’s on the prediction of extreme responses. Significant gains in the time efficiency of frequency domain simulations over time domain counterparts germinated the initiative to develop a hybrid method, which would employ both the time and frequency domain analyses.

#### 1.6.6 Chapter 6

Chapter 6 details hybrid time and frequency domain methods for the storm-based probabilistic analysis for riser responses. This chapter applies the knowledge founded throughout chapters 1 – 6 to the development of a time-efficient analysis method that would be possible to use in the response based analysis with multiple storms. One of the methods includes use of contour based turret excursion offsets inspired by environmental contours in Chapter 2. Several methods are discussed and compared starting from those that are more rigorous and potentially less time-efficient, and moving towards adopting additional simplifications which enable the computational efficiency to be further improved.

#### 1.6.7 Chapter 7

Conclusions of the thesis and an overall summary of the research project are presented in Chapter 7. These conclusions are a product of each individual chapter's findings and outcomes with emphasis on their implications to the stated research questions. The limitations of the work performed are also outlined and recommendations for future work are presented.

#### 1.6.8 Chapter 8

This is the reference chapter for the Thesis Document

#### 1.6.9 Chapter 9 – APPENDIX A

This chapter includes repeated or non-essential information that is referenced in chapters throughout the thesis.

#### 1.6.10 Chapter 10 – APPENDIX B

Progressing from the findings of riser response statistics in Chapter 3, Chapter 10 looks at short and medium term extreme response distributions caused by wave frequency motions of an FPSO system. This study provides insight into the contributions of the wave frequency motions to the predicted extreme storm response. The effect of variability on the storm distribution as well as the prediction of equivalent interval durations used for design metocean condition analyses is investigated. Asymptotic form of the storm response distributions is introduced. The work undertaken within this chapter also provided a key insight into the prohibitively long time taken by the time domain analysis of riser responses even for a single realistic storm.

This chapter was a preliminary study that lead to the findings presented in Chapter 4. For brevity of the main thesis body, it has been moved to this appendix.

#### 1.6.11 Chapter 11 – APPENDIX C

The paper presented in this chapter is a preliminary study on environmental contours performed prior to the PhD tenure. Its findings are referenced throughout the thesis, and so it has been included as an appendix.



Chapter 2 has been  
removed for copyright or  
proprietary reasons.

## Chapter 2

### INVESTIGATION INTO APPLICATION OF ENVIRONMENTAL CONTOURS FOR ANALYSIS OF FLOATING SYSTEMS

This conference paper has been peer-reviewed and accepted, and is to be presented at the ISOPE Pacific/Asia Offshore Mechanics Symposium in Jeju Island, South Korea. The citation for this conference paper is:

Armstrong, C., Drobyshevski, Y., Waterhouse, A., Chin, C., *Investigation Into Application of Environmental Contours for Analysis of Floating Systems*, PA18-139, ISOPE PACOMS 2018, Jeju Island, South Korea.

Chapter 3 has been  
removed for copyright or  
proprietary reasons.

### Chapter 3

#### COMPARATIVE STUDY ON PROBABILITY DISTRIBUTIONS OF RISER RESPONSES

This conference paper has been peer-reviewed and accepted, and is to be presented at the ISOPE Pacific/Asia Offshore Mechanics Symposium in Jeju Island, South Korea. The citation for this conference paper is:

Armstrong, C., Drobyshevski, Y., Dunn, C., Chin, C., *Comparative Study on Probability Distributions of Riser Responses*, PA18-140, ISOPE PACOMS 2018, Jeju Island, South Korea.

Chapter 4 has been  
removed for copyright or  
proprietary reasons.

#### Chapter 4

### PROBABILISTIC ANALYSIS OF EXTREME RISER RESPONSES FOR A WEATHER-VANING FPSO IN TROPICAL CYCLONES

This chapter has been accepted for publication in the Journal of Offshore Mechanics and Arctic Engineering. The citation for the journal article is:

Armstrong, C., Drobyshevski, Y., Chin, C., Penesis, I., *Probabilistic Analysis of Extreme Riser Responses for a Weather-Vaning FPSO in Tropical Cyclones*, Journal of Offshore Mechanics and Arctic Engineering, 2018, American Society of Mechanical Engineers

Chapter 5 has been  
removed for copyright or  
proprietary reasons.

## Chapter 5

### APPLICATION OF FREQUENCY DOMAIN METHODS FOR RESPONSE BASED ANALYSIS OF FLEXIBLE RISERS

This conference paper was presented at the 36<sup>th</sup> International Conference on Ocean, Offshore and Arctic Engineering in Trondheim, Norway. The citation for this conference paper is:

Armstrong, C., Drobyshevski, Y., Chin, C., *Application of Frequency Domain Methods for Response Based Analysis of Flexible Risers*, OMAE2017-61741, 36<sup>th</sup> International Conference on Ocean, Offshore and Arctic Engineering, June 25 – 30, 2017, Trondheim, Norway. DOI:10.1115/OMAE2017-61741

Chapter 6

METHODS FOR ANALYSIS OPTIMIZATION

## 6.1 Introduction

Previous studies have revealed that a full time domain analysis of riser responses for a large number of storms (100+ storm events) could exceed a year for simulation computation time alone. Therefore, the use of time domain simulations for a comprehensive response based analysis of a riser system is impractical with current software and standard hardware, and thus more efficient methods must be developed.

The key computational task of RBA method is the development of short term interval distributions of the maximum riser response. A traditional method for this task uses time domain analysis with a significantly large number of realizations (seeds) in order to obtain the maximum responses that build these distributions. Carrying out such multiple analyses turns out to be time prohibitive. Even though the computer speed and data storage technologies have been improving rapidly and the restrictions they place today may be relaxed in not far distant future, it is considered necessary to investigate more efficient analysis methods in order to significantly reduce the computational resources required for the response based analysis.

Methods that improve computational efficiency with minimum reduction in the accuracy of the short term EVD of the riser responses, are investigated in this study. Three groups of methods have been considered:

1. Methods that enable the reduction of the quantity of time domain realizations (seeds) for the development of the short term response distribution whilst using the time domain approach;
2. Methods that replace full time domain solutions with more efficient frequency domain approaches; specifically, using the more efficient frequency domain approach to generate the response component which exhibits the highest variability (seed dependency);
3. Methods that use hybrid Time Domain (TD) and Frequency Domain (FD) approaches, which minimizes required number of simulations as well as replacing certain TD tasks with those achieved by FD solutions.

Naturally, the development of more computationally efficient methods went along the way of using a balance of time and frequency domain solvers for computing the WF and LF response components. The methods presented in this chapter were developed iteratively by comparing their results with the coupled time domain analysis presented in Chapter 4. Use of turret excursion envelopes (TEE)s generated using the LF turret offsets computed by time domain analysis and the superposition of WF riser responses computed by FD analysis provides a computationally efficient method for prediction of the total LF + WF riser responses. In addition, a hybrid method proposed by Low [8,9] that uses intermittent FD WF analyses at points specified by TD LF turret tracks is investigated.

Considerations of the computational efficiency were not limited to the TD/FD simulation efficiency alone as the analysis process involves many other factors that contribute to process time:

- Pre-processing time for generation of data files that initiate numerical simulations.
- Post-processing time associated with extraction of meaningful design related results from simulation files.
- Exposure to errors related to working with large-database associated with each method, and the required pre- and post/-processing, as well as data handling during the simulation processes.
- Data storage requirements and data transfer and handling constraints.

These considerations aid in the determination of advantages and disadvantages of potential approaches, and further lead to selecting the most promising method to progress into the full riser RBA processes.

## 6.2 General Formulation for Interval Response Distribution

The short term response distribution (distribution of the maximum response in each interval) can be represented as a product of extreme value distributions computed at a number of specific “waypoints” in the horizontal x-y plane. The waypoints discretise the x-y domain swept by the riser hang off location due to the horizontal excursion of the vessel. The extreme value response distribution over Interval  $\tau$  is given by Equations 6-1 – 6-8.

$$F_i(R) = \prod_{k=1}^m F_K(R); \quad (6-1)$$

$$K = \text{number of way point intervals}; k = 1, 2, \dots, m \quad (6-2)$$

$$F_K(R) = \exp\{-\nu_Z \cdot \Delta t\}; \quad (6-3)$$

$F_K$  is the probability of the response maximum value  $e$  to be  $< R$  when the riser hang off point is in the vicinity of the way point  $k$

$$\Delta t = \tau / m \quad (6-4)$$

$$\nu_Z^{(K)} \equiv \text{mean upcrossing rate of the response level, } R \quad (6-5)$$

$$Z = R \text{ during interval } \Delta t \quad (6-6)$$

$$\nu_Z^{(K)} = \nu_Z(t = t_K); \quad (6-7)$$

$$t_k = \text{middle of } \Delta t_K \quad (6-8)$$

It should be noted that Equation (6-3) is generally applicable to the EVD of the response over the full interval duration, where it would describe the global response extrema. Several formulations for the response up-crossing rate at the interval level are described in Chapter 4.

In Equation (6-1), the same EVD format is applied to a number of sub-intervals, where the up-crossing rate takes the corresponding “local value” associated with each way point. The implied assumption is that the response extrema in these sub-intervals centered upon the way-points are independent from each other. In the following sections, the attention is focused on the methods for computing the crossing rate as a function of the response level.

## 6.3 Reduction of the number of time domain realizations

Methods of this group aim at utilizing additional information from each time domain response realization, not only a single global maximum, and using it efficiently for generating the short term response distribution. This can be achieved by different approaches.

One approach relies on the transformation of the response process into a normal Gaussian or other standard stochastic process, which enables a more comprehensive description of the original process to be obtained. The Hermite moment

model developed by Winterstein [65] transforms the original response into a Gaussian process and uses four distribution moments to approximately generate all properties of the response distribution by using the same properties of the Gaussian process. The up-crossing rate (Equation 7-5) can be described by an analytical expression involving the distribution moments. This method was described and tested in Chapter 3, and it is recommended to be investigated further. Tentatively, it may be expected that the use of first four distribution moments should enable at least a four-fold reduction in the number of time domain simulations thereby providing a significant improvement in the analysis efficiency.

Another approach relies on utilizing several or all response peaks within a single time domain realization, which are fitted with an appropriate distribution model. This method enables the MPM response to be estimated from a single or a limited number of realizations. With application to mooring responses, such method was developed and tested by Stanisic et al [66,67], and shown to provide good accuracy for the prediction of MPM responses of extreme mooring tensions and offsets of a weathervaning vessel.

A method based on a two-parameter Weibull fitting to local peaks is also available within OrcaFlex software [38]; this method was tested within a scope of extreme responses investigation in Chapter 2. Initial predictions of the MPM extreme riser responses by this method based on a single simulation produced results of considerable scatter. This limited study indicated that the subject method may have limited advantage for application to flexible riser responses. This may be attributed to stronger non-linearity of such responses compared with mooring tensions, although more in-depth studies are warranted to examine it further.

#### 6.4 Hybrid LF + WF Method

A hybrid time/frequency domain approach for efficient coupled analysis of vessel/mooring and riser dynamics was proposed by Low [8,9]. This method simulates LF motions of the floating vessel/mooring system in the time domain while performing WF analyses in the frequency domain at intervals along the LF turret movement track. This method has been shown to closely match fully coupled time domain responses.

For the investigation of the hybrid method's ability to accurately model extreme riser responses, riser responses were modeled in OrcaFlex using Ariane LF x, y positions and headings. Every 36s a position and heading were extracted at which point a FD analysis was performed to obtain WF-driven responses. This produces 50 FD simulations per TD turret track; a sample track is presented in Figure 6-1.

The process for combining the LF and WF responses is described below along with the required assumptions.

##### Notations

$$\begin{array}{ll} x_1 = WF \text{ Response} & \dot{x}_1 = \text{Time derivative of WF response (rate of change)} \\ x_2 = LF \text{ Response} & \dot{x}_2 = \text{Time derivative of LF response (rate of change)} \end{array}$$

##### Assumptions



1. LF response is assumed to be slow, such that values  $x_2(t)$ ,  $\dot{x}_2(t)$  are regarded as constant values over the duration of each “waypoint interval”  $\Delta t$ . Here  $\Delta t = \tau/m$ ;  $m \equiv$  number of points discretizing the time history of the turret motion in the horizontal plane.
2. WF response is Gaussian, with its amplitudes following Rayleigh law

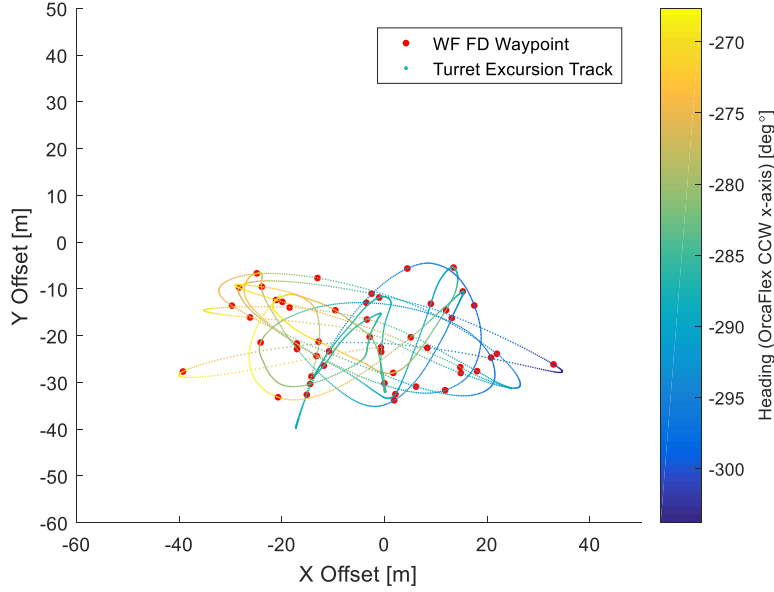


**Figure 6-1: Storm 2, Interval 76, Seed 1 Turret Track with WF FD Waypoints Distributed at 36s Intervals**

The calculation of the up-crossing rate  $\nu_z$  for use in the hybrid LF+WF method follows the method developed by Low [8,9]. The up-crossing rate is described by the following equations:

$$\nu_z = \frac{1}{2\pi} \frac{\sigma_{\dot{x}_1}}{\sigma_{x_1}} \exp \left[ -\frac{1}{2} \left( \frac{z - x_2(t)}{\sigma_{x_1}} \right)^2 \right] \cdot g \left( \dot{x}_2; \sigma_{\dot{x}_1} \right) \quad (6-9)$$

The function  $g$  accounts for the relative velocities of the LF and WF response components:

$$g \left( \dot{x}_2(t); \sigma_{\dot{x}_1} \right) = e^{-\frac{1}{2}y(t)^2} + \sqrt{\frac{\pi}{2}} y(t) \left[ 1 + \operatorname{erf} \left( \frac{y(t)}{\sqrt{2}} \right) \right] \quad (6-10)$$

Here the error function is defined as follows:

$$\operatorname{erf}(y) = \frac{2}{\sqrt{\pi}} \int_0^y e^{-s^2} ds \quad (6-11)$$

$$y(t) = \frac{\dot{x}_2(t)}{\sigma_{\dot{x}_1}} \quad (6-12)$$

Because the LF response is assumed to be slowly changing, the relative rate  $y(t)$  is expected to be small. Therefore, the following approximations must be possible:

$$g \approx g(y=0) + g'_y(y=0) \cdot y(t) = 1.0 + g'_y \cdot y(t) \quad (6-13)$$

$$g'_{y=0} = e^{-\frac{y^2}{2}} \left( -\frac{2y}{2} \right) + \sqrt{\frac{\pi}{2}} \left( 1 + \operatorname{erf} \left( \frac{y}{\sqrt{2}} \right) \right) + \sqrt{\frac{\pi}{2}} y \cdot \frac{2}{\sqrt{\pi}} e^{-y^2} = \sqrt{\frac{\pi}{2}} \quad (6-14)$$

As first approximation, for the very slow LF process:

$$g \left( x_2; \sigma_{x_1} \right) \approx 1.0 \quad (6-15)$$

Substituting the above expressions into the equation for  $F_K(R)$ :

$$F_K(R) = \exp \left\{ -\frac{\Delta t}{\tau_0} \cdot g(y_K) \cdot \exp \left[ -\frac{(R - x_2(t_K))^2}{2\sigma_{x_{1K}}^2} \right] \right\} \quad (6-16)$$

Here, the zero up-crossing period of the WF response:

$$\tau_0 = 2\pi \frac{\sigma_{x_{1K}}}{\sigma_{\dot{x}_{1K}}} \quad (6-17)$$

Consider calculation of the response MPM over a sub-interval associated with a particular way point. Invoking Equation (6-16), using notations:

$$n = \frac{\Delta t}{\tau_0}; D_1 = \sigma_{1K}^2 \quad (6-18)$$

and assuming  $g(y_K) = 1.0$ , one gets:

$$F(R) = \exp \{ n \cdot Q(R) \} \quad (6-19)$$

$$Q(R) = \exp \left[ -\frac{(R - x_2)^2}{2D_1} \right] = \exp [-a(R)] \quad (6-20)$$

The MPM value of the EVD ( $R_0$ ) is defined by the condition,

$$\frac{d^2 F}{dR^2}(R_0) = 0 \quad (6-21)$$

After differentiating Equation (6-19) and using Equation (6-21), the following equation can be obtained for the response MPM:

$$\exp \left[ -\frac{(R_0 - x_2)^2}{2D_1} \right] = \frac{1}{n} \left( 1 - \frac{D_1}{(R_0 - x_2)^2} \right) \quad (6-22)$$

Therefore,

$$R_0 = x_2 + \sqrt{2D_1 \left\{ \ln(n) - \ln \left[ 1 - \frac{D_1}{(R_0 - x_2)^2} \right] \right\}} \quad (6-23)$$

Equation (6-23) for the MPM value  $R_0$  must be solved by iterations.

Approximately, if  $D_1/(x - x_2)^2 \ll 1$  (or  $(x - x_2) \gg 0$ )

$$R_0 = x_2 + \sqrt{2D_1 \ln(n)} = x_2 + \sigma_1 \sqrt{2 \ln(n)} \quad (6-24)$$

This is the equivalent to adding MPM of response  $x_1$  to the low frequency (quasi-static) value of  $x_2$ .

## 6.5 Frequency Domain Method

The main feature of the hybrid method is the inclusion of the LF response component  $x_2$  as a slow varying response component, which can be considered quasi-statically. Another level of approximation is introduced if the LF response at each way point is replaced with the corresponding static response value. The remaining WF “dynamic” response component will be treated as a weakly non-linear process with approximately Gaussian properties. In this formulation, the way points are no longer related to a particular LF excursion of the hang off point (turret of the weathervaning vessel) but simply to its position within the turret excursion envelope (TEE).

### 6.5.1 Distribution of the Dynamic Response Component

For the “dynamic” WF responses component each local maximum is associated with a zero-up-crossing event. The maximum response in each up-crossing follows Rayleigh distribution  $F_m(R)$ , properties of which depend on the location of the riser hang off within the TEE. The short term distribution for the total interval can be presented as:

$$F_i(R) = [F(R)]^n \quad (6-25)$$

$$= \left[ \int_D F_m(R; x, y) \cdot p(x, y) dD \right]^n = \left[ 1 - \int_D Q_m(R) \cdot p(x, y) dD \right]^n \quad (6-26)$$

Here  $R$  is the dynamic response component with its local maxima following the Rayleigh law:

$$F_m(R) = 1 - e^{-\left(\frac{R^2}{2\sigma_R^2}\right)} \quad (6-27)$$

$$Q_m(R) = e^{-\left(\frac{R^2}{2\sigma_R^2}\right)} \quad (6-28)$$

In Equation (6-26), the product  $p(x, y) dD$  is the probability (or percentage time) of the turret being located in the vicinity of the way point with coordinates  $(x, y)$ , which takes into account the fact that for an arbitrary zero-up-crossing, the turret may be positioned anywhere within the TEE area.  $\sigma_R^2(x, y)$  denotes the variance of the response value when the turret is at point  $M(x, y) \in D$ , which can be estimated by the frequency domain analysis. The total number of response zero-up-crossings over the time interval  $\tau$ :

$$n = \tau / T_Z \quad (6-29)$$

Where the average zero-crossing period allows for contributions from all possible turret locations:

$$\overline{T_Z} = \left[ \int_D (T_Z(x, y))^{-1} \cdot p(x, y) dD \right]^{-1} \quad (6-30)$$

Here  $T_Z(x, y)$  is also a function of the vessel position within the TEE, which should be determined from time domain simulations.

The integral term in (7-26) is equivalent to the average response exceedance which accounts for motion of the turret in the horizontal plane. For large  $n \rightarrow \infty$ , approximately, it leads to the familiar expression for the short term distribution via the up-crossing rate (refer to Equation 7-31):

$$F_i(R) = \exp\{-Q(R) \cdot n\} = \exp\{-\nu_z \cdot \tau\} \quad (6-31)$$

Where

$$\nu_z = -\frac{Q(R)}{T_z} \quad (6-32)$$

$$Q(R) = \int_D \exp\left[-\left(\frac{R^2}{2\sigma_R^2(x, y)}\right)\right] \cdot p(x, y) dD \quad (6-33)$$

The integral in  $Q(R)$  can be discretised into a sum over m way points:

$$Q(R) \approx \sum_{K=1}^m \exp\left[-\frac{R^2}{2\sigma_R^2(x_K, y_K)}\right] \cdot p(x_K, y_K) \cdot \Delta D_K \quad (6-34)$$

Where  $\Delta D_K$  is the area of the turret envelope associated with waypoint  $K(x_K, y_K)$ . Waypoints  $K = 1, 2, 3, \dots, M$  must cover the whole area of the turret envelope:

$$\sum_{K=1}^m \Delta D_K = D \quad (6-35)$$

It is worth noting that the way-point specific number of zero-up-crossings is:

$$(p(x_K, y_K) \cdot \Delta D_K) \cdot n = n_K \quad (6-36)$$

Therefore, after using (7-49) and assuming the number of zero-up-crossings at each way point to be reasonably large, the short term response distribution (7-38) of the dynamic response component can also be written in the form:

$$F_i(R) = \exp \left\{ - \sum_{K=1}^m \exp \left[ - \frac{R^2}{2\sigma_R^2(x_K, y_K)} \right] \cdot n_K \right\} \quad (6-37)$$

### 6.5.2 Static Response Component

The static response, which represents the LF component of the total riser response, is determined by first solving for the static position of the riser when the turret is at position K prior to performing the dynamic analysis. As such, at each point K the static response values are different throughout the entire interval-defined TEE, whereas the dynamic response components are assumed not to depend directly on the respective static responses.

Therefore, before applying the integration in Equation (6-26) or summation in Equation (6-37) over all way-points, the respective static response component must be added form the total response value. Alternatively, this can be viewed as shifting the probability distribution for each way point by the corresponding static response value.

For convenience, a baseline static position of the vessel is defined, and all the outlying waypoints, K, have their static responses normalized with respect to this base static position. Naturally, the static position of the mooring system in ambient conditions, defined as (0, 0) was chosen as a basis for all intervals. A diagram of the waypoints, global static position and example TEE's is provided in Figure 6-2.

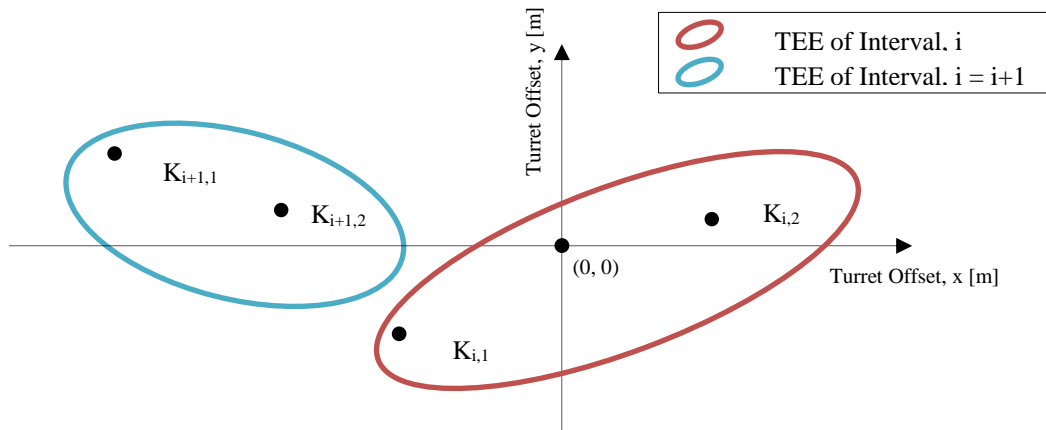


**Figure 6-2: Turret Excursion Envelope Examples With  $S_{0,0}$  and Waypoints,  $K_{x,x}$  for Two Intervals.**

At each waypoint, the turret offset would generate a unique static response  $S_K$ , therefore each dynamic response CDF must be shifted to include such response. A baseline static response at the origin  $S_{0,0}$  is subtracted to insure the common response origin is used for all way points and all intervals. A simple equation for the change in static response value at each waypoint is presented in Equation (6-38).

$$\Delta S_K = S_K - S_{0,0} \quad (6-38)$$

where,  $S_K$  = Static Response at Location K and  $S_{0,0}$  = Static Response at Origin Location.

To normalize the waypoint CDF, the addition of  $\Delta S_K$  is required. This process is presented in Figure 6-3.

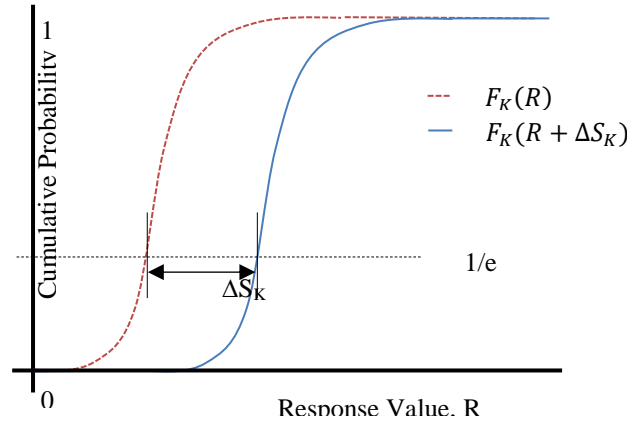


**Figure 6-3: Static Response Shift of Cumulative Probability Function for Waypoint, K**

The interval distribution function can be obtained using Equation (6-39). The probability distributions at each waypoint must be adjusted per the process shown in Figure 6-3 prior to any interval response distributions being defined.

$$F_{i(0,0)}(R) = \prod_{K=1}^m [F_K(R + \Delta S_K)] \quad (6-39)$$

All waypoint response distributions presented henceforth are inclusive of this static probability shift.

### 6.5.3 Turret Excursion Envelopes

A method of optimizing the RBA process is application of a frequency domain solver to waypoints situated about the turret excursion envelope (TEE). Firstly, the envelope is generated using time history offset tracks from the Ariane solver. Each track is representative of an individual simulation seed or realization. Three methods were investigated in order to define the TEE. The methods progressively become more complex, from a basic boundary trace to a multivariate distribution.

Figure 6-4 demonstrates the variation of offset maximums throughout the duration of a storm. To conduct RBA for an entire storm, the process that represents this range of offsets must be both flexible and robust while providing sufficient detail of each storm interval for analysis.

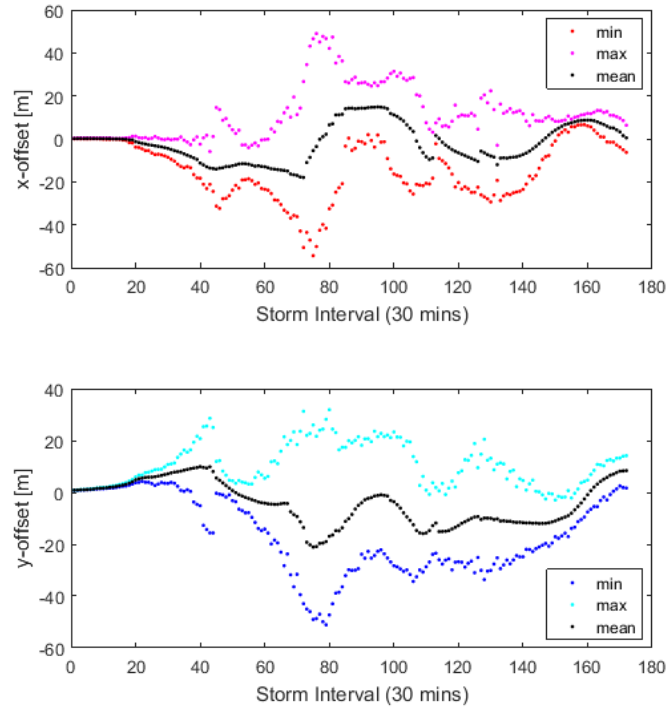


**Figure 6-4: Turret Excursion Maximums for Storm 2**

#### 6.5.3.1 Boundary Method

A rudimentary method of optimizing the RBA process is application of a frequency domain solver to waypoints situated on a turret offset envelope. The turret offset envelope is generated by applying a boundary function to all the turret excursion tracks. Once the envelope boundary is found, a user-defined number of waypoints are assigned upon this envelope; the example in Figure 6-5 has 10 waypoints shown as diamond markers.

The main assumption of this method is that the maximum riser responses will also occur at the maximum turret excursions. A limitation of this assumption is the inability to assign a probability to the maximum offset boundary and the associated uncertainty that a wave frequency motion maxima would align with these excursion maxima.

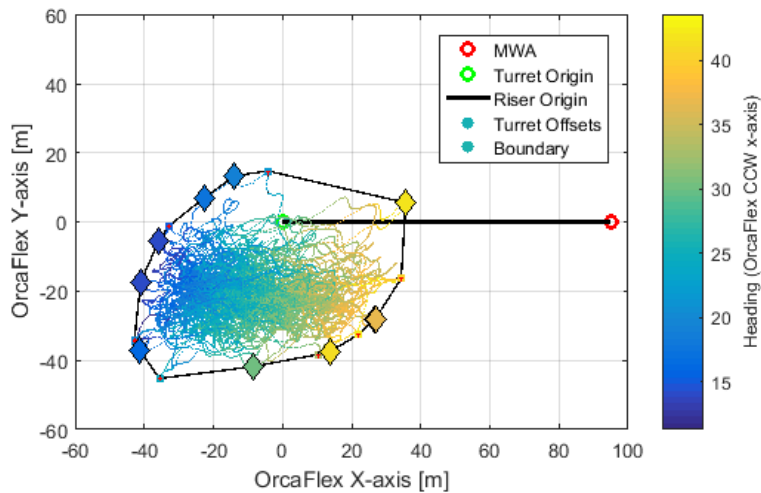


**Figure 6-5: Turret Time History Tracks, Envelope and FD Solver Waypoints**

### 6.5.3.2 Probability Density Method

Because the turret excursion tracks are subject to the global response of the system, certain excursions are less probable. Each interval has an oscillatory center where the turret has the highest probability of being located. Similarly, over the lifetime of the installation, the static position of the global system would be expected to be the most probable position of the turret. Because of this, application of a probability surface is possible. Once the surface is established, contours may be defined at certain constant probability density (CPD) levels. One immediate difficulty with any density based numerical method is the definition of bin sizes that are appropriate to the application. A further limitation of this method is the occurrence of ‘probability islands’ where contours of equal probability are not represented by a single perimeter. These ‘probability islands’ are also highly sensitive to bin sizing.

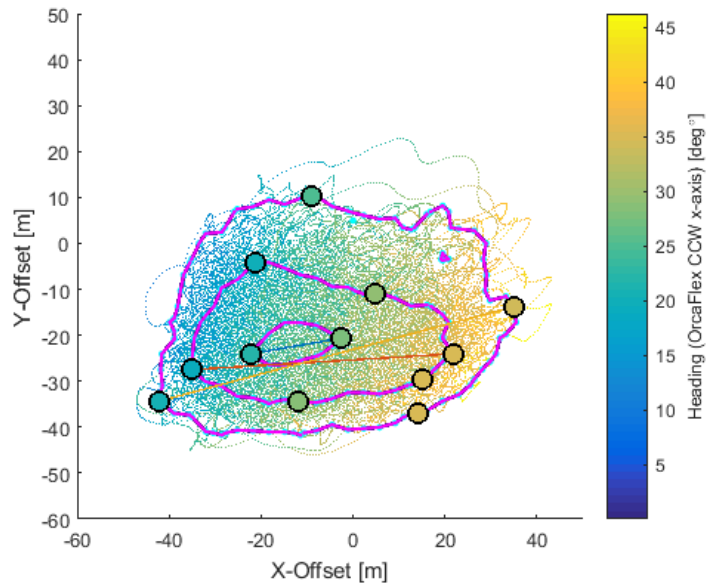


**Figure 6-6: Constant Probability Density Contours**

### 6.5.3.3 Bivariate Distribution Method

Bivariate distributions are surfaces defined by two separate distributions. If the mooring response, and concurrently the turret position is assumed to be a Gaussian process, a bivariate normal distribution based on x and y offsets may be produced using Equation (6-40).

$$p(x, y) = \frac{1}{2\pi\sigma_x\sigma_y} \frac{1}{\sqrt{1-\rho^2}} \exp \left[ -\frac{1}{2(1-\rho^2)} \left\{ \frac{(x-M_{0x})^2}{\sigma_x^2} + \frac{2\rho(x-M_{0x})(y-M_{0y})}{\sigma_x\sigma_y} + \frac{(y-M_{0y})^2}{\sigma_y^2} \right\} \right] \quad (6-40)$$

The surface that is produced when applying this bivariate normal distribution to 40 Ariane turret excursions is presented in Figure 6-7. Contours are shown as banding upon the surface and a small section of turret offset is visible on the right hand side of the extruded surface. The turret offsets that fall outside the surface plot are also seen in Figure 6-8, where a significant portion of extreme excursions are outliers at the top of the largest ellipse.



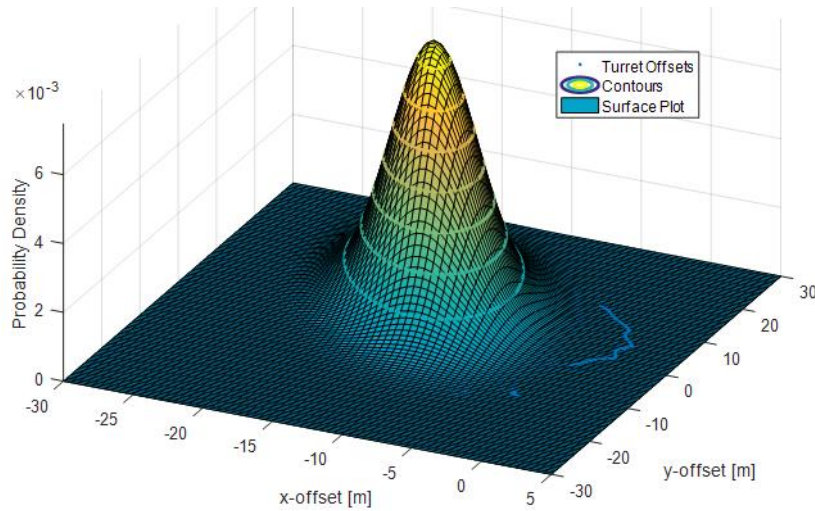


**Figure 6-7: Bivariate Normal Distribution of Turret Offset Tracks**

#### 6.5.4 Definition of Waypoints

##### 6.5.4.1 Probability Level Contours

As both CPD and the bivariate distribution methods are both surface models, contour levelling is available to define contour lines upon which waypoints may be defined. This method also allows for each waypoint to represent the probability of the vessels turret being at the location,  $K$ , which may further be used in definition of an intervals extreme value distribution (EVD). The question then arises of at what probability levels the contours should be defined.

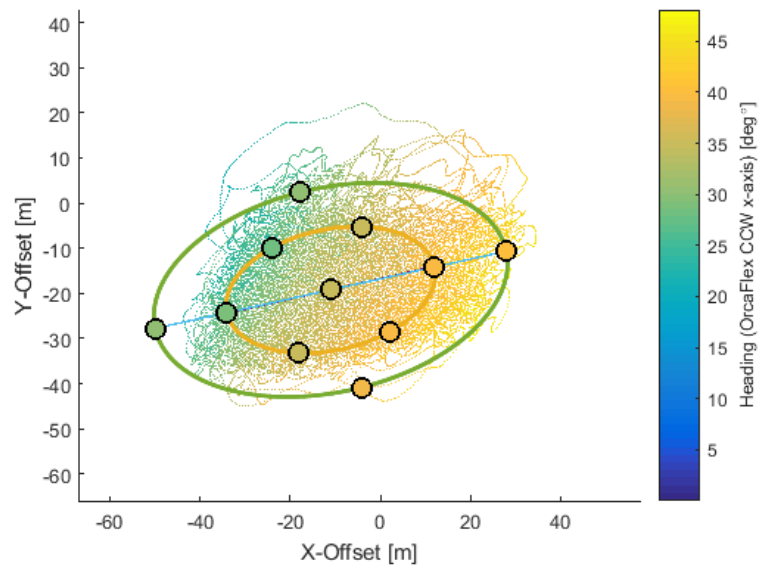


**Figure 6-8: Ellipsoidal Contours Generated by Bivariate Normal Distribution with Waypoints and Headings**

The definition of the contour levels for a bivariate normal distribution can result in an ellipse not encompassing significant amounts of excursion data (Figure 6-8 Top), whilst simultaneously predicting excursions in regions where no data is present (Figure 6-8 Left). This suggests that the Gaussian assumption of the turret offsets may oversimplify the problem. A significant benefit of the use of a bivariate normal distribution to represent the TEEs is the computational efficiency. In addition, the method does not suffer from ‘probability islands’ that are found in the probability density approach. An

improvement to this method may be inclusion of better representative distributions of the x and y excursions for the global system. The question of how to include the probabilities that each waypoint is representative of must also be addressed; this is discussed further in the following sections.

#### 6.5.4.2 TEE Mesh

Geometrical meshing is frequently used in various applications to provide numerical models with a method of distributing point-based nodes (or waypoints) in a manner that best represents geometrical shapes. Meshing involves convergence of optimized geometries within a larger geometrical boundary. For the distribution of waypoints within the TEE a Delaunay triangulation mesh was used; the Delaunay triangulation method maximizes the minimum angle of all the angles of the triangles that the mesh is composed of [68]. Definition of an approximate ideal triangle size also allows for large TEEs to have a larger number of representative waypoints, allowing for more ‘severe’ intervals within the storm to be analysed with greater resolution. Inversely, small TEEs, in more benign stages of the storm, are meshed with fewer triangles due to the defined triangle size. Therefore, these TEEs require less computational resources allocated to them, increasing overall efficiency of the process. The limitation of this method lies in the computation time for convergence of the mesh. The elliptic geometry of a bivariate normal distribution contour is generally straight-forward in solving; however, cases arise where the ellipse is significantly elongated along one of its axes. These cases can cause meshing to fail due to acute angles within the Delaunay triangles which may then inhibit convergence. Conditional requirements of elliptic elongation may be coded into the process that may override node positioning, however, further unforeseen issues may arise in significantly larger metocean datasets.

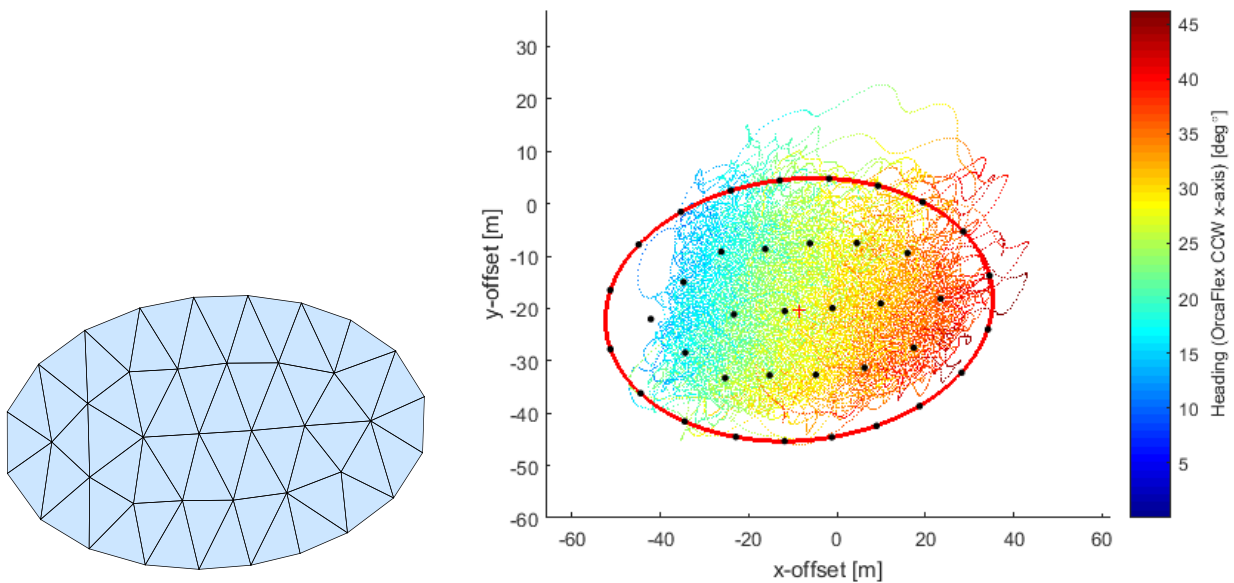


**Figure 6-9: Delaunay Triangles (LEFT) and Corresponding Waypoints Overlaid on Turret Tracks (RIGHT)**

#### 6.5.4.3 Polar Coordinate Generated Waypoints

To separate the TEE into representative areas, use of polar coordinates to define areas is a more analytical method than meshing, as it does not require distribution of polygonal shapes within a curved perimeter. The process detailed in APPENDICES Section 9.3 allows for definition of polar coordinates and their associated areas. After obtaining the polar coordinates of the waypoints, the base ellipse must be rotated and offset to re-associate it with the global x-y coordinate system as is presented in Figure 6-10.

The equation of a rotated and center shifted ellipse is presented in Equation 7-60.

$$\frac{(x-h)\cos(\varphi)+(y-k)\sin(\varphi)}{a^2} + \frac{(x-h)\sin(\varphi)+(y-k)\cos(\varphi)}{b^2} = 1 \quad (6-41)$$

where,  $h$  = ellipse centre on  $x$  axis,  $k$  = ellipse centre on  $y$  axis, and  $\varphi$  = ellipse rotation.

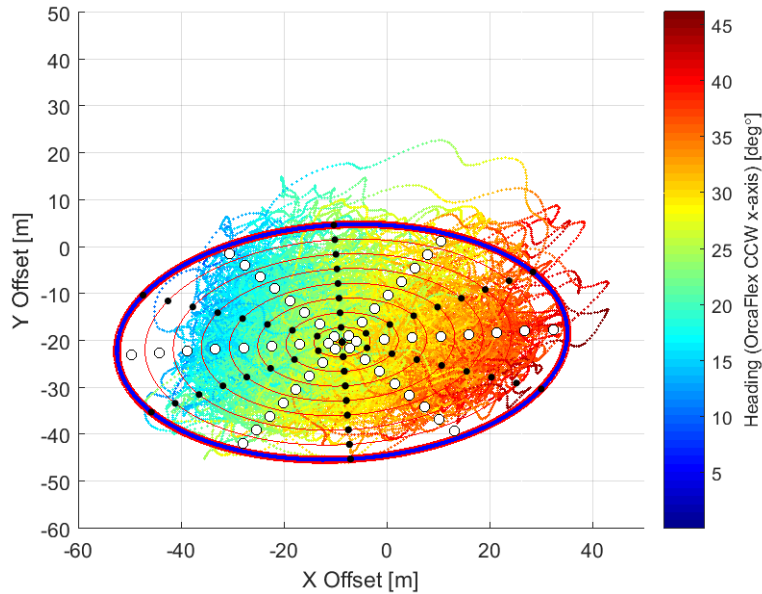


**Figure 6-10: Polar Coordinate Generated Waypoints (White Marker) with Associated Radii and Angles**

#### 6.5.4.4 Use of Dynamic Response Isoline

In addition to randomly generated waypoint methods, the use of response isolines to estimate the location at which a maximum response within a TEE is possible. For this method, a simple grid must be defined within the extents of the TEE. At each grid point, a FD simulation is run to obtain a point specific MPM. An interpolated surface model built from the grid is then used to define response isolines. Overlaying the extents of a TEE upon the isolines then allows for a maximum response location to be identified. At this location, further TD or FD simulations may be performed in order to obtain a TEE MPM response. This could potentially be used to generate catalogues of riser response isolines that are dependent on various metocean combinations. A comprehensive catalogue could then be used as a reference for extracting WF response components that could be added to the LF turret tracks in a separate process, therefore reducing the number of unique FD WF analyses that must be generated per turret track or TEE.

#### 6.5.5 Waypoint Heading Definition

Heading sensitivity of each waypoint was accounted for using the recommended practice proposed by API [69]; this involves taking three headings per waypoint, including the mean heading of the time history and  $\pm 2$  standard deviations from this mean. In addition, headings obtained from closest point averages were investigated to see if these more accurately predicted the LF+WF responses. As the turret heave is a linear response, the heading sensitivities were investigated with the heave as a baseline. Definition of the vessel heading requires the conversion detailed in APPENDICS Section 9.4 for a sample-based average heading.

## 6.6 Case Studies

The details of the simulation models used for this study as well as the metocean datasets the models were exposed to have been provided in the following sections.

### 6.6.1 FPSO Vessel/Riser System (OrcaFlex)/Mooring System (ARIANE) Details

The properties of the gas export riser as well as the FPSO vessel are identical to those used in Chapter 2 – 6. The riser system used in this study was a 16-inch gas export riser in a Lazy Wave configuration. The total riser length is 350m. The water depth at the installation location was 180m. Six responses along the riser were selected for investigation. The locations of predicted responses and their static response values are provided in Table 6-1 and a diagram of the OrcaFlex Model is provided in Figure 6-11.

**Table 6-1: Responses and their Locations**

Response	[m] from End A	Static
Hang-off Tension [kN]	0.0	111.0
Curvature: Hang-off [rad/m]	3.5	0.031
Curvature: Wave [rad/m]	170	0.0369
Curvature: Sag Bend [rad/m]	125	0.0455
Declination: Hang-off [deg]	3.5	172.8
Turret Heave [m]	0.0	0.00

All responses are dynamic and so their respective static response was subtracted from the raw response data.

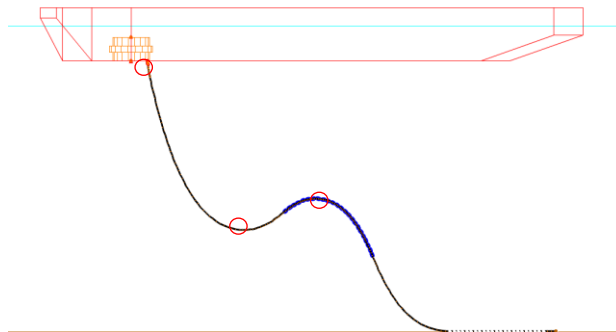


**Figure 6-11: OrcaFlex Riser Model (Red circles indicate locations of responses)**

The mooring system for this study was modeled in Ariane as a 16-line system in groupings of 4 lines. The software was used to generate the LF+WF vessel motion time histories. The mooring line properties are identical to those used in Chapter 4.

### 6.6.2 Metocean Data

The data used for this study included two cyclonic storms offshore Australia. The time histories of metocean parameters were produced by hind cast modelling using the database described in [4]. Each storm is discretized into 0.5 hour intervals, with stationary wind, wave and current magnitudes and directions defined as well as their respective wave JONSWAP spectrums. Storm 1 has an  $H_s$  maximum of approximately 7.5m and Storm 2 a maximum  $H_s$  of 15m, the intervals with these maximums were selected for the initial investigation. The metocean data components are shown in ANNEX C for Storm 1 and Storm 2 respectively. The heading angles of the metocean components are counted 'FROM' the direction.

## 6.7 Results and Discussion

### 6.7.1 Time Domain LF Responses

Isolated LF response components provide insight to where the FD TEE methods have shortcomings. The TD LF responses of the riser are computationally efficient, and so their inclusion is less prohibitive than a fully coupled LF+WF TD simulation for a riser system.

The curvature responses, most significantly the sag bend curvature in Figure 6-14, show that these responses are dominated by LF motions. This is observed when comparing the LF sag bend curvature to the fully coupled model shown in Figure 6-26. It also highlights the shortcomings of the proposed TEE methods and their limited effectiveness in capturing LF response contributions accurately. A method of combining or supplementing the TEE simulation responses with the LF TD responses may yield an analysis process that is computationally efficient and accurate.

Further insight provided by LF only simulations is that the LF turret offset can cause the quasi-static response to fall below the static response at position (0,0). This is very clear for the sag bend curvature response presented in Figure 6-14; the turret position causes the sag bend of the riser to be stretched rather than compressed, bringing the MPM below that of the static (0,0) positions curvature value for most of the storms duration.

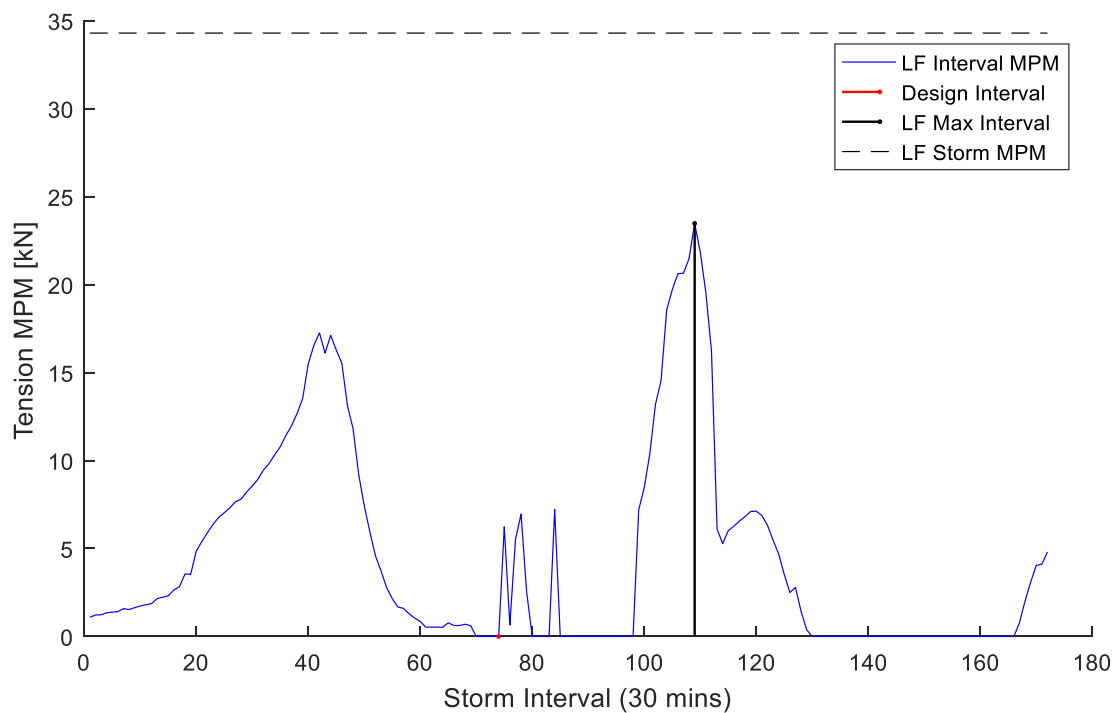


**Figure 6-12: Storm 2 LF Tension Response MPMs**

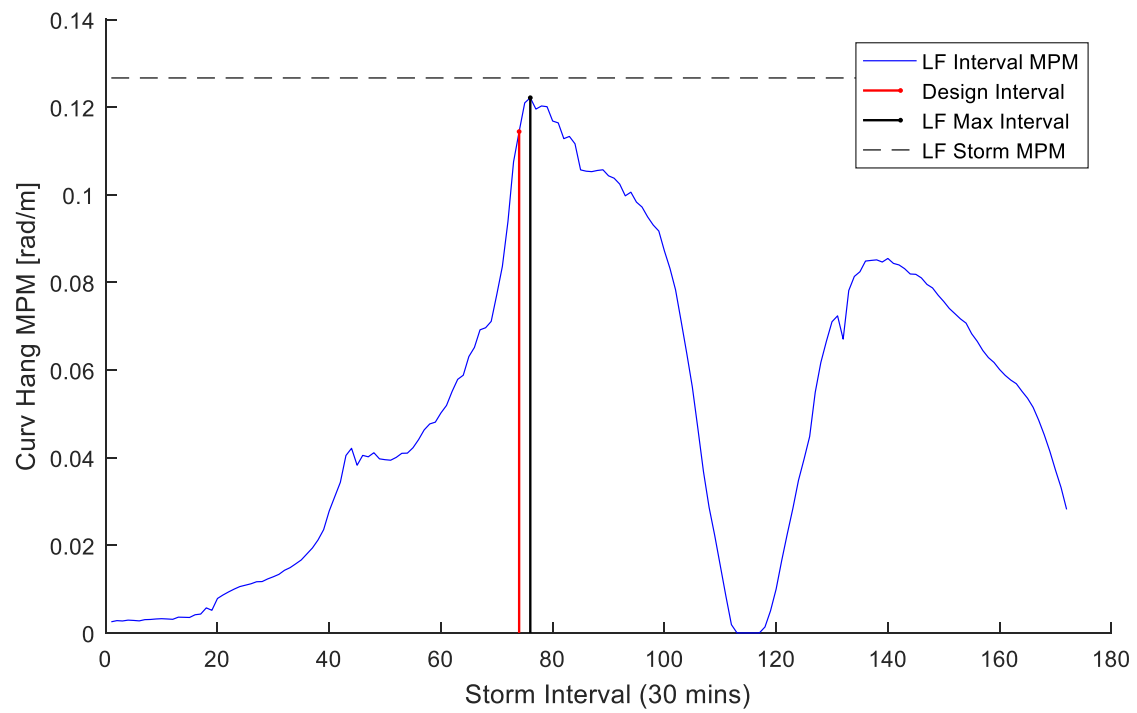


**Figure 6-13: Storm 2 LF Hang-off Curvature Response MPMs**

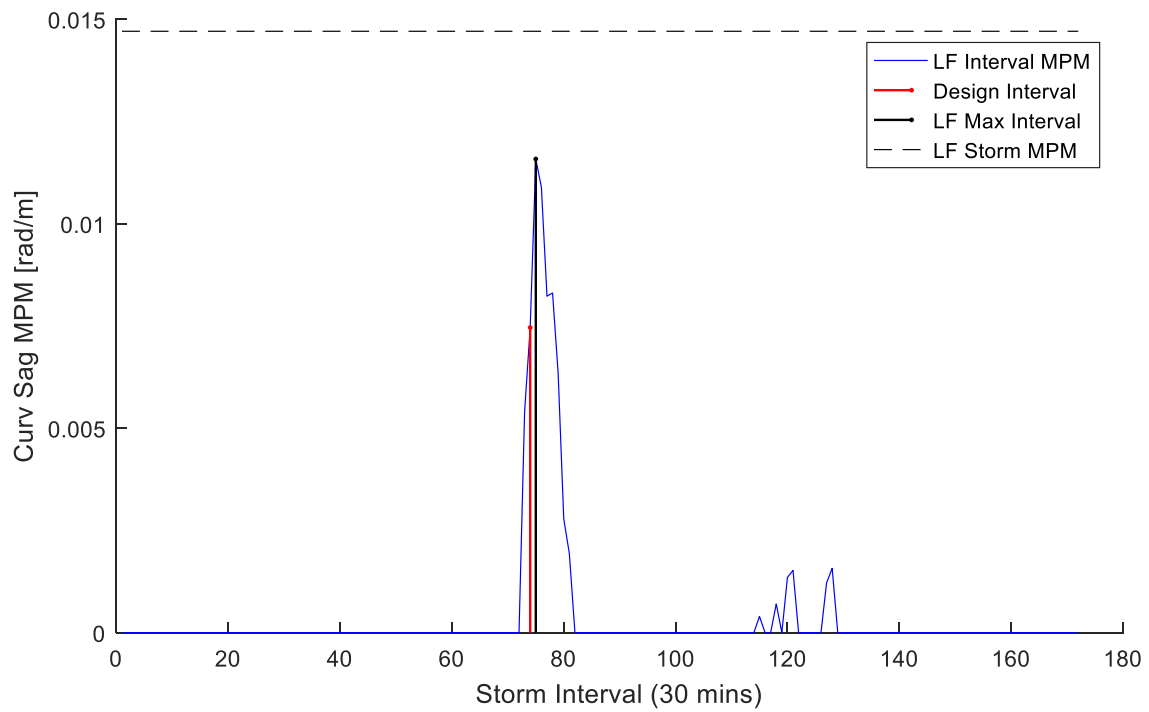


**Figure 6-14: Storm 2 LF Sag Bend Curvature Response MPMs**

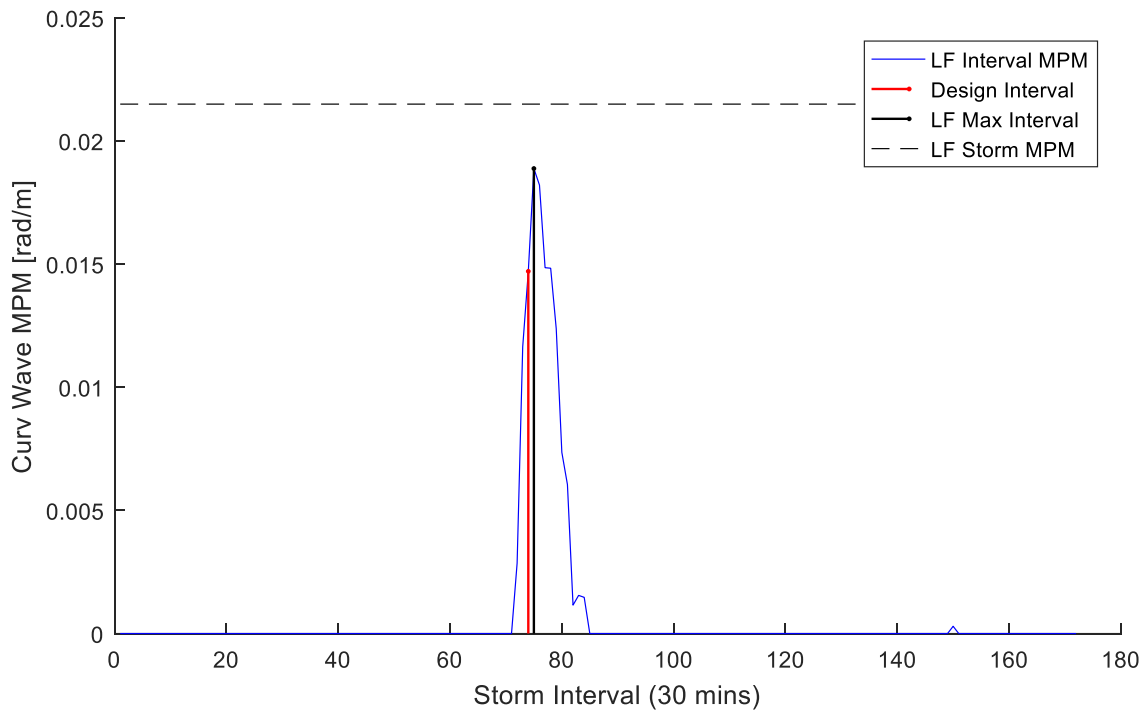


**Figure 6-15: Storm 2 LF Wave Curvature Response MPMs**

#### 6.7.2 Hybrid LF+WF Method

The Hybrid LF+WF method proposed by Low [8,9] provides a balance between the inefficient time domain and less accurate frequency domain methods. Figure 6-16 to Figure 6-20 show time histories generated using combinations of LF, WF, Time and Frequency domain solvers. The LF components shown include the static value of the riser response, whereas WF components are dynamic components only. The WF FD simulations have been fitted with a simple spline function to provide a general range for these values. The spline is also used to visualize the MPM region of WF responses about the LF time domain response.

The WF FD contribution to the sag bend curvature during Interval 76 is effectively zero as shown in Figure 6-19. This result further highlights the mismatch of peaks in Figure 6-26, where the TD response spike occurs at interval 76, but the FD polar coordinate TEE method reports an MPM of zero throughout the entire peak region.

For curvature responses, the amplitudes of the WF responses are smaller compared to those of the LF response amplitudes apart from the wave motion dominated hang-off curvature. However, the hang-off curvature's WF region does appear to be significantly inflated when compared to the complete TD LF+WF time history. This further suggests that the FD solver has difficulty predicting the magnitude of responses that are highly non-linear. For other responses, Turret Heave, Hang-off Tension sag bend and wave curvatures, the predicted range of responses ( $LF \pm WF$ ) appear to be quite accurate. In the case of the hang off curvature response presented in Figure 6-18, it can be observed that the LF response sits closely towards the base of the TD LF+WF response time history. This indicates that the WF motions of the hang-off curvature are only contributing to a positive increase of the response range, and subtraction of the WF responses is not appropriate for a response of this type.

The TD LF+WF responses shown are represented by a single realization (seed) and so consideration of the variability between seeds must be accounted for in interpretation of these results. The maximum magnitude of the time domain generated time histories' peaks are generally close to the predicted hybrid LF+WF ranges. Some peaks of the hybrid method also appear to be out of phase with the presented TD time history. A larger number of seeds may cause these time domain time history peaks to occur throughout the entire simulation duration, thus filling the hybrid LF+WF range. Further investigation of seed sample sizes and the discretization of LF and WF response contributions to time histories is needed for further development of the hybrid method.

Although this method is computationally faster for simulation times, there are other significant factors that reduce the feasibility of this method using existing software packages, particularly storage and number of required simulation files; further discussion and detail on computational efficiencies of the different methods studied are provided in Section 6.8, Summary and Conclusions.

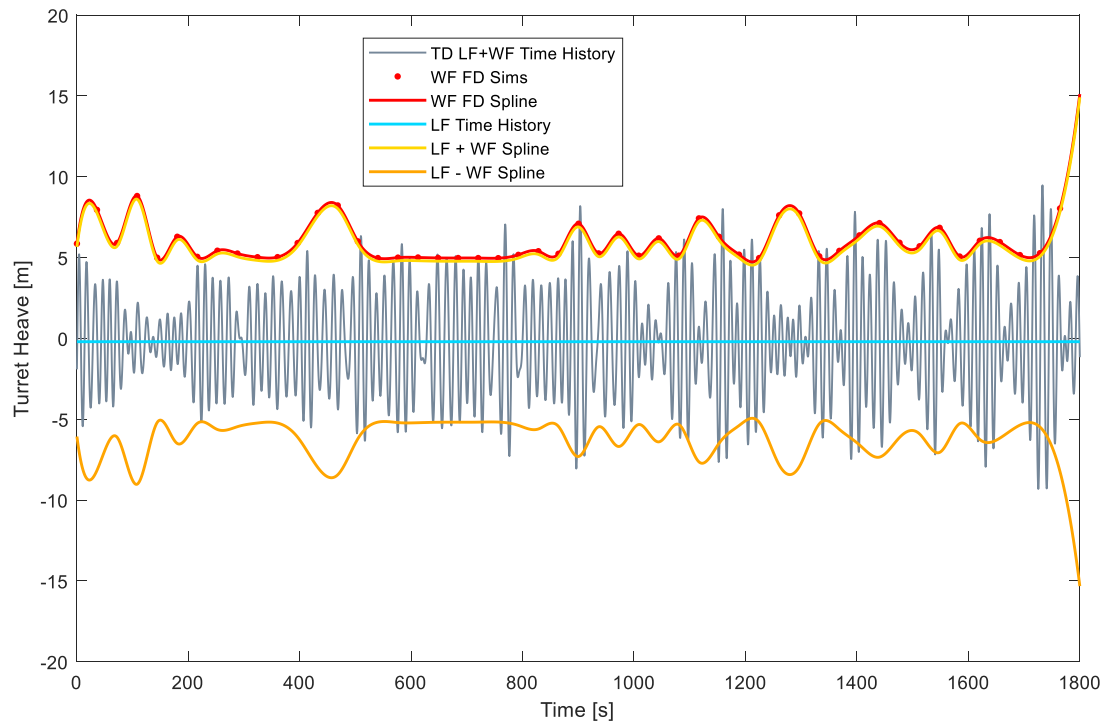


**Figure 6-16: Storm 2, Interval 76, Seed 1 LF and WF Components of Turret Heave Response**



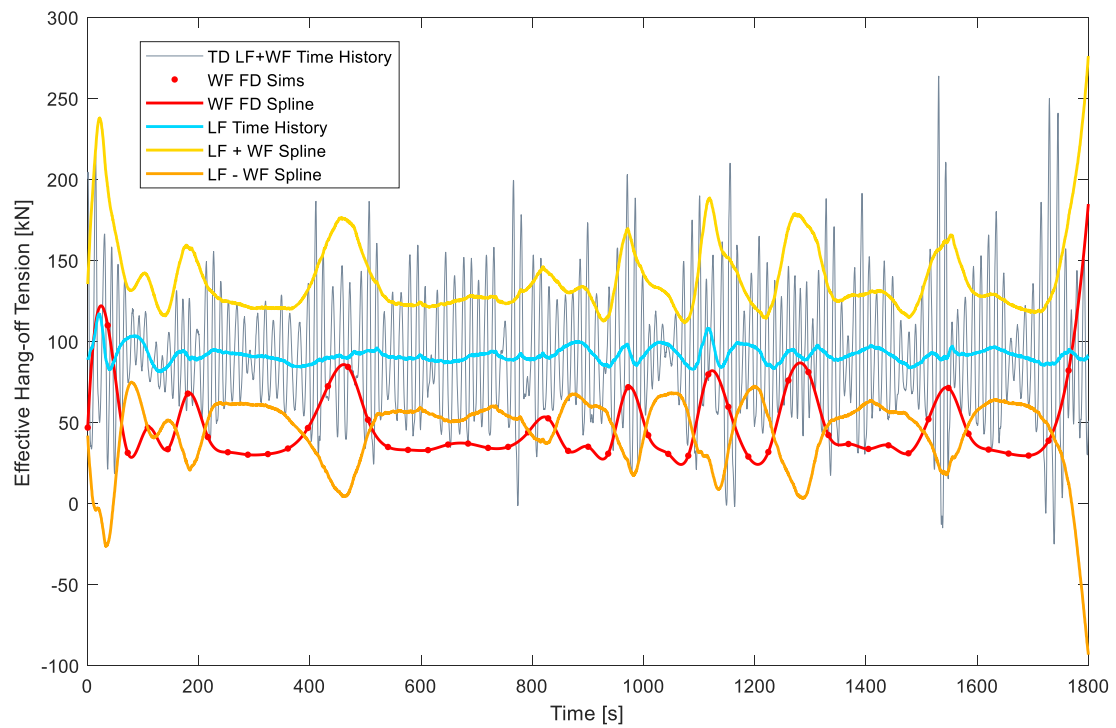


**Figure 6-17: Storm 2, Interval 76, Seed 1 LF and WF Components of Hang-off Tension Response**

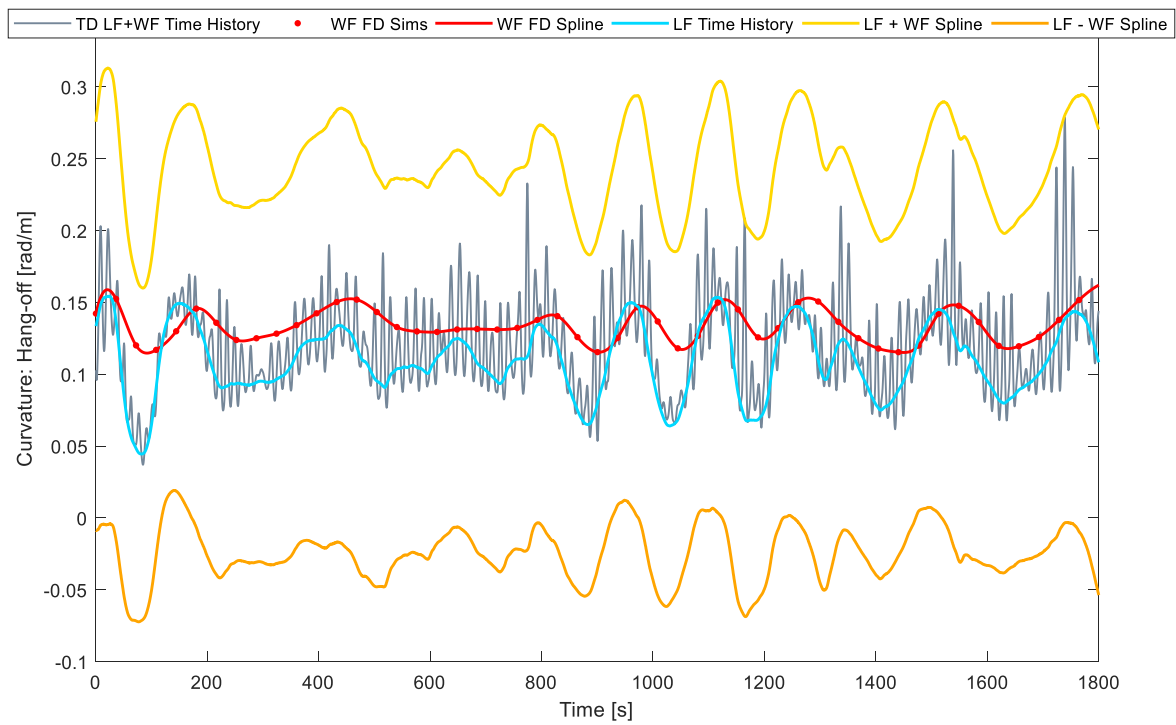


**Figure 6-18: Storm 2, Interval 76, Seed 1 LF and WF Components of Hang-off Curvature Response**

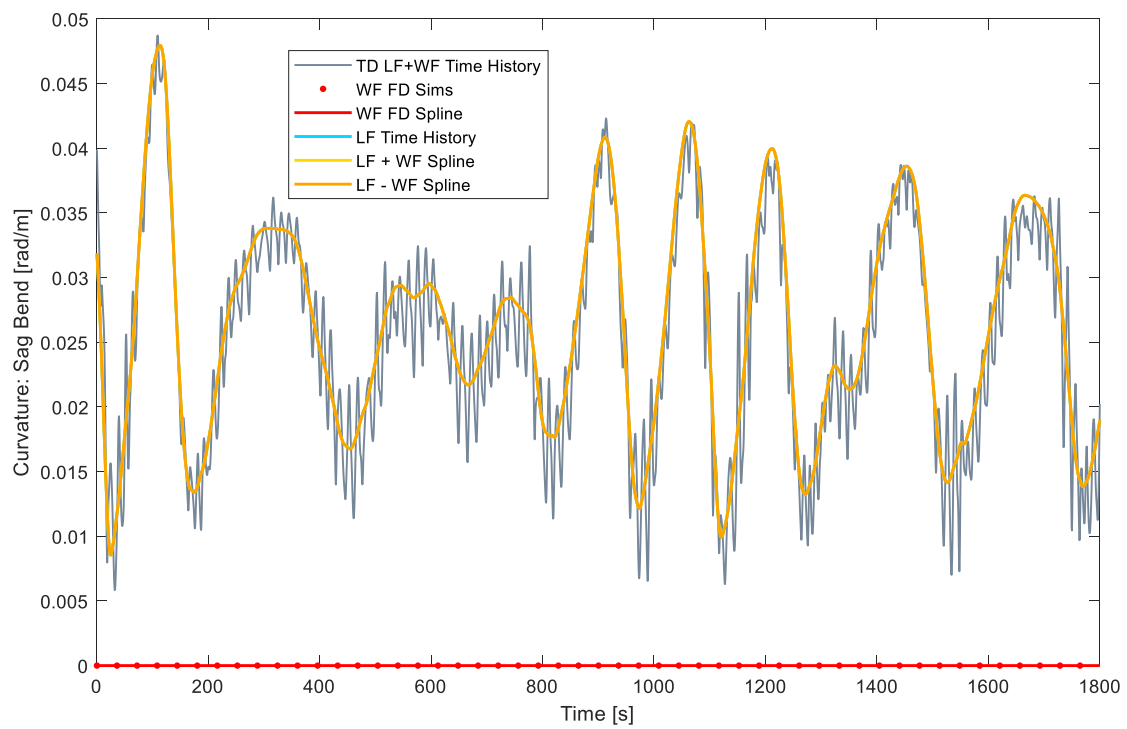


**Figure 6-19: Storm 2, Interval 76, Seed 1 LF and WF Components of Sag Bend Curvature Response**

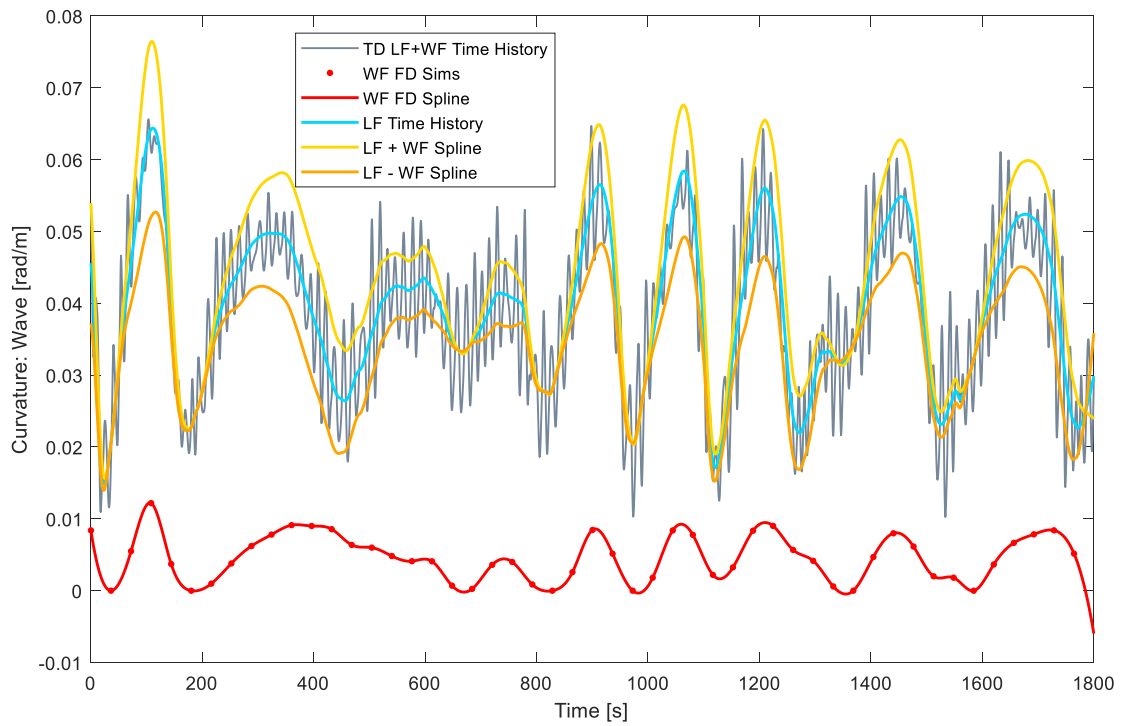


**Figure 6-20: Storm 2, Interval 76, Seed 1 LF and WF Components of Wave Curvature Response**

### 6.7.3 Polar Coordinate and Waypoint Heading Findings

The results shown in Figure 6-21 through to Figure 6-27 are generated using waypoints produced by the bivariate polar coordinate method described in Section 6.5.4.3. To check the validity of using the method described, checking the method's ability to model turret heave, a linear response independent of the riser, was investigated. The turret heave response was also used for the investigation of inclusion of waypoint headings whose method was detailed in section 6.5.3. The recommended API practice is the use of the mean vessel headings of the sampled turret excursion tracks, as well as two more cases including  $\pm 2$  standard deviations from the mean vessel heading. The results of using this API method are presented in Figure 6-21. The figure includes LF+WF response MPMs that were fully generated using time domain simulations; these are shown as the solid blue line in each figure. Ideally, the FD methods used would match the LF+WF TD simulation results, though with considerable efficiency gains.

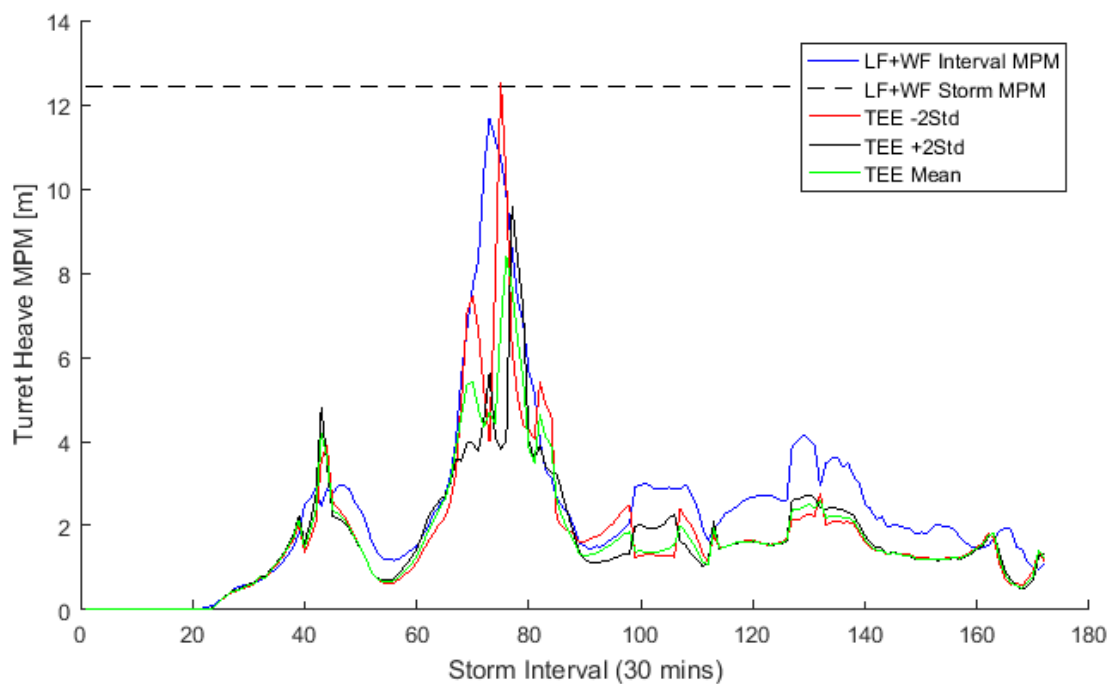


**Figure 6-21: Storm 2 Heave MPMs**

Another heading method used the average of a sample of headings that were extracted from the nearest turret track points. The nearest 2,000, 5,000, and 20,000 headings were used as sample sizes for this investigation. This method was based on observation of large TEEs that had more defined heading ranges in certain areas. In addition, the 20,000-sample case included two additional cases per waypoint that were  $\pm 2$  standard deviations from the mean vessel heading, like that of the API recommended practice. Figure 6-22 and Figure 6-23 present the sample size and hybrid 20k point/API methods. Figure 6-22 shows that there is little effect on the turret heave by the mean heading prediction being based on the sample size of headings near the waypoints. Figure 6-23 shows the merits of including  $\pm 2$  standard deviations of vessel headings for the 20,000-point sample size, as it shows the variation in response that may occur dependent on the vessels static heading in FD simulations. This is true of smaller samples sizes, though as was expected, the variation was reduced when taking a smaller sample closer to a single waypoint. The API practice accounts for the total variation within the TEE as its sample size includes all turret track data. For this reason, the API recommended practice was used in further investigation of other riser responses.

Observation of the difference between each FD method and the LF+WF TD results shows that, for turret heave, the method generally captures both the shape and magnitude of the response quite well. However, the turret heave is a relatively trivial response for a FD simulation and so investigation of other responses is more meaningful.

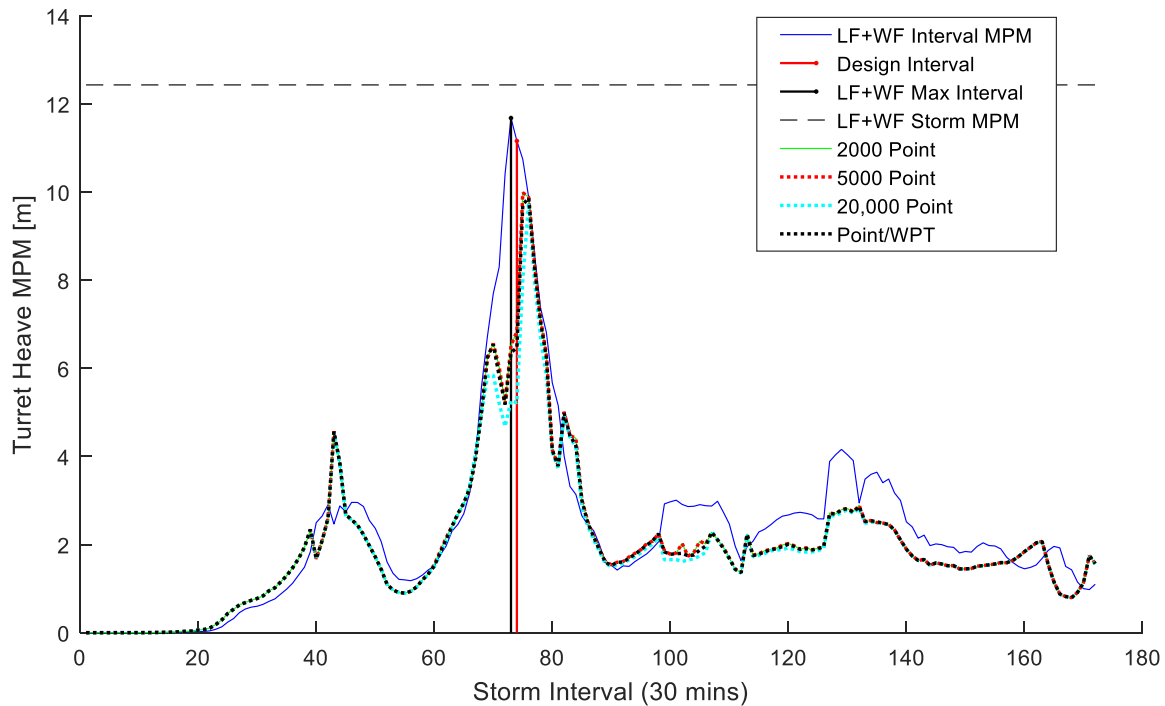


**Figure 6-22: Heading Sample Size Dependency for Storm 2 Turret Heave MPMs**

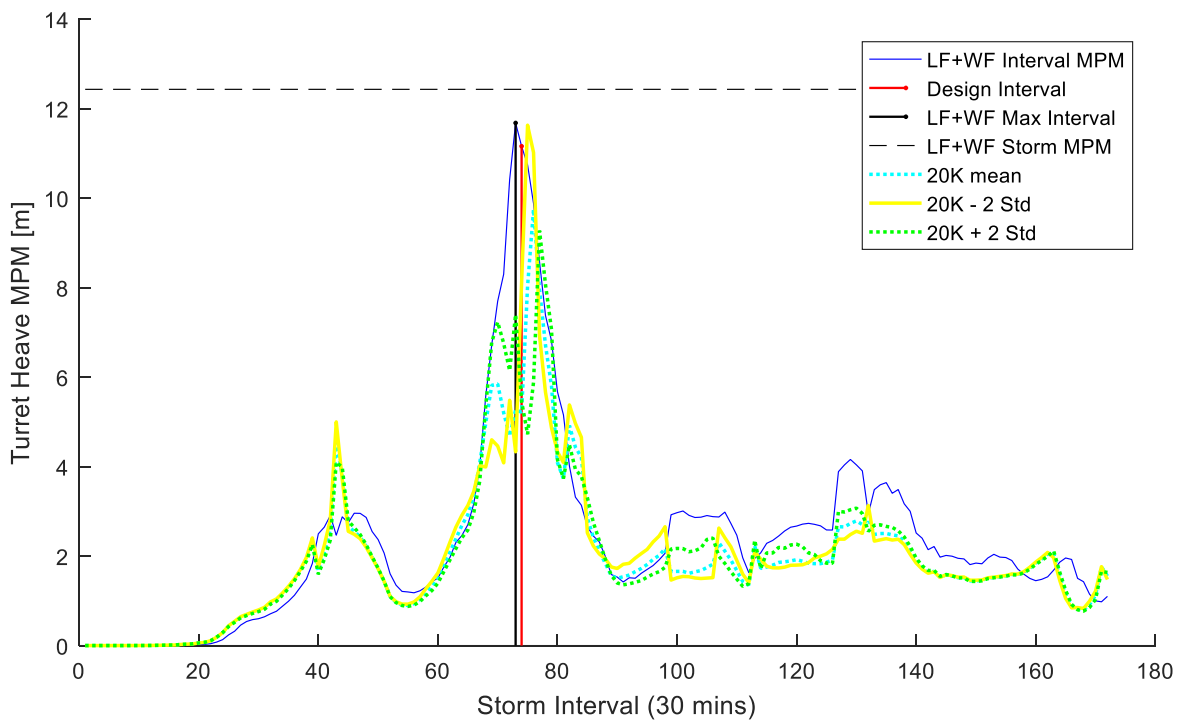


**Figure 6-23: 20K Point  $\pm$  2 Std. Dev. Heading for Storm 2 Turret Heave MPMs**

Additional riser responses are presented in Figure 6-24 through to Figure 6-27. The non-linearity and uncertainty of these responses makes their accurate prediction more difficult. The limitations of the frequency domain to account for current effects are accentuated in each of these responses. Particularly, the tension response, although largely dominated by wave-frequency motions, can be observed to be accurate in the earlier stages of the storm when there is little current effect, however in later stages the response is under-estimated during the intervals where wave height tapers off and current velocity increases.

Generally, those responses that are largely driven by wave frequency motions are well represented by this method. However, the curvature responses at locations along the riser that are more decoupled from the turret motion are less suited to representing the combined metocean effects required to model these responses. For the sag bend and wave crest curvature locations, there are erratic response predictions with little to no adherence to what was observed using LF+WF TD simulations.

Associating waypoint probabilities and their representative area significantly reduces the contribution of large turret excursion responses that are sensitive to large turret offsets. For most half hour intervals within the storm, the effect is reduced as the turret excursion envelopes are comparatively small compared to those of the extreme intervals. The less extreme excursions also have smaller ranges of responses, and because the average response is close to the extreme, the effect of probability weighting is less noticeable. The hang off curvature (Figure 6-25) is dominated by the wave frequency motions, so the reduction in hang-off curvature extremes is also minimal. On the other hand, riser tension is a maximum at far offsets, where probability weighting is lowest, thus resulting in the maximums between intervals ~65-85 being greatly reduced (Figure 6-24).

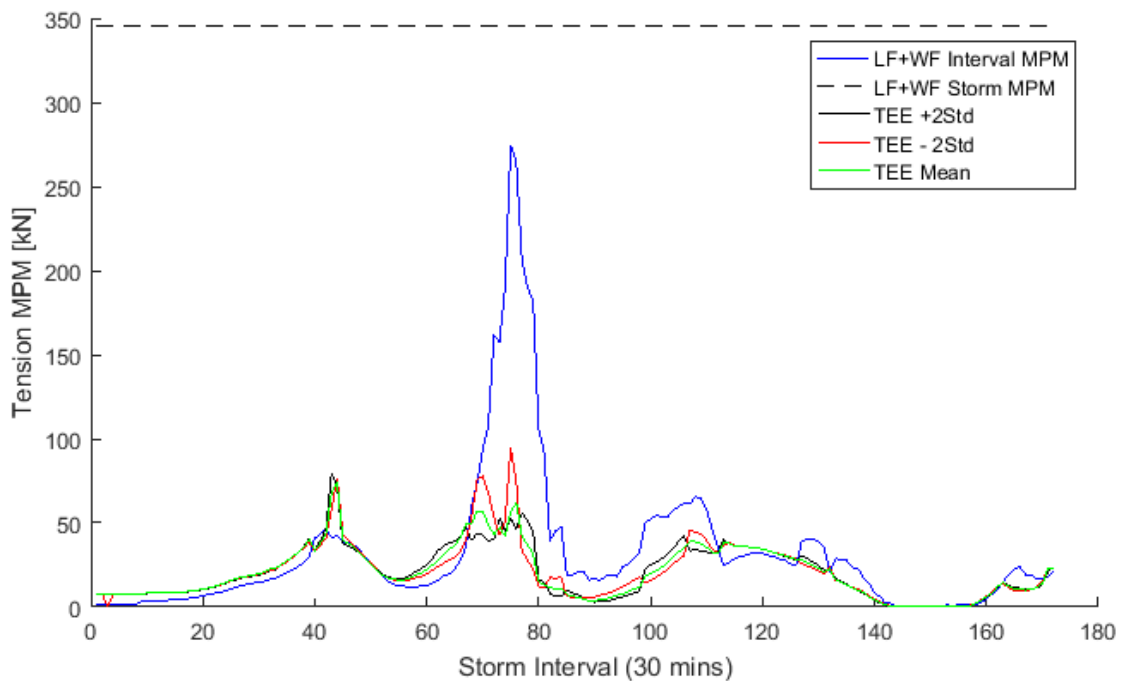


**Figure 6-24: Storm 2 Hang-off Tension MPMs**

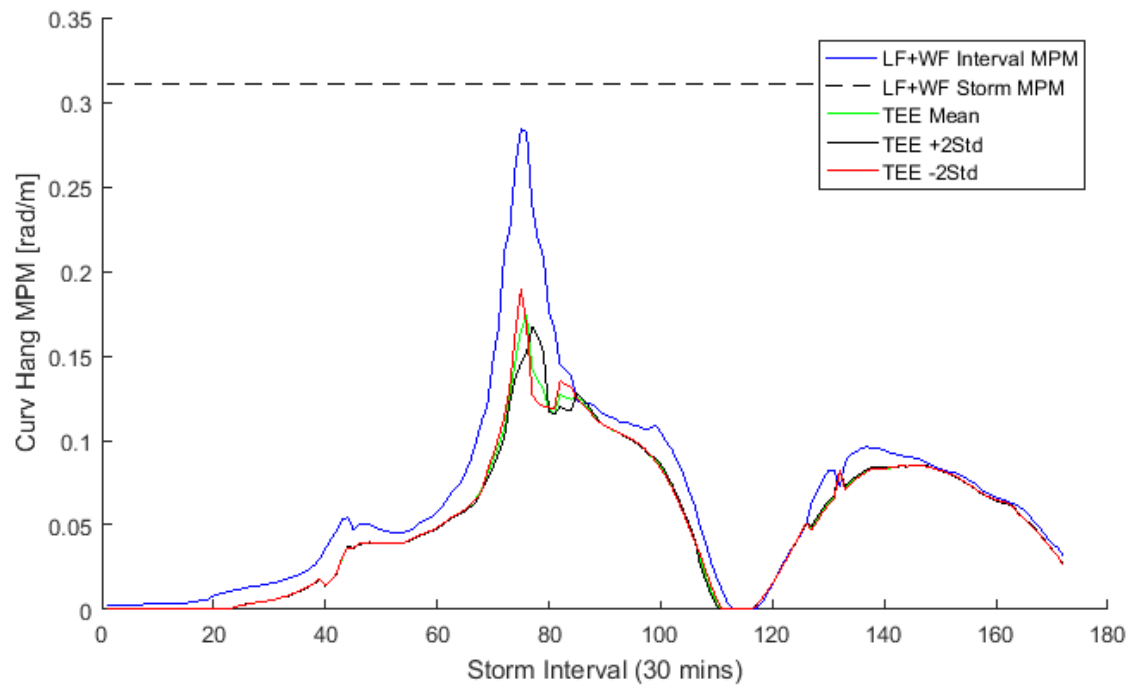


**Figure 6-25: Storm 2 Hang-off Curvature MPMs**

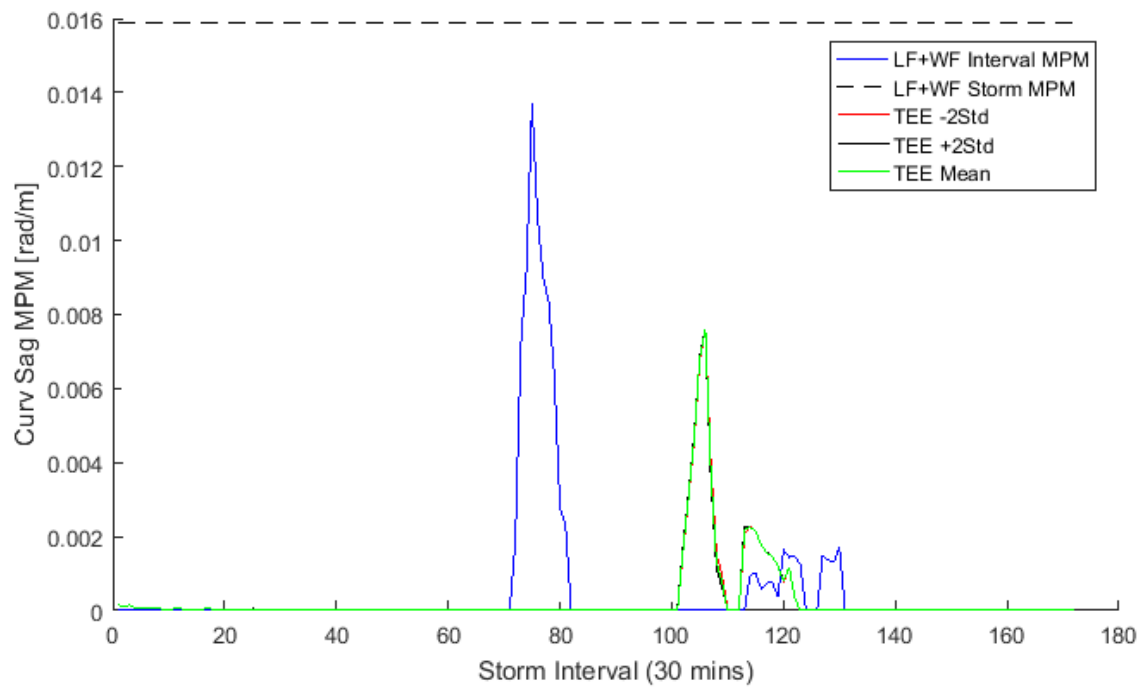


**Figure 6-26: Storm 2 Sag Bend Curvature MPMs**

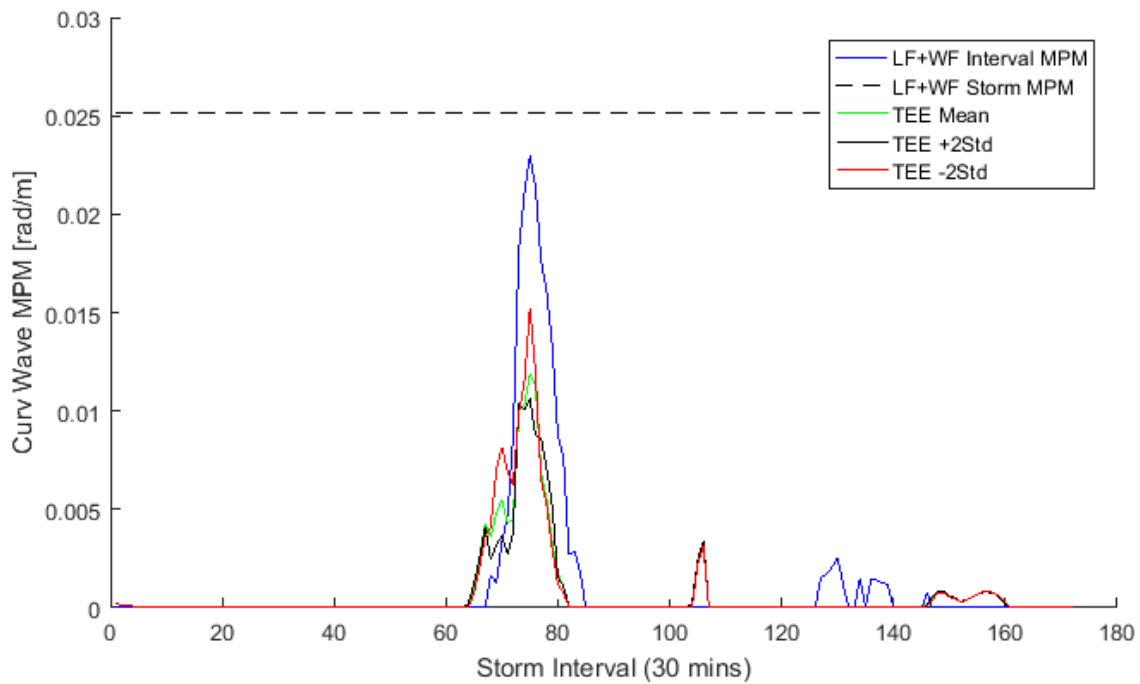


**Figure 6-27: Storm 2 Wave Curvature MPMs**

#### 6.7.4 Use of Response Isolines

The triangulation mesh provides the largest number of points within each of the contours; as such the results of this method provide insight into where the riser responses are largest within the TEE. Scatter plots of all waypoint FD MPM results are provided in Figure 6-36 through to Figure 6-35. The FD generated MPMs at each waypoint are produced with the assumption that the turret is at this location for a full half hour and no probability weighting is applied i.e. each waypoint has a probability of 1. The response magnitude is represented by the colour map shown in the right-hand colour bars. The data has been sorted to place the largest responses at the top/front of the graph. The storm interval that produces the largest response is also presented after the storms' collective scatter plots.

The general assumption is that the largest excursion will produce the largest response. Observation of each of the responses shows that this is loosely correct for individual interval TEEs; however, the maximums of some curvatures may occur at the extremities of smaller TEEs that contain metocean effects that the riser is sensitive to. For example, the sag bend and wave curvature TEEs in Figure 6-33 and Figure 6-35 are not the largest excursions of the storm. The curvature responses are also maximums when the turret is closer to the touchdown point (TDP) of the riser, rather than further, like the hang off tension response. The hang off curvature and turret heave responses are dominated by wave motions, though for the hang off curvature, the location of the turret does have some effect. When the riser is stretched and under greater tension, the hang off curvature begins to reduce as seen in the far left of Figure 6-31; the maximum occurs at an offset that is less taut, though still at a near extreme offset.

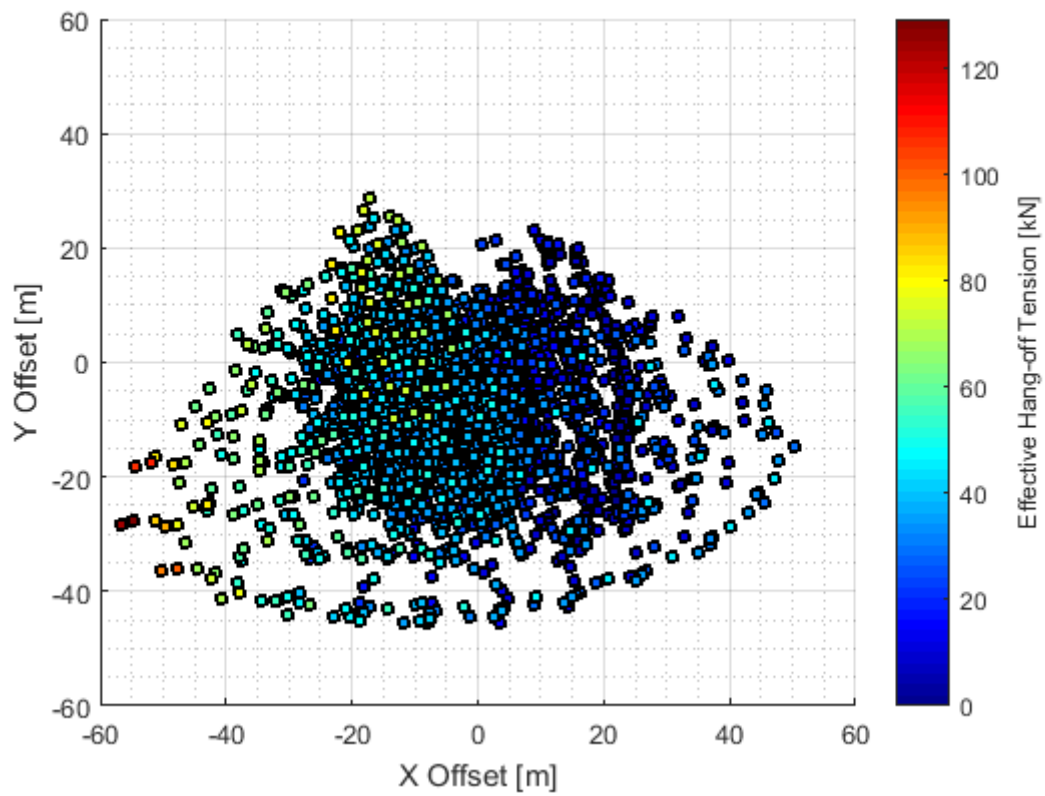


Figure 6-28: Effective Hang Off Tension FD Simulation MPMs Scatter

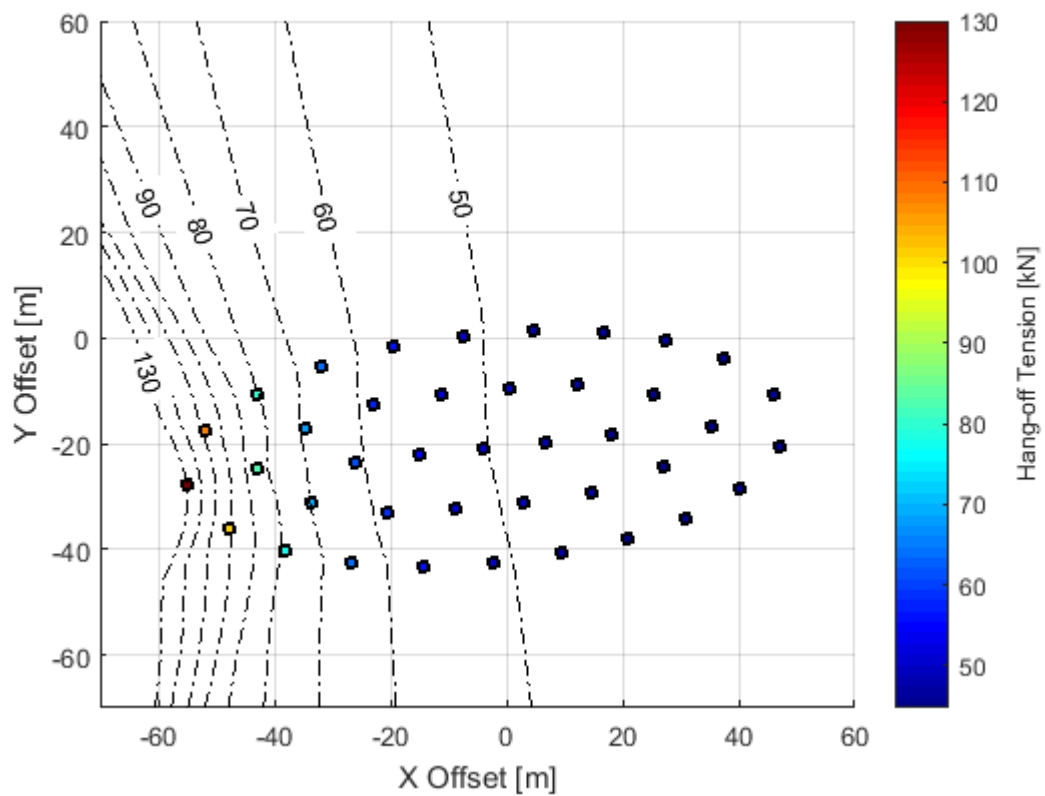


Figure 6-29: Effective Hang Off Tension Maximum Response Interval (76) Response Isolines



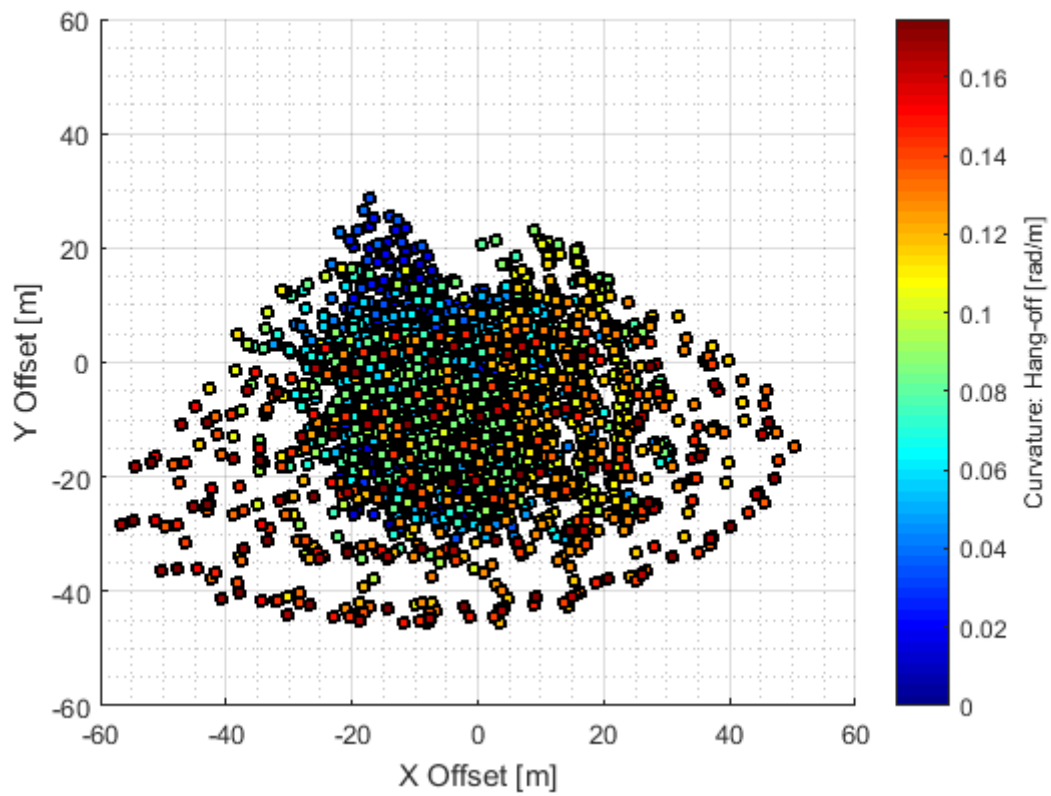


Figure 6-30: Hang Off Curvature FD Simulation MPMs Scatter

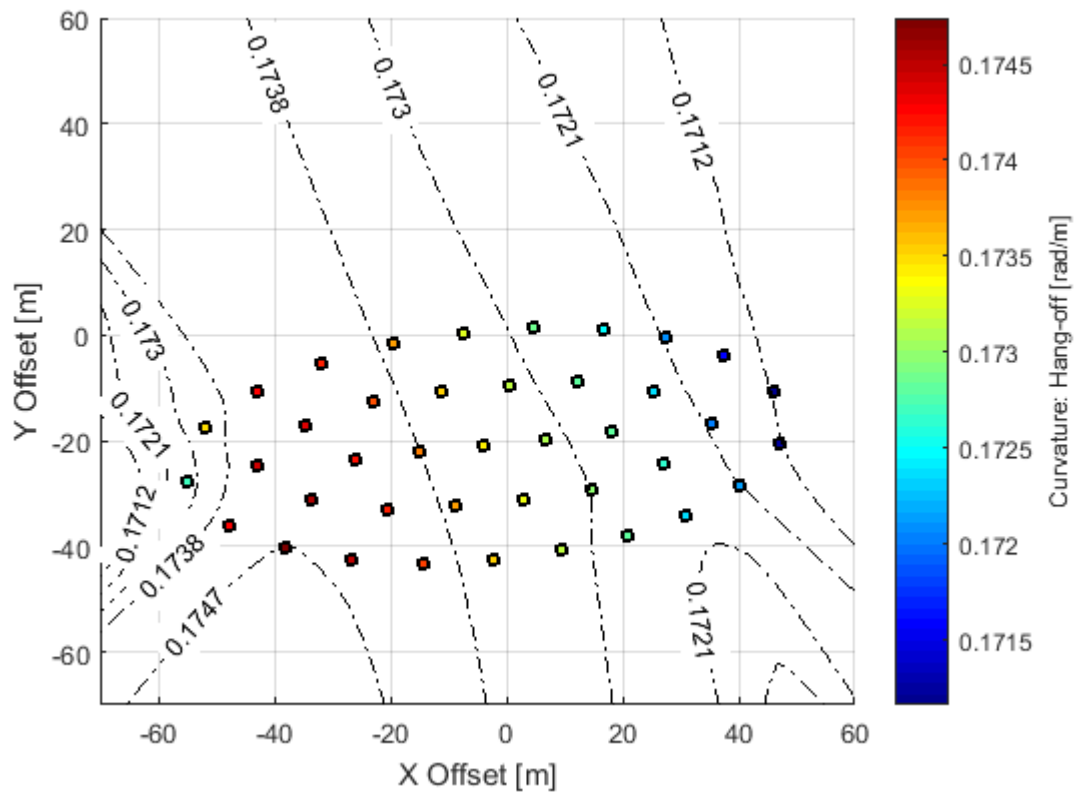


Figure 6-31: Hang Off Curvature Maximum Response Interval (76) Response Isolines

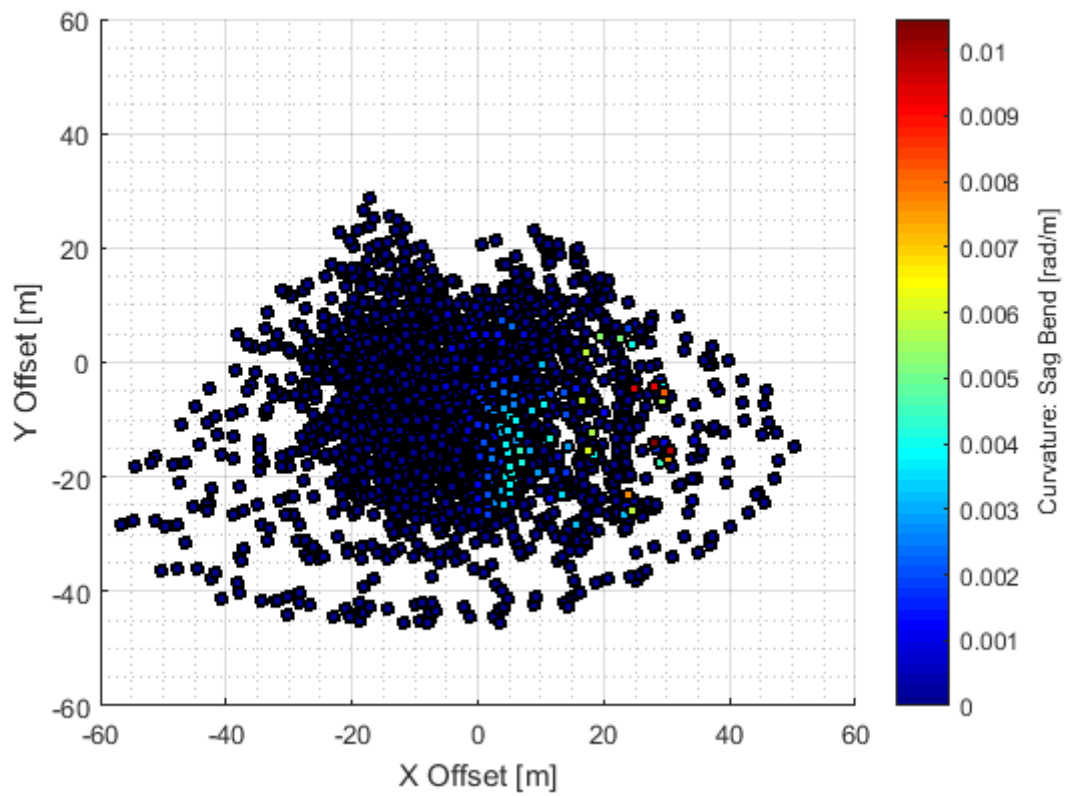


Figure 6-32: Sag Bend Curvature FD Simulation MPMs Scatter

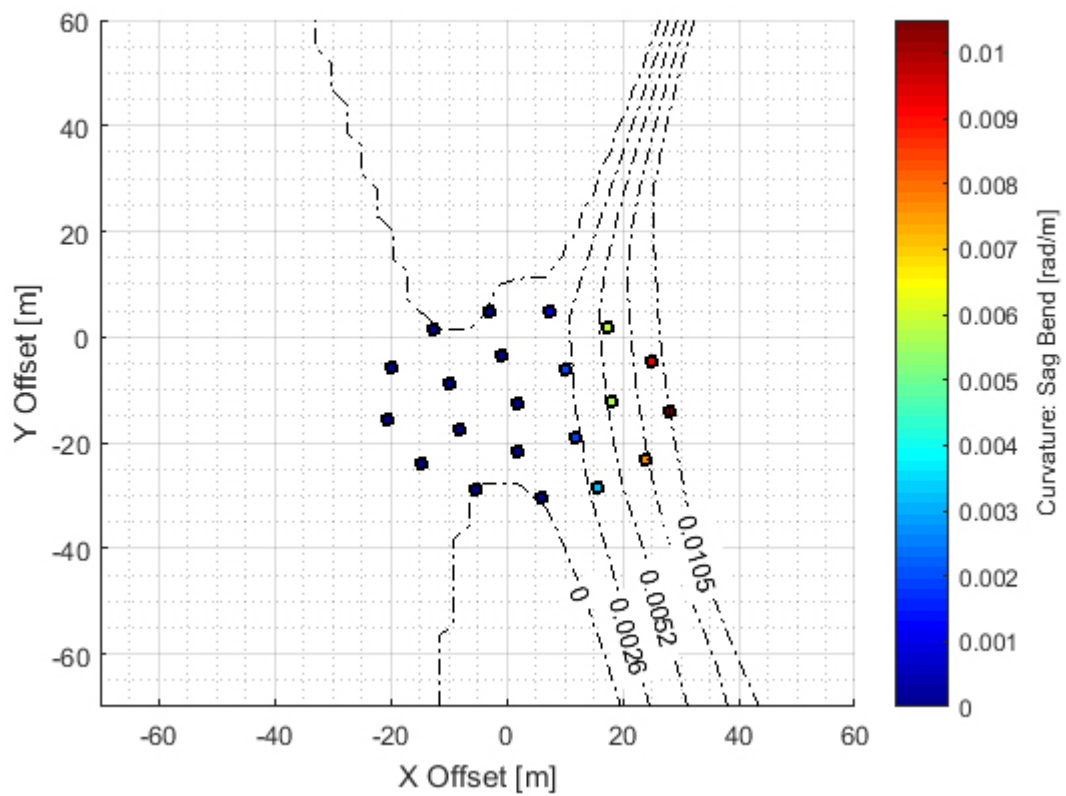


Figure 6-33: Sag Bend Curvature Maximum Response Interval (106) Response Isolines

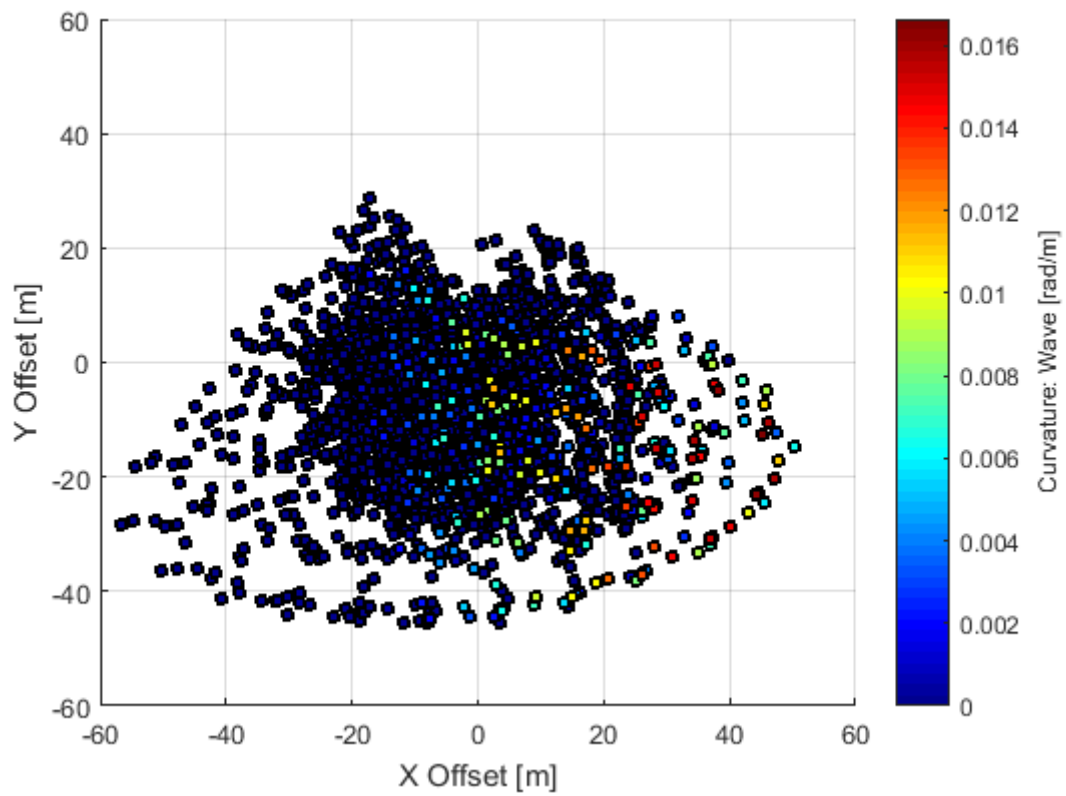


Figure 6-34: Wave Curvature FD Simulation MPMs Scatter

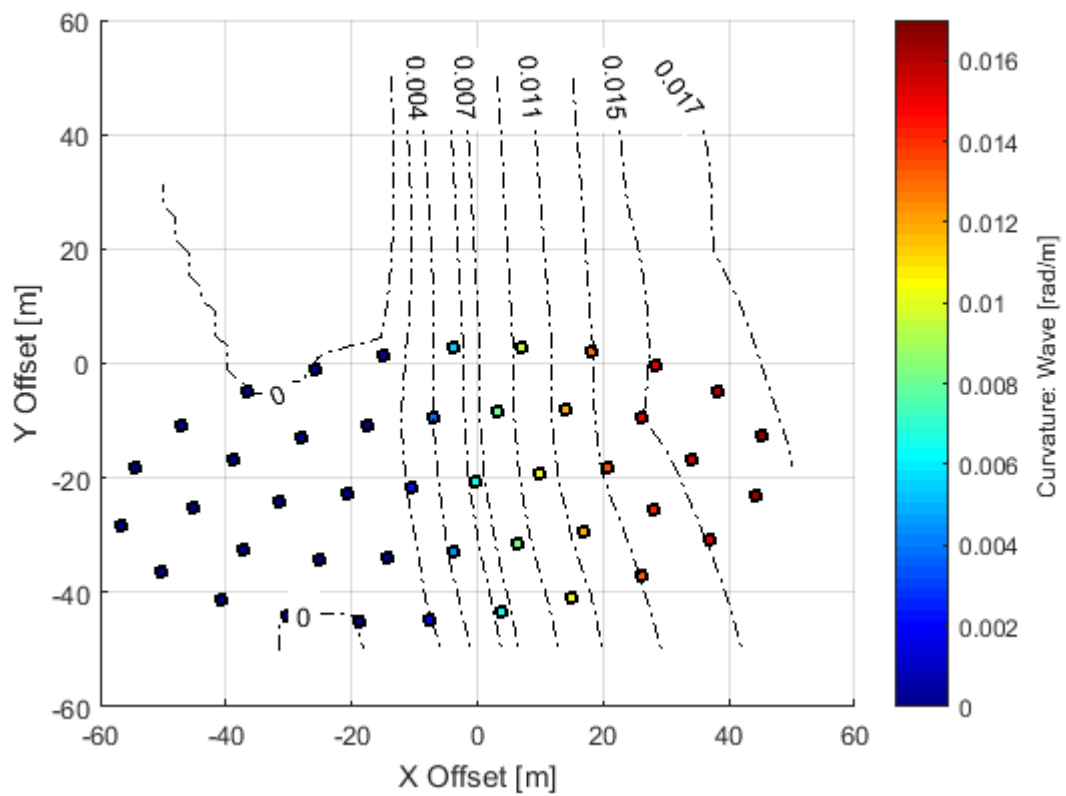
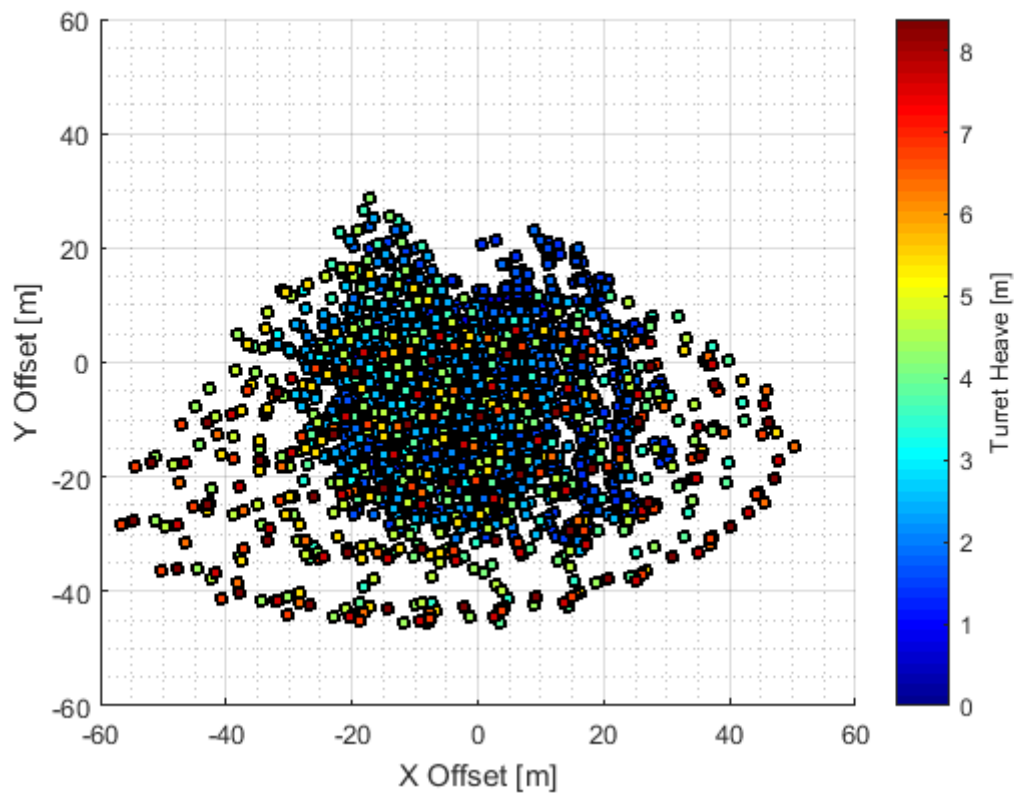


Figure 6-35: Wave Curvature Maximum Response Interval (75) Response Isolines



**Figure 6-36: Turret Heave FD Simulation MPMs Scatter**

## 6.8 Summary and Conclusions

The processing times of each method discussed in this chapter are presented in Table 6-2; a storm of 100 half hour intervals is used as a sample case. Methods inclusive of time domain simulations are assumed to have 30 seeds/realizations per interval. A balance of accuracy and computational efficiency was the objective of this investigation. Methods not presented in this chapter are also included for reference; these include the “Time Domain WF-Only” and “Frequency Domain WF-Only” studies that were conducted in Chapter 10 and Chapter 5 respectively.

**Table 6-2: Riser RBA Method Processing Times and File Requirements**

Description of Method			Storm X = 100 Intervals, 0.5 hr interval duration					
			Pre-Processing	Simulation	Post-Processing	Total Time	# of sim files	Storage
			[hrs]	[hrs]	[hrs]	[hrs]	[#]	[Gb]
T E E	Boundary		0.23	0.41	0.32	0.96	4884	18
	Constant Probability		0.25	0.41	0.32	0.98	4884	18
	Bivariate PDF	Equal Probability	0.26	0.41	0.32	0.99	4884	18
		Delaunay Meshed	0.55	0.73	0.52	1.8	7968	30
		Polar Coordinates	0.70	1.80	0.57	3.07	11644	44
Hybrid LF+WF (Low's)			11.13	30.00	475.8	516.93	150000	567
Full Time Domain (LF+WF)			0.72	123.90	2.19	126.81	3000	160
Time Domain WF-Only			0.15	5.28	0.18	5.61	3000	11
Frequency Domain WF-Only			0.0046	0.043	0.003	0.051	100	0.43

WF-only TD simulations require approximately 110 times the computation time of an equivalent WF-only FD analysis (direct WF-only comparison between Chapter 10 and Chapter 5).

Generally, for all the methods presented in Table 6-2 that utilize time domain simulations, the computation times, number of simulation files, and storage can be reduced proportionally to the number of seeds used. That is to say that, given that the Time Domain WF-Only method which is presented in Table 6-2 uses 30 seeds and requires 5.28 hours simulation time, if the seeds were reduced to 10, the simulation time would reduce approximately by a factor of 3 i.e. 10 seeds would require approximately 1.76 hours simulation time. With this consideration in mind, the feasibility of using time domain simulations for peak response regions, while using FD simulation methods for less critical intervals, has potential to be feasible in practice.

In regards to the TEE methods proposed, the LF responses being accounted for solely by turret excursion driven static shifts is limited in its ability to simulate realistic slow drift forces, dampening and other complex LF effects. A possible solution to this may be the hybridization of the TEE methods with the static offsets being replaced by TD generated LF responses. Furthermore, extension of this method for significantly large metocean datasets could be the generation of FD response isoline catalogues/databases that account for metocean parameter ranges that may be called upon by LF generated turret tracks for superposition of WF responses.

## Chapter 7

### SUMMARY, CONCLUSIONS AND FUTURE WORK

## 7.1 Summary and Conclusions

The work conducted in this thesis investigates the statistical properties and the probabilistic analysis methods applicable to flexible riser systems. Short and medium term (storm) response distributions were investigated with the intent to understand the statistical foundations and to develop the processes that can be used for generating long term riser responses for design. This chapter presents key findings of the work with summary of the conclusions and limitations of the thesis. Recommendations on future work recommendations and guidelines are also presented which expand upon the methods detailed in Chapter 6.

Each chapter of the thesis is intended to provide successive knowledge blocks leading to the development of long term (response based) analysis method of riser systems. The chapters also focus on a combination of key objectives (research questions) which were outlined in Chapter 1 of the thesis.

4. What are the statistical properties of the critical responses that govern the design of a flexible riser system (tension, curvature)? How the non-linearity of the riser system (geometrical, structural, hydrodynamic non-linearity) is reflected in the statistical properties of these critical responses?
  - a. What types of the probability distributions are applicable to modelling stochastic processes of flexible riser responses?

Chapter 3 presents an extensive study of the critical riser responses using 9 standard probability models and a more novel Hermite moment model developed by Winstertein [65]. This study provides a summary of the statistical properties of each critical response for two cases that include benign and severe metocean conditions, respectively. Findings include the conclusion of the expected normality of the hang-off tension response, though non-linearity in severe metocean conditions causes the distribution tail to deviate from the Gaussian behaviour.

Comparison of the third and fourth central moments of the standardized response processes with those of Gaussian distributions shows that all riser responses are non-Gaussian to various degrees. Depending on the value of the fourth moment, they were classified as “softening” and “hardening”, as they had wider or narrow tails. Interestingly, the declination angle and curvature at hang-off were found to be strongly non-Gaussian in the benign conditions, and they became closer to normality in a more extreme environment, even though both stayed in the “softening” category. Other riser responses changed their classification depending on the severity of the storm.

Generally, the more flexible multi-parameter distribution models, such as the Burr distribution, were found to fit the responses best. The 4-moment Hermite models performed well in both benign and severe conditions for all responses and further development of these models may provide improved fits for highly non-linear responses exhibiting skewed distributions.

- b. How to determine the maximum riser response and to estimate its variability in a stationary sea state of a given duration (e.g. from 0.5 to 3.0 hours), based on the time domain or frequency domain simulations?

Time domain analysis, which uses the finite element model of a flexible riser, remains the most appropriate method for the determination of the maximum riser responses in extreme metocean conditions, and those where the effects of current loading on the riser are significant. Frequency domain analysis is found to provide acceptable accuracy in situations where the metocean conditions are relatively benign and the effect of current is unimportant.

For the determination of maximum responses, Chapters 4 and 5 utilize fits of the Gumbel distribution model, from which and the MPM response can be easily determined using the model properties (MPM corresponds to CDF value of  $1/e = 0.368$ ). The Gumbel model is found to provide good representation of the maximum response variability in the stationary sea state of a given duration. A section of Chapter 10 investigates the goodness of fit of the Gumbel model for use on riser response extremes extracted from 30 to 40 time histories (wave realizations or seeds). The Gumbel distribution, which used the square response as a variable, was concluded to be an appropriate model for the extreme riser responses. Truncation of the Gumbel model for omission of negative maximum responses was found to not be required as the impact on the subsequent storm response distribution was negligible.

Within Chapter 2, a brief investigation was conducted on the use of a single time realization for the determination of the MPM riser response by applying a two-parameter Weibull fit to multiple local maxima. When compared with the extreme value distribution found by fitting the Gumbel model to a set of global maxima from multiple realizations, the Weibull fitting to local peaks in a single realization was found to produce significant scatter.

In Chapters 2 and 6, frequency domain analysis methods are used, and thus the MPM responses are found using power spectral density moments. In this formulation, the maximum response variability can be estimated from the Gumbel model of the squared response, with due account for the above limitations of the frequency domain predictions. The extreme non-linear curvature responses were underpredicted when compared to time-domain MPMs. A method of combining curvature x and y components through addition of spectral moments was found to accurately replicate ‘complete’ curvature of the riser. This method was used for all frequency domain generated riser curvature responses in Chapters 2, 6 and parts of 7.

- c. How to determine the maximum riser response and to estimate its variability in a storm which consists of several stationary sea states?

Chapter 10 and 5 detail the method used for combining several stationary sea states into a single storm distribution. The method used requires the product of the CDFs of all stationary sea states contributing to the ‘storm’ event being calculated, with the resulting CDF representing the storm’s response distribution. It is shown that the MPM responses over a complete storm are always higher than MPM responses in any interval making up the storm.

The effects of the wave frequency and low frequency vessel motions on the response variability were considered in isolation within each stationary sea state, and their combined effect on the storm distribution was examined. It was found that response components caused by the low frequency motions contribute a larger portion to variability of the final storm distribution for those responses that are more sensitive to turret excursion than to wave motions or turret heave. The inclusion of the LF responses always increases the overall variability of the extreme response distribution, therefore the use of quasi-static, WF-only simulations is not recommended.

In Chapter 4, the asymptotic format of the maximum response distribution in a storm was developed, conditional on the MPM storm response. In this formulation, which is an extension of that proposed by Tromans and Vandersohuren [34], the storm distribution is dependent on a single parameter. For the two tropical cyclones considered in this study, the distribution parameter takes a broader range of values than recommended by Tromans and Vandersohuren [34] for North Sea. At the same time, for the turret heave motion, there is a clear consistency between the two storms, despite very different metocean conditions and response magnitudes.



Chapters 4 and 5 present a method for the determination of the largest contributing sea state (equivalent interval) to the maximum storm response. These equivalent intervals, which provide the governing contribution to the maximum storm response, are those with the lowest percentile (non-exceedance probability) of the maximum storm response. The percentiles (or equivalent interval durations (EID)) were determined for various riser responses; they show that curvature responses that have low variability require the highest percentile or the longest durations to generate the MPM storm response. This finding may be extended to any response that exhibits low variability.

5. What is typical correlation between the maximum riser responses and metocean parameters in a storm?

Chapters 4 and 5 discuss effects of various metocean parameters. The general conclusion is that the maximum riser responses do not occur in the time intervals associated with the peak significant wave height ( $H_s$ ), or any other metocean parameters taking their peak values. With regards to  $H_s$ , the association of the maximum riser response with the maximum  $H_s$  in the storm becomes exceedingly poor for any response that is weakly coupled with the wave surface wave motion. This finding further supports the application of response based methods to the analysis of flexible risers.

6. How the time domain and frequency domain analysis methods can be used for the probabilistic analysis of riser responses?

a. What is the applicability of frequency domain analysis methods for the prediction of extreme responses of flexible risers?

Chapter 6 provides a detailed study on the prediction of the maximum riser responses by the frequency domain analysis. The method allows for extraction of the parameters required to generate CDFs for the intervals, which can be used to compute the storm response distribution in the same manner, as for the time domain analysis. The largest drawback is that the frequency domain solver can only be used to generate riser responses induced by WF motions. Therefore, the LF response components must be accounted for using some other method. This aspect is the focus of Chapter 6, where various alternative approaches are conceptualized.

The frequency domain analysis predicts the riser WF response components sufficiently for linear or weakly non-linear, such as hang-off tension and hang-off curvature. For such responses, the storm intervals where the response peaks occur are found to be consistent between the TD and FD methods. At the same time, curvature responses that are decoupled from the wave motions and significantly affected by the current do suffer from underprediction.

b. Are there any alternative (hybrid) analysis methods and what their limitations are, in terms of their accuracy to replicate a complete time-domain simulation?

Chapter 6 describes several hybrid approaches and details their limitations. Generally, the WF components of the riser response are well represented by FD analysis in their overall behaviour through the time intervals making up the storm. The FD solvers however can't predict accurately the magnitude of the response peaks due to linearization of the riser mechanics. For the curvature responses, which are effectively decoupled from wave-motions, the LF motion is dominant and the WF component is therefore less important. In such cases, however, the FD analysis may predict maximums in arbitrary (incorrect) intervals within a storm, and sensitivity studies of WF components are recommended. The methods combining the FD and TM solutions at appropriate time scales show promising results. In the future work, the priority should be given to those methods that combine time domain simulations of LF motions with frequency domain analysis of WF response components.

c. How the demands for the computational resources compare between various analysis methods?

The computational requirements of time domain methods were identified as being significantly prohibitive for a complete long term riser response based analysis. The LF + WF coupled study performed in Chapter 4 requires approximately 124 hours for a 100-hour storm to be analysed; this is inclusive of simulation, pre- and post-processing of the data. This study conclusively showed that the existing time domain solvers are inefficient to be used for the analysis undertaken for a real industry project. As such, the investigation into more time-efficient methods was required in order to extend the methods developed in this work to multiple storms in a complete response based analysis process.

Chapter 6 summarizes estimates of the processing times of each method considered. Frequency domain solvers are found to require approximately 110 times less time than the TD equivalent; TD/FD WF-only responses were the only available direct comparison for computation time. Further development of the methods presented in Chapter 6 is expected to provide an efficient and accurate modelling process.

## 7.2 Limitations and Considerations of Numerical Analyses for RBA of Flexible Risers

### Use of Numerical Simulations

- Numerical simulations are the basis of all studies within this thesis (primarily OrcaFlex and Ariane) and each of the software packages used contain simplifications that introduce numerical, modelling and analytical uncertainty. In the general framework of probabilistic (the structural reliability) analysis the aspect of modelling uncertainty is also included (or also modelled with some distributions). Although understanding and mitigating these uncertainties is important, the primary focus of the research is on the RBA component of probabilistic (reliability) analysis;
- The OrcaFlex and Ariane models were validated for project use and only the OrcaFlex model was optimised by removing additional risers and refining segmentation to allow statics to solve for every simulation with one base file. Consistent use of base cases throughout the thesis' studies was performed in order to reduce the uncertainty of the thesis as a whole.
- Model testing and full-scale analysis were not seen as viable options for this research. Model tests are not technically feasible or practical because of the scaling laws, which need to be followed: modelling both the viscous effects and riser mechanical properties (stiffness) is challenging or may require such elaborate techniques, which will very expensive and will contribute to additional uncertainty. For this reason, for example, riser sections are frequently tested in scale 1:1 but this is not possible for the full system. Full scale data is valuable for calibration of analytical models, but also expensive. This then points towards the use of analytical models, calibrated wherever possible by full scale measurements. For this reason, riser properties are usually validated by vendors carrying out full scale testing of sections and detailed structural FEA.

### Metocean Datasets

- The work conducted in this thesis focuses on two storm events that may be categorized as benign and severe. A limitation of this small event sample size is the potential oversight of metocean combinations that the simulated riser configurations/floating and mooring systems are sensitive to. A large metocean dataset with a broad range

of metocean magnitudes and combinations (100+ storms) is required for a robust response based design. Inclusion of additional metocean events was unable to be performed due to the limited computational efficiencies of the available software. Further development of the riser RBA methods will require the simulation of large datasets, which will include multiple storms.

#### Time Domain Solvers

- Time domain solvers used in this thesis had limitations with respect to two aspects: (1) – long simulation time and (2) - the program ability to compute a static riser configuration prior to the dynamic analysis. Both limitations required the flexible riser model to be simplified in order to reduce its physical complexity. Modification of the models required removal of additional risers as well as the omission of some mid water arch components in applicable models. As such, mass, stiffness and other interaction effects that these omitted structures may have had on the subject system were assumed to be negligible. For comprehensive analysis of a riser system, all the risers may need to be included, and the real riser configuration may result in additional simulation time.

#### Frequency Domain Solvers

- The frequency domain solver used is limited to wave frequency motions, and so inclusion of LF motions required conceptual processes to be developed in Chapter 6. The solver used does not include all the responses that time domain offers. Specifically, for the studied responses, declination angle was not offered by the frequency domain solver. Furthermore, initial studies using the frequency domain solver did not allow for modelling of bend stiffeners at the riser-turret interface. In later versions of software releases, bend stiffener modelling in frequency domain was available and this feature was implemented in Chapter 6. Various limitations of frequency domain solver abilities to predict non-linear responses exist as system mechanics require linearization in the frequency domain.

#### Coupling of Independent Solvers

- Coupling of independent solvers requires conversion of coordinate systems and various parameters that must be transferred for replication of the simulated conditions. Each solver uses its own assumptions that must be accounted for throughout the simulation process. One such assumption in coupling LF motions from Ariane with WF motions in OrcaFlex is that the wave trains experienced by both models are consistent. The time history of the wave motions in Ariane are recorded at the FPSO turret center, this is then used by OrcaFlex to generate its own wave history for the entire model's water surface. The wave motions beyond the turret center are therefore assumed to be consistent between the two solvers.
- Coupling of multiple software solvers causes a significant bottleneck to simulation efficiency. Transfer of results from one solver to another requires generation of intermediate files that require large storage banks to be retained. Thus, the read-write speed of the simulation hardware becomes an additional inhibitor for computation time.
- The retention of large databases of results requires modification of data naming conventions. In large databases, the identification of problematic, corrupted or incomplete simulations is essential for efficient quality assurance, troubleshooting and maintenance. The use of multiple hardware devices and server based simulation also requires that the file origins be traceable.

## Riser Configurations

- For the conceptualization of more efficient analysis processes, the riser configuration with a mid-water arch (MWA), which was initially used, has been swapped for a less computationally demanding Lazy-Wave configuration. This was also required for the riser model to be simple enough to enable the static solution for a range of turret excursions to be obtained; the MWA model used initially resulted in a large number of static analysis “failures”, which imposed serious limitation on the study. Such failures of static analysis for complex riser configurations are therefore expected to be a common occurrence when a large number of storms is considered; thus, some work-around is required to mediate the gaps left by these failures.
- The work in this thesis focuses on six responses, including 5 riser responses and the turret heave. The responses and their locations investigated were identified as critical for each riser configuration in an initial parametric study. Although other critical responses exist, the scope of this work did not permit analysis of all critical responses. Expansion of this work to include further responses, or further preliminary design assessment of the riser to identify the critical responses is recommended.

### 7.3 Future Work

Direct extension of the work conducted in this thesis may include the following research topics, which are grouped in several areas:

#### Short Term and Medium Term (storm) Riser Responses

- Extended use of the Hermite moment model detailed in Chapter 3 to include the generation of extreme value distributions of the maximum riser response in each interval;
- Investigation into variability of the distribution moments to understand the potential of significantly reducing the number of time domain simulations, which are processed using the Hermite model;
- Investigation into the Hermite models inclusive of higher order moments to determine if it can be improved to better fit strongly non-Gaussian responses;
- Developing a methodology for finding “design wave” events (which include wave elevation and also wind gust and current), which cause a given maximum riser response in a storm. Logically, such “design wave” should be identified within the equivalent interval, which is already found, where the riser MPM response is most likely to be exceeded. To simplify this approach further, single wave frequencies (regular wave analysis) could be investigated to find a regular wave capable of reproducing the target response.

#### Methodology and Software for Hybrid Analysis

- Investigation into one of the identified hybrid methods (Chapter 6) for the accurate and efficient probabilistic analysis of risers in multiple storms;
- Investigation into the application of the riser WF response isolines generated by the frequency domain analysis (and possibly catalogued) for efficient addition to LF responses in place of the frequency domain WF simulations performed for each way points.

#### Comparison and Validation of Different Software Packages

- Investigation regarding the use of different software packages to replace OrcaFlex and Ariane solvers;
- Comparison of the results from different software packages and development of a methodology for modelling the associated uncertainty, to be used within the framework of the structural reliability analysis of flexible risers;
- Analysis of Multiple Storms (complete RBA)
- Simulation of a complete metocean dataset consisting of 100+ storm events to establish the long-term riser responses as well as validating the more efficient processes that are to be developed.

#### Other Critical Responses for Design

- Investigation of further critical responses, flexible riser types and their configurations, as well as inclusion of additional floating systems to which the risers are connected;
- Non-linear responses of the floating system are expected to add further variability to the riser responses. Investigation and quantification of the effects that the FPSO's non-linear responses have on the riser is recommended;
- Investigation of wind loads and wind gust phasing with waves; the effect these loads have on the dynamic responses of the whole system. In addition, phasing would be of significant interest to the previously mentioned "design wave" methodology development;
- Understanding and inclusion of the directional spread of wind and wave loads when performing RBA.

In addition to the above research tasks, there are additional tasks related to software Development

- Programming of a standalone hybrid time and frequency domain solver for riser responses to reduce the data handling requirements when the two independent programs are combined;
- Development of a suite of programs and graphical user interfaces for the simplified application of riser RBA is recommended for consistency and quality control when performing numerous simulations.

## Chapter 8

### REFERENCES

- [1] Winterstein, S. R., 1990, “An Introduction to Structural Reliability, FORM, and LRFD Design,” *GC/MS*, John Wiley & Sons, Inc., Hoboken, NJ, USA, pp. 113–118.
- [2] Det Norske Veritas, 2009, *DNV OS F201 Dynamic Risers*.
- [3] Det Norske Veritas, 2010, *DNV RP F204 Riser Fatigue*.
- [4] Det Norske Veritas, 2009, *DNV OSS 302 Offshore Riser Systems*.
- [5] American Petroleum Institute, 2014, *API 17B, Recommended Practice for Flexible Pipe*, Washington, DC.
- [6] American Petroleum Institute, 2014, *API 17J, Specification for Unbonded Flexible Pipe*.
- [7] Garrett, D. L., 2005, “Coupled Analysis of Floating Production Systems,” *Ocean Eng.*, **32**(7), pp. 802–816.
- [8] Low, Y. M., 2008, “Prediction of Extreme Responses of Floating Structures Using a Hybrid Time/Frequency Domain Coupled Analysis Approach,” *Ocean Eng.*, **35**(14–15), pp. 1416–1428.
- [9] Low, Y. M., and Langley, R. S., 2008, “A Hybrid Time/Frequency Domain Approach for Efficient Coupled Analysis of Vessel/Mooring/Riser Dynamics,” *Ocean Eng.*, **35**(5–6), pp. 433–446.
- [10] Vasudevan, S., and Westlake, P., 2012, “Investigation on the Use of Different Approaches to Mooring Analysis and Appropriate Safety Factors,” *Volume 1: Offshore Technology*, ASME, p. 755.
- [11] Witz, J. A., and Tan, Z., 1992, “On the Axial-Torsional Structural Behaviour of Flexible Pipes, Umbilicals and Marine Cables,” *Mar. Struct.*, **5**(2–3), pp. 205–227.
- [12] Majed, A., and Cooper, P., 2014, “A Nonlinear Dynamic Substructuring Approach to Global Dynamics of Flexible Riser Systems,” *33rd International Conference on Ocean, Offshore and Arctic Engineering*, ASME, p. 6B: Pipeline and Riser Technology.
- [13] Forristall, G. Z., Larrabee, R. D., and Mercier, R. S., 1991, “Combined Oceanographic Criteria for Deepwater Structures in the Gulf of Mexico,” *Offshore Technology Conference*, Offshore Technology Conference.
- [14] Tromans, P. S., and Vandersohuren, L., 1995, “Response Based Design Conditions in the North Sea: Application of a New Method,” *Offshore Technol. Conf.*
- [15] Incecik, A., Bowers, J., Mould, G., and Yilmaz, O., 1998, “Response-Based Extreme Value Analysis of Moored Offshore Structures Due to Wave, Wind, and Current,” *J. Mar. Sci. Technol.*, **3**(3), pp. 145–150.
- [16] Winterstein, S. R., Alok, K. J., and Satyendra, K., 1999, “Reliability of Floating Structures: Extreme Response and Load Factor Design,” (August), pp. 163–169.
- [17] Ahilan, R. V., and Standing, R. G., 2002, “Response Based Design for FPSOs - Compromise on Physics or Statistics,” *ASRANet Colloquium*.
- [18] Standing, R. G., and Eichaker, R., 2002, “Benefits of Applying Response-Based Design Methods to Deepwater FPSOs,” *Offshore Technology Conference*, p. 1, pp. 1–12.
- [19] Perdrizet, T., and Averbuch, D., 2008, “Long Term Failure Probability Calculation Method Applied to Riser Design,” *Volume 2: Structures, Safety and Reliability*, ASME, pp. 847–852.
- [20] Jorge Mendes de Sousa, F., Sudati Sagrilo, L. V., de Lima, E. C. P., and Papaleo, A., 2012, “Calibration of Design Conditions

Based on Long Term Top Tension for Catenary Risers,” *31st International Conference on Ocean, Offshore and Arctic Engineering*, ASME, p. 2: Structures, Safety and Reliability.

- [21] Drobyshevski, Y., Whelan, J. R., Wadhwa, H., and Anokhin, V., 2014, “Determination of Design Metocean Conditions by Response Based Analysis,” *33rd International Conference on Ocean, Offshore and Arctic Engineering International Conference on Ocean, Offshore and Arctic Engineering*, ASME, p. 1B: Offshore Technology.
- [22] Zhang, Y., Tan, Z., Hou, Y., and Yuan, J., 2014, “A Study for Statistical Characteristics of Riser Response in Global Dynamic Analysis With Irregular Wave,” *33rd International Conference on Ocean, Offshore and Arctic Engineering*, ASME, p. 6A: Pipeline and Riser Technology.
- [23] Connaire, A., Kavanagh, K., Ahilan, R. V., and Goodwin, P., 1999, “Integrated Mooring & Riser Design: Analysis Methodology,” *Offshore Technology Conference*, Offshore Technology Conference, pp. 1–14.
- [24] Goodwin, P., Ahilan, R. V., Kavanagh, K., and Connaire, A., 1999, “Integrated Mooring and Riser Design: Reliability Analysis Methodology and Preliminary Results,” *Offshore Technology Conference*, Offshore Technology Conference.
- [25] Martens, M., Whelan, J. R., and Drobyshevski, Y., 2011, “Integrated Analysis of Mooring and Riser Systems for FPSO’s in Harsh Shallow Water Environments,” *30th International Conference on Ocean, Offshore and Arctic Engineering*, ASME, p. 4: Pipeline and Riser Technology.
- [26] Cruces Girón, A. R., Corrêa, F. N., Jacob, B. P., and Senra, S. F., 2012, “An Integrated Methodology for the Design of Mooring Systems and Risers of Floating Production Platforms,” *31st International Conference on Ocean, Offshore and Arctic Engineering*, ASME, p. 1: Offshore Technology.
- [27] Winterstein, S. R., Ude, T. C., Cornell, C. A., Bjerager, P., and Haver, S., 1993, “Environmental Parameters for Extreme Response: Inverse FORM with Omission Factors,” *ICOSSAR*, pp. 9–13.
- [28] Haver, S., and Winterstein, S. R., 2008, “Environmental Contour Lines- A Method for Estimating Long Term Extremes by a Short Term Analysis,” *Trans. Soc. Nav. Archit. Mar. Eng.*, **116**(October), pp. 116–127.
- [29] Haver, S., and Kleiven, G., 2004, “Environmental Contour Lines for Design Purposes: Why and When?,” *23rd International Conference on Offshore Mechanics and Arctic Engineering*, ASME, pp. 1, Parts A and B, pp. 337–345.
- [30] Bitner-Gregersen, E. M., 2005, “Joint Probabilistic Description for Combined Seas,” *24th International Conference on Offshore Mechanics and Arctic Engineering*, ASME, p. 2, pp. 169–180.
- [31] Ruichao, W., “Prediction of Design Response for North Sea,” NTNU.
- [32] Armstrong, C., Chin, C., Penesis, I., and Drobyshevski, Y., 2015, “Sensitivity of Vessel Responses to Environmental Contours of Extreme Sea States,” *34th International Conference on Ocean, Offshore and Arctic Engineering*, p. 3A: Structures, Safety and Reliability.
- [33] Baarholm, G. S., and Haver, S., 2010, “Application of Environmental Contour Lines on a Flexible Riser,” *29th International Conference on Ocean, Offshore and Arctic Engineering*, ASME, p. 5, Parts A and B.
- [34] Tromans, P. S., and Vandersohuren, L., 1995, “Response Based Design Conditions in the North Sea: Application of a New Method,” *Offshore Technology Conference*.
- [35] Hawkes, P. J., Gouldby, B. P., Tawn, J. A., and Owen, M. W., 2002, “The Joint Probability of Waves and Water Levels in Coastal Engineering Design,” *J. Hydraul. Res.*, **40**(3), pp. 241–251.
- [36] Drobyshevski, Y., Whelan, J. R., McConochie, J. D., and Martin, H. A. C. S., 2008, “Response Based Design Metocean Conditions for a Permanently Moored Vessel in Cyclone-Affected Area,” *Deep Offshore Technology International*.
- [37] Det Norske Veritas, 2010, *DNV-RP-C205: Environmental Conditions and Environmental Loads*, Det Norske Veritas.

- [38] Orcina Ltd., 2016, *OrcaFlex Manual Version 10.0e*.
- [39] Armstrong, C., Drobyshevski, Y., and Chin, C., 2017, "Application of Frequency Domain Methods for Response Based Analysis of Flexible Risers," *36th International Conference on Ocean, Offshore and Arctic Engineering*, ASME, p. 3A: Structures, Safety and Reliability.
- [40] Fergestad, D., and Løtveit, S. A., 2014, *Handbook on Design and Operation of Flexible Pipes*, Norsk Marinteknisk Forskningsinstitutt AS, Trondheim.
- [41] Li, H., Du, J., Wang, S., Sun, M., and Chang, A., 2016, "Investigation on the Probabilistic Distribution of Mooring Line Tension for Fatigue Damage Assessment," *Ocean Eng.*, **124**, pp. 204–214.
- [42] Izadparast, A. H., and Duggal, A. S., 2013, "Empirical Estimation of Probability Distribution of Extreme Responses of Turret Moored FPSOs," *Proceedings of the International Offshore and Polar Engineering Conference*, pp. 877–884.
- [43] Johnson, N. L., Kotz, S., and Balakrishnan, N., 1994, *Continuous Univariate Distributions, Volume 1, Second Edition*, Wiley.
- [44] Johnson, N. L., Kotz, S., and Balakrishnan, N., 1995, *Continuous Univariate Distributions, Volume 2, Second Edition*, Wiley.
- [45] The Mathworks, I., "MATLAB and Statistics Toolbox Release 2016b."
- [46] Winterstein, S. R., 1987, *Moment-Based Hermite Models of Random Vibration.*, Technical University of Denmark, Department of Structural Engineering, Lyngby.
- [47] Winterstein, S. R., 1988, "Nonlinear Vibration Models for Extremes and Fatigue," *J. Eng. Mech.*, **114**(10), pp. 1772–1790.
- [48] NIST/SEMATECH, 2012, "E-Handbook of Statistical Methods" [Online]. Available: <http://www.itl.nist.gov/div898/handbook/>.
- [49] Nematrian Limited, 2017, "Standard Statistical Tests for Normality: The Cramer von Mises Test." [Online]. Available: [www.nematrian.com/CramervonMises](http://www.nematrian.com/CramervonMises).
- [50] Stephens, M. A., 1970, "Use of the Kolmogorov-Smirnov, Cramer-Von Mises and Related Statistics Without Extensive Tables," *J. R. Stat. Soc. Ser. B*, **32**(1), pp. 115–122.
- [51] Armstrong, C., Drobyshevski, Y., Chin, C., and Penesis, I., 2017, "Variability of Extreme Riser Responses Due to Wave Frequency Motions of a Weather-Vaning FPSO," *36th International Conference on Ocean, Offshore and Arctic Engineering*, ASME, p. 3A: Structures, Safety and Reliability.
- [52] Bury, K. V., 1975, *Statistical Models in Applied Science*, John Wiley & Sons.
- [53] Naess, A., 1984, "Technical Note: On a Rational Approach to Extreme Value Analysis," *Appl. Ocean Res.*, **6**(3), pp. 173–174.
- [54] Gumbel, E. J., 1959, *Statistics of Extremes*.
- [55] Fergestad, D., and Løtveit, S. A., 2014, *Handbook on Design and Operation of Flexible Pipes*, NTNU, 4Subsea, MARINTEK.
- [56] Huseby, A. B., Vanem, E., and Natvig, B., 2015, "Alternative Environmental Contours for Structural Reliability Analysis," *Struct. Saf.*, **54**, pp. 32–45.
- [57] Campbell, B. L., Lawes, H. D., and Standing, R. G., 2001, "The Use of Response-Based Design Methods Applied to Floating Structures," *16th Annual Floating Production Systems Conf., London*.
- [58] Larsen, C. M., and Olufsen, A., 1992, "Extreme Response Estimation of Flexible Risers by Use of Long Term Statistics," *International Offshore and Polar Engineering*, p. 2, pp.14–19.
- [59] Tucker, M. J., and Pitt, E. G., 2001, *Waves in Ocean Engineering (Elsevier Ocean Engineering)*, Elsevier.
- [60] Bureau Veritas Marine Division - Research Department, 2009, *Ariane 7 Theoretical Manual*, Neuilly-sur-Seine Cedex, France.



- [61] Mazaheri, S., and Downie, M. J., 2005, "Response-Based Method for Determining the Extreme Behaviour of Floating Offshore Platforms," *Ocean Eng.*, **32**(3–4), pp. 363–393.
- [62] Ormberg, H., Sodahl, N., and Steinkjer, O., 1998, "Efficient Analysis of Mooring Systems Using De-Coupled and Coupled Analysis," *17th International Conference on Offshore Mechanics and Arctic Engineering*, Lisbon, Portugal.
- [63] Ran, Z., Kim, M. H., and Zheng, W., 1999, "Coupled Dynamic Analysis of a Moored Spar in Random Waves and Currents (Time-Domain Versus Frequency-Domain Analysis)," *J. Offshore Mech. Arct. Eng.*, **121**(3).
- [64] Press, W. H., Teukolsky, S. A., Vetterling, W. T., and Flannery, B. P., 1992, "Numerical Recipes in C, Second Edition."
- [65] Winterstein, S. R., 1987, "Moment-Based Hermite Models of Random Vibration."
- [66] Stanistic, D., Efthymiou, M., Kimiaei, M., and Zhao, W., 2017, "Evaluation of Conventional Methods of Establishing Extreme Mooring Design Loads," *36th International Conference on Ocean, Offshore and Arctic Engineering*, Trondheim, p. V03AT02A017.
- [67] Stanistic, D., Efthymiou, M., Kimiaei, M., and Zhao, W., 2018, "Design Loads and Long Term Distribution of Mooring Line Response of a Large Weathervaning Vessel in a Tropical Cyclone Environment," *Mar. Struct.*, **61**, pp. 361–380.
- [68] Edelsbrunner, H., Tan, T. S., and Waupotitsch, R., 1992, "An  $O(N^2 \log n)$  Time Algorithm for the Minmax Angle Triangulation," *SIAM J. Sci. Stat. Comput.*, **13**(4), pp. 994–1008.
- [69] American Petroleum Institute, and API, 2005, *API RP 2SK, Recommended Practice for Design and Analysis of Stationkeeping Systems for Floating Structures*.

## Chapter 9

### APPENDICES

#### 9.1 Storm #1 (Benign) and Storm #2 (Severe) Metocean Parameters

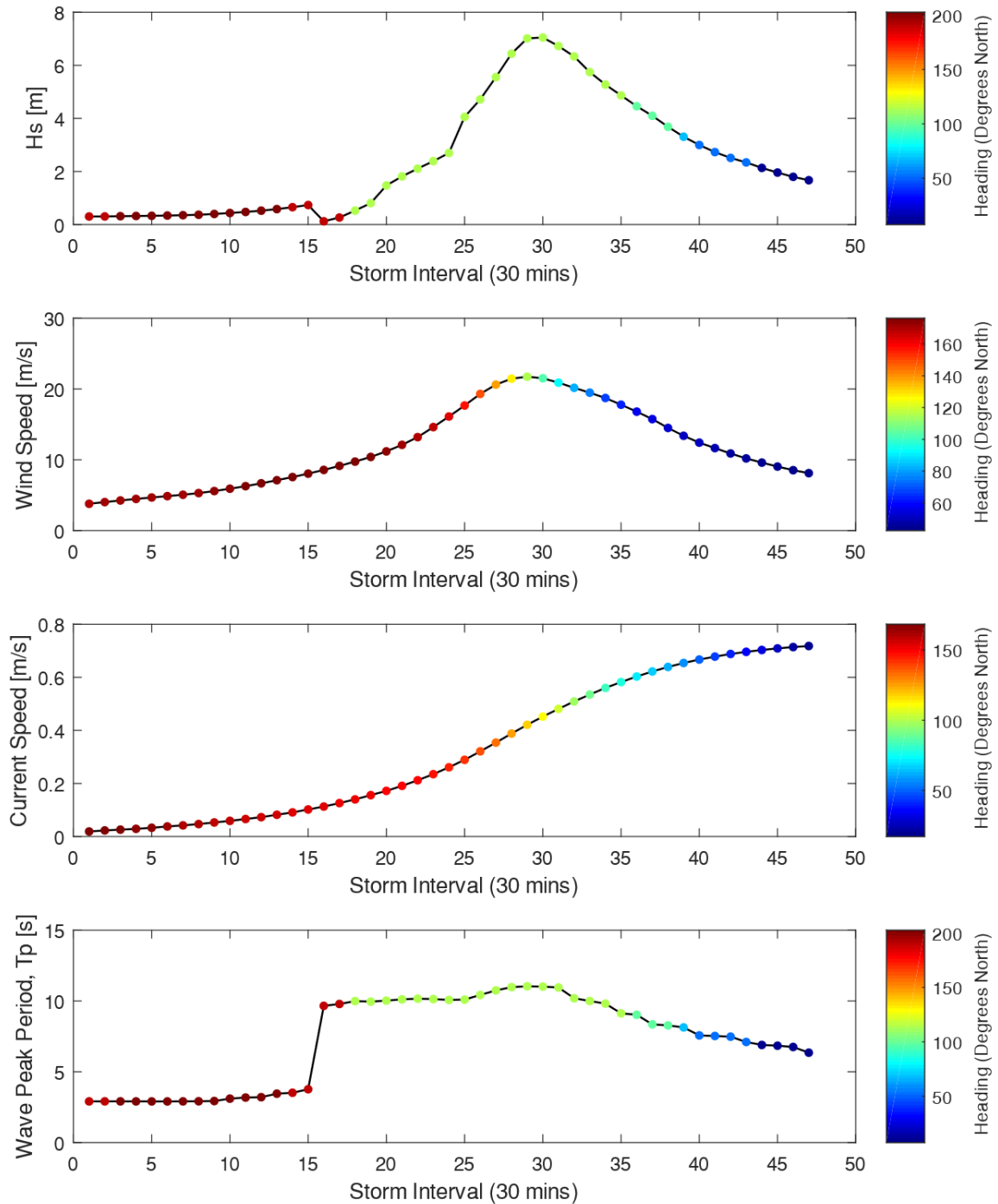


**Figure 9-1: Storm 1 Metocean Parameters**

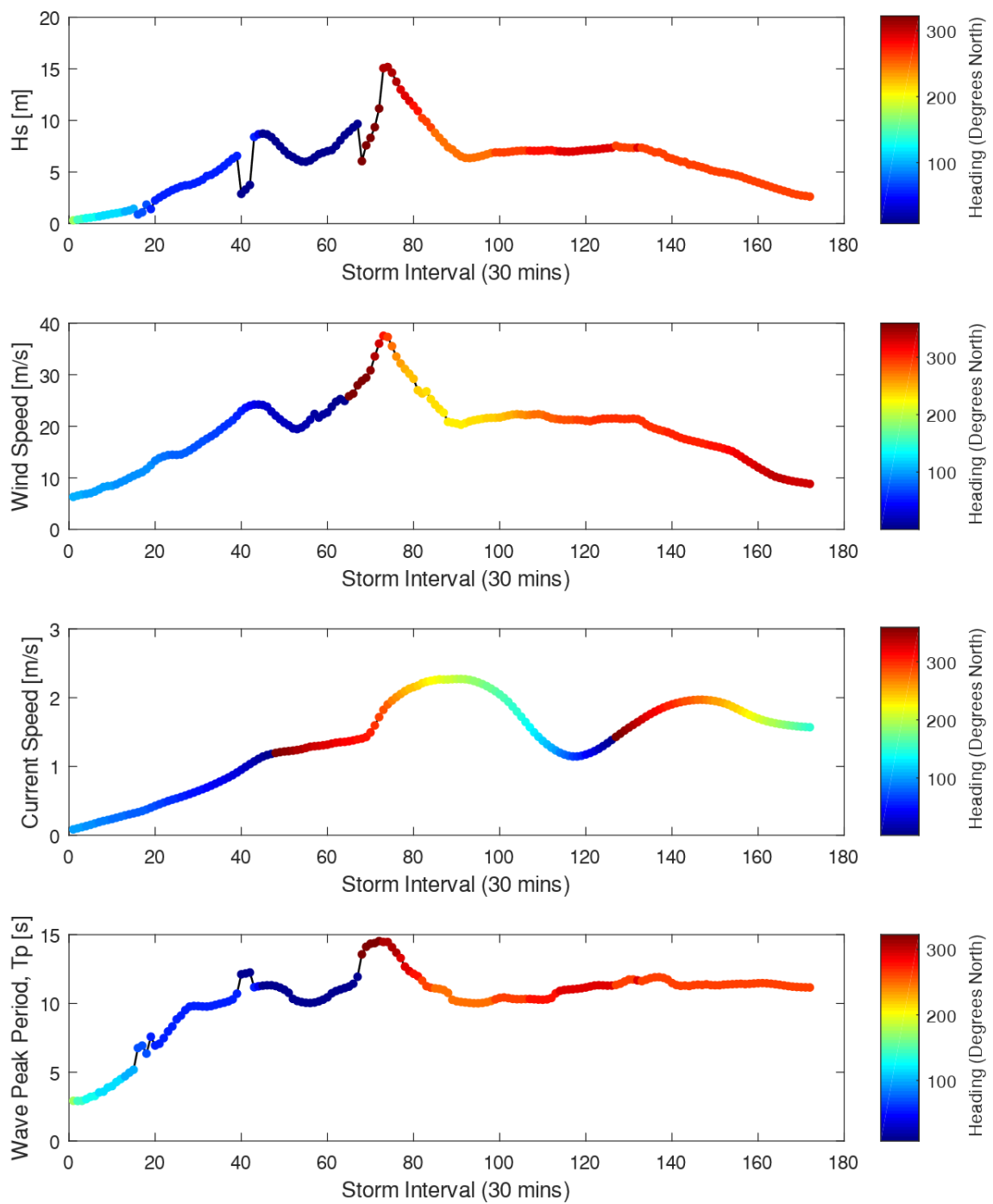


**Figure 9-2: Storm 2 Metocean Parameters**

## 9.2 Hermite Extreme Value Distribution

The Hermite PDF is given by Equation 10-1.

$$f(x) = \varphi(u) \frac{du}{dx_0} \frac{1}{\sigma_x} \quad (9-1)$$

The Hermite CDF equation is

$$F(x) = \Phi(u) \quad (9-2)$$

The extreme value distribution that may be obtained using the Hermite model is detailed in Equation 10-3.

$$F_m(x) = \exp[-Tv(x)] = \exp\left[-Tv_0 \exp\left(-\frac{u^2}{2}\right)\right] \quad (9-3)$$

Here,  $Y(x) = Y_0 \exp\left(-\frac{u^2}{2}\right)$  is equivalent to the crossing rate of response level  $x$  from below.

$$\Phi(u) = \frac{1}{\sqrt{2\pi}} \int_{-\infty}^u e^{-\frac{t^2}{2}} dt \quad (9-4)$$

Equation (10-4) is equivalent to the CDF of the standardized normal distribution.

## 9.3 Polar Coordinate Equations of an Ellipse

To associate the TEE with polar coordinates, let  $a$  and  $b$  be the large and small semi-axes of an ellipse respectively. These should be selected to describe conveniently the domain (for example,  $a, b$  = MPM excursions).

The basic equation of an ellipse centered on the origin with no rotation is:

$$\frac{x^2}{a^2} + \frac{y^2}{b^2} = 1 \quad (9-5)$$

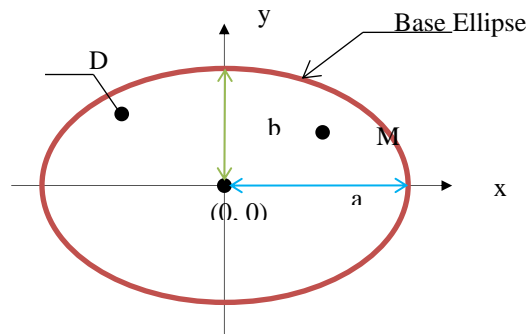


**Figure 9-3: Base Ellipse Diagram**

Coordinates  $M(r, \theta)$  are used to describe all the equations for the polar coordinate method.

$$x = ar \cdot \cos\theta \quad (9-6)$$

$$y = br \cdot \sin\theta \quad (9-7)$$

$$\text{when } r = 1 \rightarrow M(1, \theta) \in \text{Base Ellipse} \quad (9-8)$$

$$\text{when } r > 1 \rightarrow M(r, \theta) \in \text{Some Ellipse Outside Base} \quad (9-9)$$

$$\text{when } r < 1 \rightarrow M(r, \theta) \in \text{Some Ellipse Inside Base} \quad (9-10)$$

Jacobian of this coordinate transformation:

$$J = abr \rightarrow (dx \cdot dy) = abr \cdot (dr \cdot d\theta) \quad (9-11)$$

Integration Over Base Ellipse

$$\iint_D f dx dy = \int_0^1 \int_0^{2\pi} f(r, \theta) \cdot (abr) \cdot dr d\theta \quad (9-12)$$

Similarly, one can integrate over any ellipse larger than the base or smaller, by only changing the upper integration limit of r. Say, set a new ellipse size as:

$$S = \frac{a_1}{a} = \frac{b_1}{b} \rightarrow \int_0^S \int_0^{2\pi} f(r, \theta) \cdot (abr) \cdot dr d\theta \quad (9-13)$$

Grid Setting and Replacing Integral by a Finite Sum

$$\{r_i\}_{i=1}^{M_r} = \{0; \Delta r; 2\Delta r; 3\Delta r; \dots; (M_r - 1)\Delta r\} \quad (9-14)$$

$$M_r = \text{number of subdivisions in } r \quad (9-15)$$

$$(M_r - 1) \cdot \Delta r = r_{max} \quad (9-16)$$

$$\{\theta_j\}_{j=1}^{M_\theta} = \{0; \Delta\theta; 2\Delta\theta; 3\Delta\theta; \dots; (M_\theta - 1)\Delta\theta\} \quad (9-17)$$

$$(M_\theta - 1) \cdot \Delta\theta = 2\pi \quad (9-18)$$

Midpoints of the grid:

$$\bar{r}_i = \frac{1}{2}(r_i + r_{i+1}); \quad \bar{\theta}_j = \frac{1}{2}(\theta_j + \theta_{j+1}) \quad (9-19)$$

$$\bar{x}_{ij} = a\bar{r}_i \cos \bar{\theta}_j (\equiv \text{matrix}(M_r \times M_\theta)) \quad (9-20)$$

$$\bar{y}_{ij} = b\bar{r}_i \sin \bar{\theta}_j (\equiv \text{matrix}(M_r \times M_\theta)) \quad (9-21)$$

The values of function  $f(x, y)$  at midpoints of the grid must be calculated, along with the integral over domain (S x D):

$$\int_{S \times D} f \Delta D = a \cdot b \sum_{i=1}^{M_r} \sum_{j=1}^{M_\theta} f(x_{ij}; y_{ij}) \cdot \bar{r}_i (\Delta r \cdot \Delta \theta) \quad (9-22)$$

Therefore,

$$\Delta D_i = a \cdot b \cdot \bar{r}_i \cdot \Delta r \cdot \Delta \theta \text{ for } j=1, 2, \dots, M_{\theta i} \quad i=1, 2, \dots, M_r \quad (9-23)$$

#### 9.4 Equations for Vessel Headings

Definition of the vessel heading requires the following conversion for a sample-based average heading to be applied.

$$\bar{\varphi} \rightarrow \bar{\cup}(\cos \varphi : \sin \varphi) \quad (9-24)$$

where,  $\cos \varphi$  and  $\sin \varphi$  are the mean components of the sampled headings.

$$\overline{\cos \varphi} > 0 \rightarrow \text{atan} \left( \frac{\overline{\sin \varphi}}{\overline{\cos \varphi}} \right) = \bar{\varphi} \quad (9-25)$$

$$\overline{\cos \varphi} < 0 \rightarrow \text{atan} \left( \frac{\overline{\sin \varphi}}{\overline{\cos \varphi}} \right) - \pi = \bar{\varphi} \quad (9-26)$$

$$\varphi \in [-180 : +180] \quad (9-27)$$

Chapter 10 has been  
removed for copyright or  
proprietary reasons.

## Chapter 10

### VARIABILITY OF EXTREME RISER RESPONSES DUE TO WAVE FREQUENCY MOTIONS OF A WEATHER-VANING FPSO

This conference paper was presented at the 36<sup>th</sup> International Conference on Ocean, Offshore and Arctic Engineering in Trondheim, Norway. The citation for this conference paper is:

Armstrong, C., Drobyshevski, Y., Chin, C., Penesis, I., *Variability of Extreme Riser Responses due to Wave Frequency Motions of a Weather-Vaning FPSO*, OMAE2017-61745, 36<sup>th</sup> International Conference on Ocean, Offshore and Arctic Engineering, June 25 – 30, 2017, Trondheim, Norway. DOI:10.1115/OMAE2017-61745

Chapter 11 has been  
removed for copyright or  
proprietary reasons.

## Chapter 11

### SENSITIVITY OF VESSEL RESPONSES TO ENVIRONMENTAL CONTOURS OF EXTREME SEA STATES

This conference paper was presented at the 34<sup>th</sup> International Conference on Ocean, Offshore and Arctic Engineering in St Johns, NL, Canada. This paper was published prior to the PhD candidature. The citation for this conference paper is:

Armstrong, C., Chin, C., Penesis, I., Drobyshevski, Y., *Sensitivity of Vessel Responses to Environmental Contours of Extreme Sea States*, OMAE2015-41680, 34<sup>th</sup> International Conference on Ocean, Offshore and Arctic Engineering, May 31 – June 5, 2015, St. Johns, NL, Canada. DOI:10.1115/OMAE2015-41680



## ANNEX A

### Sensitivity of Vessel Responses

#### Ship Shaped FSO

Table 6 – Response Sensitivity: Heave [m]

Return Period	Parameter at max	North Atlantic			Word Wide Trade			West Shetlands		
		IFORM	CPD	% Diff	IFORM	CPD	% Diff	IFORM	CPD	% Diff
100	$H_s$	16.21	16.30	-0.58	14.07	14.12	-0.38	16.70	16.72	-0.11
	$T_p$	19.98	20.21	-1.17	19.47	19.93	-2.34	17.79	17.80	-0.03
	$A_{MPM}$	10.65	10.81	-1.54	9.04	9.26	-2.44	9.76	9.77	-0.15
1000	$H_s$	18.15	18.28	-0.70	16.12	16.17	-0.32	19.03	19.05	-0.10
	$T_p$	20.78	20.96	-0.87	20.48	20.96	-2.33	18.70	18.70	-0.01
	$A_{MPM}$	12.30	12.47	-1.33	10.80	11.03	-2.06	11.75	11.76	-0.10
10000	$H_s$	20.04	20.11	-0.38	18.15	18.26	-0.63	21.24	21.24	0.01
	$T_p$	21.46	21.73	-1.24	21.35	21.73	-1.76	19.58	19.60	-0.10
	$A_{MPM}$	13.89	14.05	-1.17	12.54	12.76	-1.77	13.71	13.72	-0.08

Table 7 – Response Sensitivity: Vertical Bending Moment [ $1.0 \times 10^7$  Nm]

Return Period	Parameter at max	North Atlantic			Word Wide Trade			West Shetlands		
		IFORM	CPD	% Diff	IFORM	CPD	% Diff	IFORM	CPD	% Diff
100	$H_s$	16.21	16.00	1.28	14.71	14.55	1.10	13.92	13.90	0.12
	$T_p$	13.02	12.99	0.27	12.74	12.73	0.04	13.93	14.04	-0.80
	$A_{MPM}$	4.38	4.34	1.11	4.03	3.99	1.08	3.54	3.51	1.03
1000	$H_s$	17.92	17.78	0.79	16.66	16.47	1.18	14.91	14.80	0.77
	$T_p$	12.93	12.99	-0.45	12.76	12.73	0.22	14.11	14.13	-0.18
	$A_{MPM}$	4.87	4.82	1.07	4.56	4.51	1.08	3.74	3.71	0.98
10000	$H_s$	19.65	19.40	1.27	18.52	18.33	1.03	15.58	15.50	0.51
	$T_p$	12.95	12.90	0.41	12.72	12.73	-0.12	14.10	14.15	-0.35
	$A_{MPM}$	5.33	5.28	1.02	5.08	5.02	1.08	3.91	3.87	0.93

#### Semisubmersible

Table 8 – Response Sensitivity: Surge [m]

Return Period	Parameter at max	North Atlantic			Word Wide Trade			West Shetlands		
		IFORM	CPD	% Diff	IFORM	CPD	% Diff	IFORM	CPD	% Diff
100	$H_s$	16.31	16.40	-0.55	14.17	14.27	-0.68	16.79	16.82	-0.18
	$T_p$	19.83	20.06	-1.15	19.30	19.67	-1.92	17.71	17.70	0.07
	$A_{MPM}$	10.15	10.29	-1.43	8.63	8.82	-2.23	9.50	9.51	-0.12
1000	$H_s$	18.27	18.43	-0.91	16.24	16.38	-0.87	19.07	19.05	0.11
	$T_p$	20.60	20.70	-0.48	20.27	20.57	-1.47	18.66	18.70	-0.23
	$A_{MPM}$	11.68	11.83	-1.22	10.27	10.47	-1.89	11.28	11.29	-0.09
10000	$H_s$	20.27	20.32	-0.28	18.40	18.46	-0.30	21.24	21.24	0.01
	$T_p$	21.06	21.35	-1.33	20.88	21.35	-2.20	19.58	19.60	-0.10
	$A_{MPM}$	13.14	13.28	-1.05	11.87	12.06	-1.59	13.08	13.09	-0.07

Table 9 – Response Sensitivity: Heave [m]

Return Period	Parameter at max	North Atlantic			Word Wide Trade			West Shetlands		
		IFORM	CPD	% Diff	IFORM	CPD	% Diff	IFORM	CPD	% Diff
100	H <sub>s</sub>	13.93	14.20	-1.95	11.74	12.00	-2.20	16.82	16.82	0.02
	T <sub>p</sub>	22.25	22.48	-1.01	22.02	22.46	-2.00	17.67	17.70	-0.18
	A <sub>MPM</sub>	10.88	11.34	-4.18	8.94	9.57	-6.84	8.28	8.29	-0.12
1000	H <sub>s</sub>	16.31	16.60	-1.74	14.35	14.70	-2.40	18.98	19.00	-0.09
	T <sub>p</sub>	22.91	23.07	-0.71	22.76	23.04	-1.20	18.74	18.74	-0.01
	A <sub>MPM</sub>	13.47	13.85	-2.77	11.73	12.24	-4.21	9.92	9.93	-0.10
10000	H <sub>s</sub>	18.57	18.90	-1.78	16.74	17.14	-2.38	21.02	21.00	0.10
	T <sub>p</sub>	23.39	23.45	-0.25	23.40	23.53	-0.56	19.73	19.75	-0.11
	A <sub>MPM</sub>	15.76	16.08	-2.04	14.22	14.64	-2.95	11.97	11.99	-0.13

Table 10 – Response Sensitivity: Pitch [deg]

Return Period	Parameter at max	North Atlantic			Word Wide Trade			West Shetlands		
		IFORM	CPD	% Diff	IFORM	CPD	% Diff	IFORM	CPD	% Diff
100	H <sub>s</sub>	17.40	17.36	0.19	15.14	15.04	0.63	16.70	16.69	0.06
	T <sub>p</sub>	15.95	15.95	0.01	13.87	13.89	-0.11	16.76	16.80	-0.23
	A <sub>MPM</sub>	5.75	5.74	0.19	5.18	5.15	0.65	5.42	5.41	0.21
1000	H <sub>s</sub>	19.36	19.33	0.17	17.14	17.03	0.62	18.59	18.63	-0.25
	T <sub>p</sub>	15.98	16.07	-0.56	13.83	13.89	-0.38	17.30	17.40	-0.59
	A <sub>MPM</sub>	6.39	6.38	0.25	5.87	5.83	0.68	5.89	5.88	0.24
10000	H <sub>s</sub>	21.23	21.16	0.31	19.10	19.00	0.53	20.59	20.67	-0.38
	T <sub>p</sub>	16.10	16.07	0.14	13.88	13.98	-0.71	18.08	18.20	-0.67
	A <sub>MPM</sub>	7.00	6.98	0.28	6.54	6.49	0.74	6.29	6.27	0.21